Republic of Iraq
Ministry of Higher Education
and Scientific Research
University of Babylon
College of Materials Engineering
Department of Metallurgical Engineering

Effect of Silicon and Boron Carbids on Mechanical and Machining Properties of Aluminium 7075-T6 Matrix Composite

A Thesis
Submitted to the Council of the College of Materials Engineering, University of Babylon in Partial Fulfillment of the Requirements for the Master Degree in Materials Engineering/Metallurgical.

By:

Mohammed Shakir Nahi Sayer

Supervised by:

Prof. Dr. Saad Hameed Al-Shafaie
Assist. Prof. Sundus Abbas Jasim

2022A.M **1443A.H**

بسم الله الرحمن الرحيم

وَلَقَدْ آتَيْنَا دَاوُودَ وَسُلَيْمَانَ عِلْمًا ۖ وَقَالَا الْحَمْدُ لِلَّهِ

الَّذِي فَضَّلَنَا عَلَىٰ كَثِيرٍ مِنْ عِبَادِهِ الْمُؤْمِنِينَ ()

صدق الله العظيم

سورة النمل
آية (15)

Supervisor Certificate

I certify that this thesis entitled ***(Evaluation of Mechanical and Machining Properties of Metal Matrix Composites*)** is Prepared by **(Mohammed Shakir Nahi)** under my supervision at the Department of Metallurgical Engineering, College of Materials Engineering, University of Babylon in partial fulfillment of the requirements for the degree of Master of Science in Material's Engineering/Metallurgical**.**

Signature***:***
Supervisor: Prof. Dr. Saad Hameed Al-Shafaie

Signature***:***
Supervisor: Asst. Prof. Sundus Abbas Jasim
Date: / / 2022

Acknowledgments

Many thanks to God Almighty, my Creator, who gave me strength and health.

Adequate thanks and gratitude to the two supervisors

, Prof. Dr. Saad Al-Shafaei and Assistant Professor. Sundus Abbas Jasim for their support and assistance in my research.

It was a great honor to work and study under their supervision.

My thanks to all the workers in the Metallurgical and Ceramic Engineering laboratories in the College of Materials Engineering, University of Babylon.

A heartfelt thank you to my family for their continuous support that made this work possible.

I am also very grateful to my friends for their fraternal support and to everyone who contributed to this work.

Mohammed Shakir Nahi

2022

Dedication

I dedicate my humble work;

... To the one who was the first to be credited with getting me to this stage and

first teacher in my life

(My beloved father), God give him long life.

To the one who set me on the path of life and made me calm, (My dear mother), my

sun, God have mercy on her

To all my family, my wife, my brothers, my sisters, and my friends; you are a source

of support, My world is more beautiful with you

To all my dear teachers; Who helped me

Mohammed Shakir Nahi

2022

Abstract

Metal matrix composites (MMCs) are widely employed in different industrial and engineering applications because of their superior properties, like high specific strength, high impact strength, and high fracture toughness when compared to traditional materials. Al 7075 was widely used in transportation applications, particularly aerospace, aviation, Marin, and vehicle, because of high strength to low weight ratio. Even though the Al 7075 series alloys have better mechanical and thermal properties as well as high wear resistance, they still need to be improved to be used in engineering applications.

The mechanical and machining properties of Al-7075 metal matrix composite (AMMCs) reinforced with (3, 6 and 9) of B_4C and/or SiC incorporated in the stir casting method are investigated in this study. The mechanical properties of AMMCs, such as Vickers hardness, tensile strength, compression strength, flexural strength, and elongation; were explored after reviewing the literature on the mechanical and machining behavior of AMMCs. The materials were characterized using the XRD, particle size analyzer, SEM, and optical microscope. Mechanical properties results demonstrate that all reinforcing materials have a considerable impact on these properties. The reinforcing material (4.5% B_4C + 4.5% SiC) provided better mechanical properties. Mechanical properties have improved by 54.95% in Vickers hardness VH, 31.1% in yield strength YS, 32.46 % in ultimate tensile strength UTS, 34.42% in ultimate compression strength UCS, and 39.4% in flexural strength FS, when compared to the base alloy. The optimization method used facilitated the improvement of the properties of hybrid AMMC. The best specimen in terms of mechanical properties Al7075 (4.5 % B_4C + 4.5 % SiC) was subjected to the Electrical Discharge Machining (EDM) procedure to determine the optimal combination of machining parameters in the same optimization technique (GRA) at a confidence level of 95%, the results collected from experimental runs were analyzed using Minitab17 software.

The main response was chosen to assess the impact of EDM process parameters like voltage (V), current (I), pulse duration (Ton) and pulse interval (Toff) on the performance characteristics such as Materials Removal Rate (MRR), Electrode Wear Rate (EWR) and Surfaces Roughness (Ra). Some EDM process factors have a considerable impact on performance attributes, according to the findings. GRA findings reveal that the optimal process parameter set is V 140 volts, Ip 10 A, Ton 50 µs, and Toff 25 µs.

List of Contents

List of Subscripts & Superscripts &Latin Symbols

Symbol	Meaning	Units
I_p	Pulse Current	Amp
T_{on}	Pulse On Time	µsec
T_{off}	Pulse off time	µsec
R^2	Coefficient of Determination	
R^2_{adj}	Adjusted Coefficient Of Determination	
V	Discharge Voltage	Volt
W	Weight	g
Wt	Percentage weight	%

List of Abbreviations

Symbol	Meaning
Adj MS	Adjust Mean Square
AMC	Aluminum matrix composites
ANOVA	Analysis of variance
ASTM	American Society for Testing and Materials
Adj SS	Adjust Sum Square
EDM	Electro-Discharge Machining
EWR	Electrode Wear Rate
F-test	Fisher Test
GRA	Grey Relational Analysis
MMCs	Metal Matrix Composites
MRR	Material Removal Rate
Ra	Surface Roughness
P	Probability
Seq SS	Sum of Squares
UCS	Ultimate Compression Stress
UTS	Ultimate Tensile Strength
VHN	Vickers Hardness
XRD	X Ray Diffraction
YS	Yield Stress

Chapter One

Introduction

1.1 General background

Current engineering applications require products that are harder, lighter, and inexpensive. A good example is a current advantage in the production of materials with good strength to weight ratio suitable for automotive applications where fuel economy with increased engine efficiency is becoming more important. In-service performance specifications for certain new infrastructure systems include materials with a wide variety of properties that are difficult to satisfy with monolithic material, these properties mentioned above can be achieved only by using composite materials [1].

A composite material can be defined as a system of materials in which a combination of two or more materials or stages of the same material is insoluble in each other is present. Their properties are usually intermediate between the properties of the matrix material and the reinforcements. The Two kinds of constituent materials in all existing composites are classified as matrix and reinforcement materials[2].

Composites of metal matrices are metals reinforced with other compounds of metal, ceramics, or organics. By dispersing the reinforcements in the base metal matrix, they are made. Reinforcement particles are typically used to strengthen the base metal's properties, such as strength, hardness, etc.[3].

MMCs are now widely used in modern engineering and industrial applications due to their excellent mechanical properties like strength-to-weight ratio, impact resistance, fracture toughness and higher corrosion and oxidation resistance than conventional materials. MMCs with various matrix metals; Such as aluminum, reinforced with different ceramic particles such as; Al_2O_3, SiC, B_4C … etc.[4].

One of the types of composite materials with excellent properties is hybrid composite materials, and it consists of at least two types of reinforcement materials embedded in the base material. The production of this material results in a significant improvement in mechanical, physical, and thermal properties and an improvement in corrosion and wear resistance. The reinforcement materials are either continuous or discontinuous and the widely used discontinuous reinforcement materials are Whiskers, particles, and short fibers [5].

Aluminum-based composites are among the most important metal composite materials because it has many important properties such as good specific strength, low thermal expansion coefficient, and low density. continuous study in materials science has been done over the current years, supporting the engineering and development of aluminum metal matrix composites (AMMCs)due to their many industrial application [6], [7].

The advantages of using these materials compared with non-reinforced aluminum alloys in high-tech structural and functional applications, including aircraft, military, and automotive [6], [7].

Hybrid composite materials based on aluminum are considered one of the modern generations of metal composite materials, which can fulfill the modern demands of many advanced engineering applications. This is due to improved mechanical properties, the possibility of using conventional manufacturing processes, and the potential of reducing the cost of production of aluminum hybrid composites.

Aluminum hybrid composites(AHC) are the most needed composites in the realm of advanced lightweight materials due to their low density, superior mechanical properties, improved wear and corrosion resistance, and reduced thermal expansion coefficient in comparison to traditional metals. Their low production costs and good mechanical properties make them the right choice [1], [8]. Key processes for the processing of AMC on an industrial scale may be divided into two primary groups; liquid State processes like Stir Casting, and Solid-state processes like powder metallurgy.

The stir casting process's key advantage is its flexibility for mass production and low cost. When compared to other fabrication processes, the stir casting method is one of the most frequent commercial ways of manufacturing aluminum-based composites. In the stir casting process, mechanical stirring is often utilized to disperse particle reinforcement into the metal melt. This approach relies heavily on mechanical stirring. Particle distribution in the final solid is influenced by mixing speed, particle wetting condition with the melt, solidification rate, and relative density. The mechanical stirrer's design, its position in the liquid, the molten temperature, and the particle properties introduced all influence particle dispersion in a molten matrix[9][10].

1.2 Machining of Metal Matrix Composites (MMCs)

Most reinforcing materials have been observed to be very hard during the machining of MMCs compared to the more widely used carbides and the tools of high-speed steel (HSS). The traditional machining of MMCs then posed a critical problem. These products can be machined Conventionally by Processes such as rotating, milling, or drilling, with the appropriate design of the tools and their use inappropriate operating conditions, however, the strengthening leads to rapid wear of the tools and this leads to lower machinability and more costs[11]

Due to the presence of hard reinforcements such as SiC, B_4C, TiC, ZrC, WC, Al_2O_3, etc. in (AMMC) products, this presents a challenge to the conventional machining methods resulting in the disadvantages described above. An unconventional technique, such as electrical discharge machining (EDM), has been accepted as the best possible process for machining AMMCs. EDM can machine materials, regardless of their hardness, to produce complex shapes. EDM is one of the unconventional ways of machining materials that have the property of electrical conductivity, by generating controlled electric sparks, between the electrode and the workpiece immersed in a dielectric fluid [7].

The EDM method does not include mechanical energy; the hardness, strength, or toughness of the workpiece does not influence the metal removal rate While the performance of conventional cutting methods is constrained by the mechanical properties of the workpiece .EDM is one of the most commonly used non-conventional material removal methods for the material that has been processed [12]. Its distinctive characteristic of using thermal energy for electrically conductive materials, regardless of their hardness, has been its unique advantage in the manufacture of die, mold, aerospace, automobile, and surgical components etc. In addition, EDM does not make direct contact between the electrode and the workpiece [13][14] EDM is used in a broad variety of industries, such as automotive, electronics, domestic devices, machines, packaging, telecommunications, watches, aeronautics, toys, surgical instruments, etc. [15].

1.3 Objectives of the present work

This work's purpose is to:

- Improve the mechanical properties of Al7075 by adding various percentages (3, 6, 9) % of B_4C and/or SiC fabricated by stir casting. The mechanical properties include Vickers hardness (VHN), yield strength (YS), ultimate tensile strength (UTS), ultimate compression strength (UCS), elongation (e), flexural strength (FS). And then select the optimum sample with best mechanical properties.
- Study the effect of the electric-discharge machining (EDM) parameters such as voltage (V), current (Ip), pulse on-time (T_{on}) and pulse off-time (T_{off}) on the machining performance include; material removal rate (MRR), electrode wear rate (EWR), and surface roughness (Ra), for the optimum sample to reach the better machining parameters. Grey relational analysis (GRA) based on the Taguchi method will be used to achieve the optimal mechanical and machining parameters.

Chapter Two

Theoretical Part and Literature Review

2.1 Introduction

This chapter will focus on composites materials Particularly Al7075 matrix composites, manufacturing of (AMMCs) reinforcing with Boron Carbide, Silicon carbide, and some other reinforcement materials by stir casting, machinability of (AMMCs), using GRA Base on Taguchi method approach for optimization of mechanical and machining condition, and Literature Review for researches close to the present study.

2.2 Composites Materials

A composite material is a mixture of a matrix and a reinforcement that, when mixed, has properties that are superior to the individual materials' properties. Because of their properties such as high strength and stiffness, wear resistance, thermal and mechanical fatigue resistance, and creep resistance, composite materials have a special role in the manufacturing sector. Until now, a substantial number of composites have been developed and successfully used in a variety of applications [16].

2.2.1 Metal Matrix Composites(MMCs)

Metal matrix composite (MMC) is a composite material made up of at least two components, one of which must be metal and the other may be metal or mostly ceramic [9]. (MMCs) have been found to provide a better property combinations required in a variety of engineering applications. High specific strength, low coefficient thermal expansion, and high thermal resistance are some of these property combinations, as are reasonable damping capacities, superior wear resistance, high specific stiffness, and acceptable degrees of corrosion resistance [1]. Continuous fibers, discontinuous fibers, whiskers, wires, and particulate are the five main types of MMC reinforcements. Reinforcements are normally

constructed of ceramics, except wires, which are made of metal. These ceramic materials are mostly nitrides, oxides, and carbides, and their use is preferred due to excellent strength and high hardness at ambient and high temperatures [17].

2.2.1.1 Hybrid Metal Matrix Composites

Hybrid composites are made up of at least three components (matrix and two or more reinforcements) to obtain a specific property in the product or part they are used to create. To change physical or functional properties such as wear, mechanical, or thermal properties, a few reinforcement particles are embedded into a matrix. The hybrid composites outperformed the unreinforced alloy in terms of stiffness and impact strength [5][1]. Silicon carbide, Silica, Boron carbide, Titanium carbide, Titanium dioxide, tungsten carbide, and Fly ash, are some of the reinforcements used in hybrid composites [8].

2.2.1.2 Aluminum 7075 Metal Matrix Composites

One of the key reasons for choosing aluminum is that it is available in the earth's crust, making it available for more than 8% of the planet's mass. Aluminum binds to the other components quite easily. It has a lot of useful properties. It is one of the lightest metals, about three times as light as Iron (Fe) [18]. Because of their good mechanical properties, minimal investments, and low manufacturing and maintenance costs, aluminum metal matrix composites are the most promising and commonly utilized materials. They may also be formed using traditional metal processing techniques. The aim of creating an aluminum matrix composite (AMC) is to incorporate the desirable properties of metal and ceramics into one material. [19] Ceramic reinforcements in aluminum-based composites are generally oxides, carbides, or borides like Al2O3, TiO2, SiC, TiC, B4C, and so on. The composite's microstructure, physical, tribological, and other desirable properties of the composite are influenced by the production methods, shape, size, and chemical affinity of reinforcement materials with matrix content [20].

Among all-aluminum alloy series, the 7075 series of aluminum alloys have the highest strength and the widest range of uses of all the aluminum alloy types. Because the maximum zinc content varies between 5.1 and 6.1 percent, the Al-7xxx series alloy is sometimes known as an aluminum-zinc alloy, figure (2.1) show the Al-Zn phase diagram. This series was initially created in secret by the Japanese company Sumitomo Metal in 1943 for usage in the construction of Japanese Navy airframes. Because aluminium-7075 has a wide range of applications, it requires further reinforcing. Aluminum-7075 series alloys are widely used in transportation applications such as aerospace, aviation, automobiles, and marine because of their exceptional mechanical properties such as low density, and high strength-to-weight ratio [21].

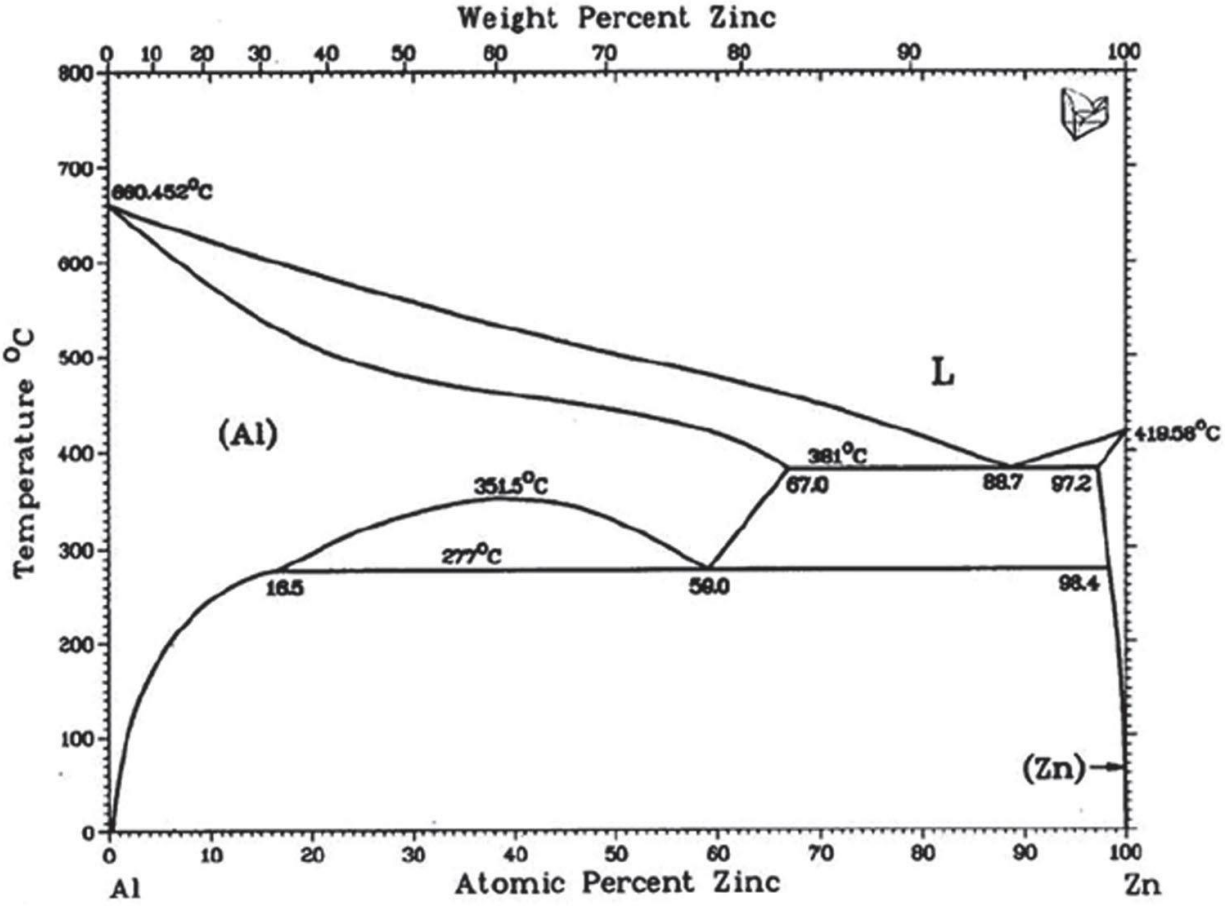

figure (2.1) show the Al-Zn phase diagram[22]

2.3 Particle-Reinforced Composites

Hard particles embedded in a soft matrix are referred to as particulate composites. Particle-reinforced composites are divided into two types: Large-particle and dispersion-enhanced composites The difference is dependent on the mechanism of reinforcement or strengthening. The term "large" refers to the fact that particle-matrix interactions should not be treated at the atomic or molecular level. The hard reinforcing particles tend to restrict matrix phase motion in the vicinity of each particle. The matrix transmits a portion of the applied load to the particles, which only carry a small portion of the load. The degree of reinforcement or enhancement in mechanical behavior is determined by strong bonding at the base alloy–particle interface. Dispersion-strengthened composite particles are often much smaller. Particle-matrix interactions lead to strengthening at the atomic or molecular level. Despite the fact that the matrix carries the majority of the load applied, the smaller dispersed particles impede or obstruct dislocation motion. As a result, plastic deformation is restricted, leading to greater yield, tensile, and hardness values [23].

2.4 Silicon Carbide

Silicon carbide (SiC) is a good abrasive material that has been used to make grinding wheels and other abrasive materials. SiC provides an excellent lubricating effect while also reducing noise and vibration during relative motion. Abrasives, refractories, ceramics, and a variety of other high-performance applications use SiC. Silicon Carbide ceramics provide superior anti-oxidation, wear resistance, creep resistance, and corrosion resistance properties. Silicon carbide (SiC) has found a wide range of applications due to its superior properties such as low density, exceptional thermal shock resistance, high-temperature strength, chemical stability, melting point, and low thermal expansion coefficient [24]. Table 2.1 shows the properties of silicon carbide.

Table (2.1) properties of SiC particles [25] - [26].

Property	value
Density	3.1 g/cm^3
Melting Point	2700-2200 C
Modulus of Elasticity	400 GPa
Hardness	2800 Kg/mm^2
color	Black

2.5 Boron Carbide (B_4C)

Boron carbide is a black solid with a shiny appearance that is the third hardest ceramic compound in nature after diamond and cubic boron nitride. B4C has a rhombohedra crystal lattice structure that gives good chemical and thermal stability, high hardness, young's modulus, impact and wear resistance, and low density. Table 2.2 displays the mechanical and physical properties of B4C ceramic particles. Because of its high refractoriness, it is used in high-temperature (melting point of 2450 °C) applications. Al/B4C is a lightweight composite with high hardness, low density, and excellent thermal and chemical stability [27].

Table (2.2) properties of B4C particles [28] [29].

Property	**Value**
Density	2.52 g / cm^2
Melting Point	2445 °C
Young modulus (E)	448 GPa
Hardness	2900 -3580 kg / mm^2
color	Black

2.6 Fabrication of Particulate Reinforcing Metal Matrix Composites

As mentioned earlier, various fabrication techniques that were used to fabricate particulate reinforcing metal matrix composites during the last few years. The following processes are the most commonly used for MMC fabrication: Liquid-state processes like stir casting and Solid-state processes like powder metallurgy.

2.7 Stir Casting Process

Earlier about 5500 years ago, metals cast in the carved or impressed shapes of cavities were utilized as molds created by clay and soft materials. Stir casting is a simple approach that produces consistent mixing of diverse metal elements, low moisture levels, high adhesion, and few chemical interactions between the particles and the base material. AMMCs were made using the stir casting technique, which is the simplest and most cost-effective method for making particle reinforced metal matrix composites. Uniformly distributed reinforcements particle in the matrix material gave the composites their best properties. The stirrer is used to ensure that the reinforcing material is evenly distributed throughout the matrix material. The matrix alloy was melted at temperatures ranging from 600 to 800 degrees Celsius. Generally, the stirrer is put into the molten metal and stirred at a speed that starts from 200 rpm for 10–20 minutes by an electric motor to generate a vortex. After that, preheated particle reinforcement was supplied at the vortex area to achieve a uniform distribution of reinforcement particles in the matrix as shown in Figure (2.1) [21].

Among the various fabrication techniques, the liquid metallurgical route is the most suitable and widely accepted as a promising route to composite fabrication due to its simplicity, cost-effective production, little reinforcement damage, flexibility, applicability to mass production, and stir cast products are not limited by their size and shape [30] [31].

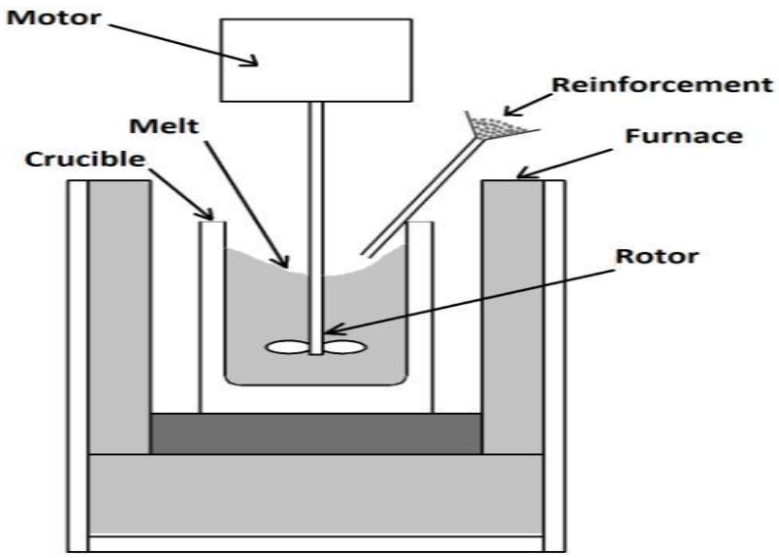

Figure. (2.2). Stir casting setup [32].

2.8 Electric Discharge Machining Process EDM

Electrical discharge machining (EDM) is one of the most commonly used non-traditional machining technologies due to it has been recognized as a common method for manufacturing mold and dies of aerospace, industrial, nuclear, medical, petroleum, and marine parts, etc [33]. In EDM, the electrode is pushed down toward the work component until the spark gap (the closest space between the two electrodes) is small enough to allow the impressed voltage to ionize the dielectric[12]. Rapid, repetitive spark discharges from a pulsating direct-current power supply with dielectric flow between the workpiece and the electrode remove electrically conductive materials. EDM avoids mechanical stresses, chatter, and vibration issues during machining since the electrode does not make any contact with the work material. As a result, even the hardest and brittle materials may be machined simply and precisely. In the EDM technique, performance-determined variables or output parameters include material removal rate (MRR), electrode wear rate (EWR), and surface roughness (Ra)[33]. Only the electrical conductivity of the workpiece material limits machinability. Other challenges with EDM include tool wear and irregularity of tool wear, as well as the tool's inability to create very sharp edges owing to the distance (gap) between the tool and the workpiece [34].

2.8.1 Advantages of EDM process[35]

• The EDM process may be used to cut any electrically conducting material.

• Hardened workpieces may be machined without the distortion caused by heating.

• The X, Y, and Z axes may be varied to create complex profiles using simple electrodes.

• Complex die parts and molds can be made more precisely, faster, and inexpensively.

• The EDM process has no burrs.

• Webs and fins, for instance, are thin and delicate portions that may be machined without causing the product to deform.

2.8.2 Types of EDM Processes[36]

- Sinking EDM.
- Wire EDM.
- Micro EDM.
- Powder Mixed EDM.
- Dry EDM.

2.9 Machining of Metal Matrix Composites by EDM.

When conventional machining was used, the machining of MMCs was complicated owing to the extremely abrasive nature of ceramic reinforcements. The machining process is removing unwanted content from a workpiece (raw material) to turn it into the desired shape (final product). Conventional machining removes unwanted content in the shape of chips by applying power using a very hard cutting tool. Owing to the existence of abrasive particles (reinforcement), the key problems faced during conventional machining of MMCs are high tool wear and poor surface quality. MMC machining by traditional techniques is highly

challenging. As a consequence, advanced machining processes are needed for machining MMCs. Among newly established advanced machining techniques, EDM is a very prominent machining method. The benefits of the EDM process are most visible when machining MMCs with the greatest hardness in reinforcement. Since the EDM method does not use mechanical energy, the workpiece's stiffness, weight, or durability have little effect on the MRR. Notably, tensile residual stress and a heat-affected zone (HAZ) are frequently found during the EDM technique. Furthermore, the EDM finishing process is more time-consuming than the roughness process. This improved technique for machining MMC materials is recognized as one of the most significant processes in the manufacturing industry [12].

The reinforcement mixed into the aluminum matrix greatly improves the elastic modulus, wear resistance, strength, and fatigue resistance of AMMCs. Furthermore, the use of reinforcement particles decreases the matrix material's coefficient of thermal expansion. These types of property improvements are usually not possible for traditional alloying processes. This fact encourages researchers to concentrate on their advanced industrial applications. Non-conventional machining techniques, such as electric discharge machining (EDM), are being used effectively for easy machining of AMMCs, Figure. (2.3). [37]

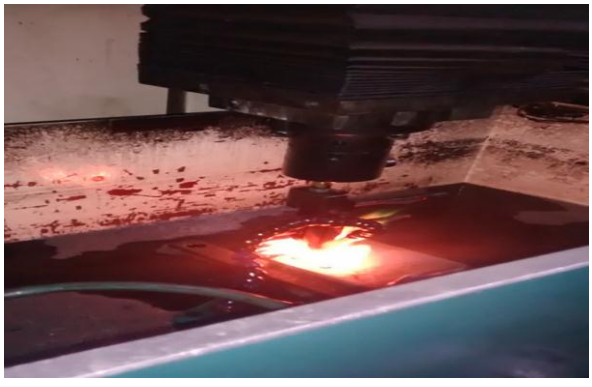

Figure. (2.3). EDM machining of Aluminum Metal matrix composites [37].

2.10 Effect of Electrical Parameter

2.10.1 Peak Current

is defined as the amount of power used in discharge machining and is recognized as the most significant process parameter. During each pulse on time, the current increases until it reaches a preset level, which is known as peak current. Peak current is determined by the surface area of the cut. During roughing operations, a higher peak current is used due to a wide surface area. Because the machined cavity is a duplicate of the tool electrode, excessive wear will affect machining accuracy. New electrode materials, such as graphite, can withstand high currents with minimal damage.[38]

2.10.2 Discharge Voltage

Discharge voltage is proportional to the breakdown strength of dielectric fluid and the spark gap. Before an electric discharge, the open-gap voltage increases until an ionization channel forms between the workpiece and the electrode. When the current starts flowing, the voltage drops and stabilizes at the operating gap level. As a result, a higher voltage setting widens the gap, improving cleansing conditions and supporting the stabilization of the cut until an ionization route forms between the workpiece and the electrode. [38].

2.10.3 Pulse Duration

Pulse duration, it can also be called (T_{on}), can be defined as the time it takes for the current to flow from the tool (electrode) to the workpiece via the spark gap figure (2.4). This period is estimated in microseconds. Pulse length is also known as a pulse on time. MRR is proportional to the amount of energy that propagates during T-on. The MRR is affected by T-on length. When is set longer the T-on, the more eroded particles are removed from the machining area, which has an impact on the EWR. The melting and vaporization process erodes the material from the tool and workpiece in the EDM operation. This amount of melting and evaporation depends on the (T_{on}), that is, the longer the (T_{on}), the greater the melting and evaporation, and vice versa [24].

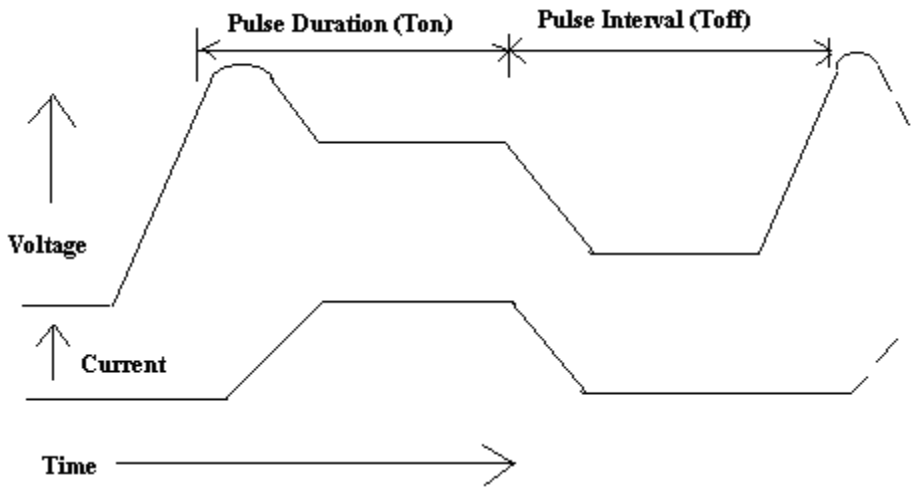

Figure. (2.4). The actual profile of a single EDM pulse [35].

2.10.4 Pulse Interval (T_{off})

It is the time interval between two pulses on periods. As shown in Figure.(2.5), it is the period during which no machining occurs (idle period), allowing the melt content to vaporize and be removed from the area. This parameter can influence the cut's speed and stability. If the T_{off} is too short, MRR increases, but in the machining area, more sparks become unstable. MRR steadily decreased as the pulse interval time increased. Because of the very short(T_{off}), the arcing risk is increased due to dielectric in the gap does not regain its dielectric strength [39].

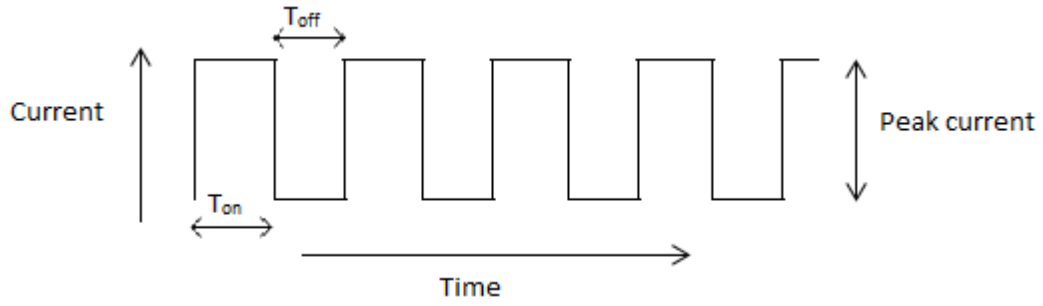

Figure.(2.5) Pulse waveform of pulse generator[12].

2.10.5 Electrode Gap

(Spark Gap): A proper gap between the tool and the workpiece is needed for effective machining. The servomechanism automatically maintains the constant gap between the tool and the workpiece. The gap width between the tool and the workpiece cannot be directly measured, but it can be estimated using the voltage of the average gap. [40].

2.10.6 Polarity

It may be linked to the tool electrode or the work material either positively or negatively Polarity can have an impact on the EDM operation's processing speed, finish, wear, and stability. MRR is higher when the tool electrodes are linked in a positive polarity (+) than when they are connected in a negative terminal (-). This might be because the energy transfer during the charging process is greater in this machining condition[41].

2.11 Effect of Nonelectrical Parameter

2.11.1 Dielectric Flushing

Flushing is the process of removing debris from the cutting zone. The flushing process is carried out with dielectric fluid, which is used to cool the tool and workpiece. To quench the spark, dielectric fluid is also employed. Dielectric fluid must have high dielectric strength and quick recovery after a breakdown. Dielectric fluid behaves as a conducting medium when ionized [40].

2.11.2 Tool Geometry

The form of the electrode, which might be square, rectangular, or circular, is referred to as tool geometry. The electro-discharge machining efficiency metric is also influenced by the form of the electrode. And the shape influences the aspect ratio. For any form of the electrode, the aspect ratio is known as the length/diameter ratio, and for rotational disc electrodes, it is known as the

thickness/diameter ratio. As a result, increasing the size of the electrode enhances machining efficiency [40].

2.12 EDM Performance Measures

2.12.1 Material Removal Rate(MRR)

MRR is the weight differential between the workpiece material before and after machining divided by the machining time. The migration of material elements between the workpiece and the electrode is referred to as material removal. The amount of elements that diffuse from the electrode to the workpiece. These elements are carried as solids, liquids, or gases and alloyed with the contacting surface via a solid, molten, or gaseous-phase process [14]. The current intensity was the most important element for the MRR performance parameter, followed by its quadratic influence and pulse–off duration. As the current intensity rises, the MRR increases significantly. When the pulse–off time was increased, the same effect was found [36]. MRR) depends on the amount of energy used during the pulse duration. Increased pulse duration also allows more heat to sink into and spread via the workpiece, resulting in a wider recast layer and a deeper heat-affected zone. After an optimum value of pulse length, the material removal rate tends to decrease [38].

2.12.2 Surface Roughness

Surface roughness is one of the most critical EDM performances when compared to tool wear and material removal rate. The roughness of the surface is a technical requirement for mechanical items. Practically, for the machine parts and its play an important role in fatigue strength, wear resistance, tensile, and ductility. Surface roughness value generally influenced by many factors such as machining parameters, work piece properties, cutting phenomena and type of cutting tools. . The value of surface roughness is controlled by the discharge energy and duration as shown in Figures (2.6) and (2.7) during the machining process, The higher energy applied leads to the higher amount of material removed which can be also causing a rougher surface finish [24].

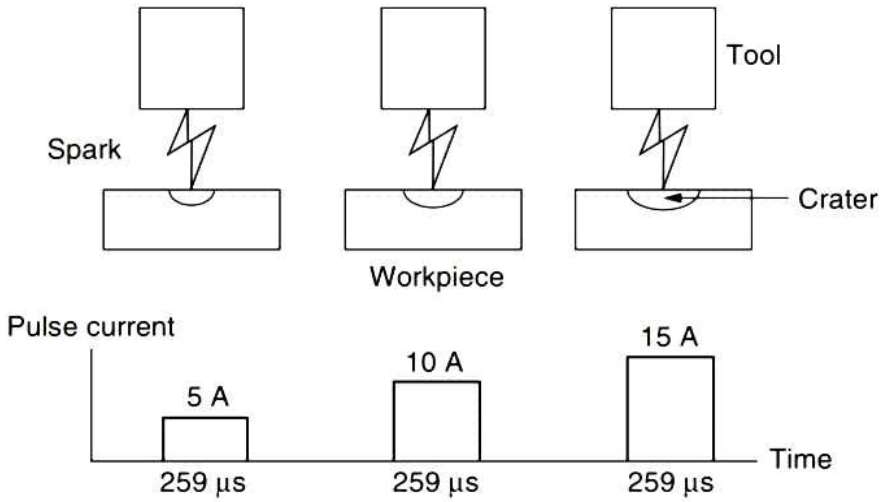

Figure. (2.6)Effect of pulse current (energy) on the removal rate and surface roughness[42].

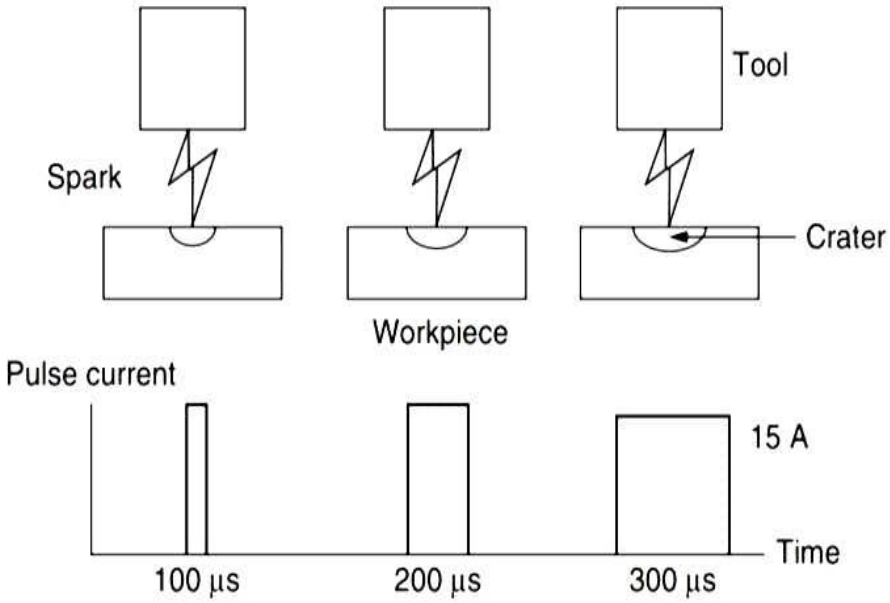

Figure.(2.7) effect of pulse on-time (energy) on the removal rate and surface roughness [42].

2.12.3 Electrod Wear Rate (EWR)

Since the tool and workpiece are considered as a set of electrodes in EDM, the tool wear operation is similar to the MRR. Carbon precipitation from the hydrocarbon dielectric onto the electrode surface during sparking effects tool wear. The rapid wear on the electrode edge was caused by carbon failure to precipitate in difficult-to-reach areas of the electrode . The most influential factor in electrode wear parameters is current, followed by its quadratic effect and pulse – on time. Low intensity and pulse – on-time values can be used for low electrode wear [36].

2.13 Grey Relational Analysis

Grey relational grade can be used to convert a multiobjective optimization issue to a single-objective optimization problem. The optimization of process parameters has been discovered in this work to maximize some properties while minimizing the others at the same time. As a result, grey relational analysis (GRA) was employed in this paper. To transform a multi-objective optimization problem into a single-objective problem, use the approach below. The initial stage is to use grey relational generation to normalize the experimental data according to the kind of performance response (in the range of 1 to 0). In this work, some properties or outputs were taken as the larger the better, the sequence can be normalized according to Eq (2.1)[43]. Nevertheless, the others were to be minimized (a smaller-is-better characteristic), It is needed to normalize the original sequence as equation (2.2) [44]

$$x_i^*(k) = \frac{X_i(k) - \min X_i(k)}{\max X_i(k) - \min X_i(k)} \dots\dots\dots\dots\dots\dots\dots\dots\dots (2.1)$$

$$x_i^*(k) = \frac{\max X_i(k) - X_i(k)}{\max X_i(k) - \min X_i(k)} \dots\dots\dots\dots\dots\dots\dots\dots\dots (2.2)$$

where, $x_i^*(k)$ is the sequence after the data preprocessing and x_i (k) is the comparability sequence, min x_i (k) is the smallest value of x_i (k) for the k^{th} response, and max X_i (k) is the largest value of X_i (k) for the k^{th} response.

In the second stage, the grey relational coefficient (GRC) is calculated using normalized data to represent the connection between the ideal and real experimental data. Equation (6) may be used to compute the GRC$\xi_i(k)$[16].

$$\xi_i(k) = \frac{\Delta_{min.} + \xi\Delta_{max.}}{\Delta_{0i}(k) + \xi\Delta_{max.}} \dots\dots\dots\dots\dots\dots\dots\dots\dots\dots\dots\dots (2.3)$$

where $\Delta_{0i}(k)$ represents the sequence of deviation for the reference sequence, $x_0^*(k)$ and the comparability sequence, $x_j^*(k)$. Δ_i is the difference between $x_0^*(k)$ and $x_j^*(k)$ in absolute value as shown in equation (2.4). $\Delta_{\min}$ is the smallest value of Δ_i, $\Delta_{\max}$ is the largest value of Δ_i, [45].

$$\Delta_{0\mathrm{i}}(\mathrm{k}) = |X_0^*(\mathrm{k}) - X_i^*(\mathrm{k})| \dots\dots\dots\dots\dots\dots\dots\dots\dots\dots\dots (2.4)$$

ξ is the distinguishing coefficient ($\xi \in [0, 1]$) and is used to adjust the difference of the relational coefficient. In general, ξ is 0.5.

In the third step, the weight of GRC corresponding to each response is averaged to compute grey relational grade (GRG). GRG is calculated as equation (2.5) and shows the relation among the series[46].

$$\gamma_i = \frac{1}{n}\sum_{k=1}^{n} \xi_i(k) \dots\dots\dots\dots\dots\dots\dots\dots\dots\dots\dots\dots\dots\dots (2.5)$$

where n is the number of performance characteristics or responses.

In the last stage, the optimal parameter is found by reference to the maximum value of GRG. The higher the GRG value, the closer the experimental value is to the ideal normalized value. As a result, a larger GRG implies that the associated parameter combination is approaching the ideal.

2.14 Literature Review

This part Includes studies related to mechanical and machining properties of Aluminum matrix composites

2.14.1 Studies Related to Mechanical Properties of Aluminum Matrix Composites.

In 2013 Senthilvelan et al., [47] studied the mechanical properties of three aluminum metal matrix composites reinforced with 10 wt% of B_4C, SiC, and Al_2O_3 particles were processed by stir casting method followed by hot rolling. The mechanical characteristics of Al/B_4C exhibited the strongest bonding among the three MMCs. Because of the poor interface and porosity, which caused agglomeration, the result of Al/SiC was determined to be the lowest of the other two MMCs. In terms of tensile strength, Al/B4C improves by 143 percent, Al/Al_2O_3 improves by 88 percent, and Al/SiC improves by 46 percent. Even though Al/B_4C delivers 4.33 percent elongation, which is larger than the other two MMCs, reduced ductility was attained. Al/B4C has a Vickers hardness of 138 VH, whereas Al/Sic has a hardness of 121 VH and Al/Al_2O_3 has a hardness of 112 VH.

In 2014, Baradeswaran and Elaya Perumal [48] investigated the effect of graphite on the wear and mechanical behavior of Al 7075/(2, 4, 6 and 8)Al_2O_3 +5 % wt Gr composites. The liquid metallurgical technique was used to create percent graphite hybrid composites. The results demonstrate that the hardness of hybrid composites rises with increasing Al_2O_3 and is greater than the hardness of base alloy in all compositions. The inclusion of Al_2O_3 particles boosts the tensile, compression, and flexural strength of the hybrid composite, which is greater than the basic alloy. The presence of graphite reduces mechanical characteristics, which was countered by the addition of Al_2O_3 particles in hybrid composites.

In 2014 Krishna and Xavior[49], studied the manufactured and compared the mechanical characteristics of Al6061-SiC and Al6061-SiC/Graphite hybrid composites. The stir casting procedure was used to create the composites, with reinforcement ranging from 5 to 15% in 5wt% increments. The results show that weight fractions have a substantial influence on the mechanical characteristics of the composites, such as tensile strength; the greatest tensile strength recorded was 192.45 MPa at 15% SiC/Gr. The mechanical characteristics of SiC/Gr reinforced hybrid composites outperformed those of single reinforcement.

In 2015 Pugalethi et al., [50] Investigated and evaluated The mechanical characteristics of aluminum 7075 in the presence of silicon carbide, aluminum oxide, and their combinations were investigated and produced using the stir casting process. The results reveal that the addition of SiC and Al_2O_3 increases tensile strength and hardness while decreasing ductility. The sample with the greatest percentage of Al_2O_3 (89 percent Al7075 +2 percent SiC+9 percent Al2O3) had a high tensile strength of 402.5 MPa, a high hardness of 115 VHN, and a minimum percent elongation value of 2.789 percent.

In 2016 Kittali, et al. [51] presented a review on the effects of Al_2O_3, B_4C, Gr, Y_2O_3, and SiC reinforcements on the tribological and mechanical behavior of AMMCs fabricated by various methods such as stir casting. The results obtained from this work showed that Reinforcements added to Aluminum alloy will improve mechanically and wear properties, Aluminum matrix composites have better properties than unreinforced materials.

In 2017 Verma [52], studied the effect of various reinforcement particles on the mechanical behavior of Aluminium Alloys (Al7075and Al6061) based composite. The composite material is fabricated by various advanced processes like Stir Casting, by introducing different weight percentages of reinforcement material. the results show that the Al 7075 based composite has superior properties as compared to the Al 6061 based composite, the composite has smaller size reinforcement which has more yield Strength as compared to

composite having large size reinforcement particles, Magnesium can be used to increase the wettability between the matrix material and reinforcement in Al 6061 and Al 7075, stir casting process is considered as best fabrication process for Al 6061 and Al 7075 matrix composite. There were increases in mechanical properties like tensile strength, compression strength, hardness with the addition of hard ceramics like B_4C, SiC, and Al_2O_3 with Al 6061 and Al7075.

In 2017 Fadhil [53], investigated the effect of B4C particles on the mechanical and physical properties of Al –base matrix. All samples were prepared by a two-step stir casting method with squeezing the melt during its solidification. Aluminum metal matrix samples of 2wt%Mg with (0,2,4, and 6wt%) of B_4C particles were prepared. The results show that the Stir casting with squeezing during solidification is suitable to prepare MMC reinforced with B_4C particles, Particles of B_4C improve the mechanical properties of Al-matrix, the greatest improvement of 53% in the hardness was recorded for the specimen with 6wt% of B_4C, while an improvement of 50% was achieved via the addition of 4wt% of B_4C. The maximum improvements in the tensile properties were recorded for the specimen with 4wt% of B_4C, so as the yield stress, tensile strength, and the modulus of elasticity were increased by 11%, 51%, and 51% respectively.

In 2017 Raju and Principal [54], studied the mechanical properties such as tensile strength, hardness, and impact strength and compare the different levels by the addition of Fly ash % and evaluated the best metal from the four samples. The results reveal that the aluminum-based metal matrix composite was effectively cast by stir casting for three different ranges of fly ash particles of 15%, 20%, and 25%. The increase in reinforcing results in a decrease in tensile strength and an increase in hardness. Sample 3 with a reinforcement of 20% fly ash shows a consistent distribution of particles and a satisfactory hardness of the AMMC. The tensile property of the AMMC declines at a slower pace, but the weight ratio of the material reduces significantly, which is a good indicator for a lightweight

material. When compared to other samples in this investigation, sample 3 exhibits good mechanical properties and a height hardness of BHN 80.

In 2018 Subramaniam et al. [55] reported the manufacture and assessment of the mechanical characteristics of Aluminium 7075 reinforced with boron carbide (B4C) and coconut shell fly ash particles. (CSFA). manufactured using the stir casting process The Al7075 samples were made using varying weight percentages of (0, 3, 6, 9, and 12wt. percent) B4C and 3wt. percent CSFA. The results reveal that the mechanical characteristics of hybrid composites, such as hardness and tensile strength, improve with increased reinforcement particles in the matrix, but ductility decreases. The maximum tensile strength rose by 66% when compared to unreinforced aluminium 7075. Multiple reinforcements result in reduced porosity and improved interface bonding.

In 2019 Sharma et al. [8] investigated the impact of various reinforcement combinations on the mechanical properties of 7075 hybrid composites. It was concluded that the higher hardness in most of the 7075 hybrid composites was mostly attributable to hard reinforcement particles, increased dislocation density, uniform distribution of reinforcements in the matrix, and good interfacial bonding of phases present. The tensile strength of the hybrid composite was higher when the grains were refined and there was less porosity. The compressive strength was primarily determined by the type of reinforcement utilized, as well as the density of dislocations. The impact strength of a hybrid composite can be increased by obtaining high matrix strength.

In 2019 Imran and Khan[21] investigated the mechanical, tribological, and corrosion behavior of Al-7075 metal matrix composites (AMMCs) produced by stir casting with desired reinforcements. The results demonstrated that the inclusion of different weight percentages of ceramic particles reinforcing in aluminum alloys resulted in significant enhancements in mechanical characteristics. The addition of silicon carbide and other reinforced particles to aluminum improves tensile strength, hardness, yield strength, compressive

strength, and flexural strength while decreasing ductility. The wear resistance assessment demonstrates that the introduction of carbide particles reinforcement in the Al7075 matrix alloy greatly improves the wear rate.

In 2019. Suresh et al. [56] investigated the impact of mechanical stir casting on 7075-based lightweight aluminum alloy improved by nano-Al_2O_3 with average particle size (20–30) nm and weight percent of nano-Al_2O_3 (1.0, 2.0,3.0, and 4.0). When compared to as-cast, the experimental results reveal that the heat treatment technique boosted the mechanical performance of nano aluminum oxide composites. When the weight percent of nano-reinforcement is increased, the density decreases when compared to the base alloy, and the tensile strength, hardness, and toughness steadily improve.

In 2021 K. Kumar, et al. [57] Studied the influence of B_4C and SiC particles on aluminum metal matrix composites fabricated by the stir casting technique. It has been found that Reinforcement of aluminum alloys is a useful method for improving mechanical and physical properties, the mechanical properties of hybrid Al MMCs reinforced with SiC/B_4C are better than those of Al MMCs reinforced with B_4C or SiC, adding B_4C and SiC as reinforcement to Al MMCs improves mechanical properties significantly When compared to the base metal.

2.14.2 studies related to machining properties of Aluminum matrix composites.

In 2009 Habib[13] investigated the effect of process parameters (current, voltage, pulse on time, and weight percent SiC) on machining properties (MRR, EWR, gap size, and SR) in EDM of Al/SiC composite. Four different volume fraction percentages of silicon carbide in the aluminum matrix were chosen (5, 10, 20, and 25). The experiments were carried out using copper electrodes. The results indicate that process parameters; peak current, pulse on time, gap voltage, and SiC percentage have a significant impact on the metal removal rate, electrode wear rate, gap size, and surface roughness.

In 2012 S. Gopalakannan et al. [58], investigated the effect of EDM process parameters; voltage (V), current (I), pulse-on time (*Ton)*, and pulse-off *(Toff)* of Aluminium 7075 Metal Matrix Composites reinforced with 10% B4C fabricated by Stir Casting method on performance characteristics; (MRR), (EWR) and (SR). The research result shows that factors effect on MRR are current, pulse-on time, and the EWR significantly affected by current, pulse-on time, pulse-on time, and pulse-off time. Current, pulse-on time, and voltage have a statistical significance on SR.

In 2014 Kumar et al. [59] studied the impacts of tool wear rate (EWR), surface roughness (Ra), and energy consumption on the electrical discharge machining (EDM) parameters of an aluminum alloy (Al 6351) matrix reinforced with 5% silicon carbide (SiC) and 10% boron carbide (B4C) particles fabricated via the stir casting route. The results show that the input parameters have a significant impact on the output parameters, with the pulse current having the highest influence on the total output responses (83.94 percent).

In 2015 Vinoth Kumar, et al. [60] studied the machining of Al–MMC with 10% SiCp reinforcing, conventional electrical discharge machining (CEDM), and an electrical discharge machining procedure with a cryogenically cooled electrode. (CCEDM). Discharge current, pulse on time, and gap voltage were among the machining parameters. The output replies included EWR, Ra. Discharge current, pulse on time, and gap voltage were found to have the most significant effect on EWR, while pulse on time with discharge current had the most significant effect on SR.

In 2016 P. Kumar and R. Parkash [61]studied the effect of EDM process parameters current, (Ton), (Toff) and electrode material on (MRR), (EWR), and (SR) during machining of aluminum boron carbide Al–B4C composite fabricated by stir casting method using 5% (wt) B4C particles in Al 6061 metal matrix. According to the results, the current is the most important factor for MRR and

SR, whereas tool material is the most critical component for EWR. ANOVA also supports comparable outcomes.

In 2016 V.K. Jain [62]investigated the electro-discharge machining of an aluminum matrix reinforced with SiC particles. It is concluded that the presence of SiC particles affects EDM efficacy owing to their tendency to not melt, raising discharge current, leading to a large material removal rate as well as a higher tool wear rate. High peak current levels are harmful to the process.

in 2017 Lalmuan et al. [63] published a review of machining investigations of several hybrid MMCs in terms of process parameters employed and their impacts on machining performance. MRR is shown to rise with increasing current, pulse on time, and flushing pressure and decrease with increasing voltage. Tool wear rate is similarly affected by current and voltage, and it reduces as a (T on) and flushing pressure rise.

In 2018 K. Ponappa et al.,[64]investigated The influence of EDM parameters such as pulse current and pulse duration on EWR, MRR, and SR during machining of a stir cast hybrid composite Al 7075-TiC-B_4C. The Al 7075 was strengthened with TiC and B_4C at 2.5, 5, and 7.5 vol. percent. It is concluded that among the process parameters studied, the pulse current was determined to be the most influential in impacting MRR, EWR, and SR. The other variables have little influence on the response variable.

In 2018 Mahanta et al. [65] investigated the machining of aluminum alloy (Al 7075)-based hybrid composites enhanced with boron carbide (B_4C) (1.5 wt%) and fly ash produced using a stir-casting method by (EDM) process and studied the effect of four process parameters; voltage, current, pulse-on time, and pulse-off time on three sustainable measures MRR, PC, and Ra. The results show that the current (I) and pulse-on time (Ton) are important factors for performance measurements; high values of I and Ton offer significant discharge energy, which results in high melting and vaporization of material, resulting in high MRR and

SR. It had a significant influence on PC, and the increased length of Ton increases power consumption.

In 2019 Malhotra et al. [66] studied the effect of EDM process parameters on EWR and MRR of the stir casting-produced Hybrid reinforcement of Aluminum 7075, 10% SiC, and Magnesium nanoparticles. The Taguchi technique was used to improve the machining process's efficiency. According to the experimental results, rotary EDM has a greater MRR and a lower EWR than traditional EDM.

In 2019 Palanisamy et al. [67] optimized the input parameters (I, Toff, and Ton) of LM6-Alumina Stir cast Metal Matrix Composites (MMC) to get the best MRR, EWR, and SR. The attributes were designed and optimized using grey relation analysis. According to the findings of this study, the discharge current is the most significant parameter influencing MRR and surface finish.

In 2020 Dinesh Kumar et al. [42] examined the numerous process parameters and their effects on the EDM process in several aspects such as discharge energy, electrode feed rate, pulse on time, and pulse off time. They discovered that the current is the most influencing component that has a significant impact on the Material Removal Rate and Surface Roughness during the EDM machining of Metal matrix composites.

In 2021R. Vijaya Prakash and V. Chittarangan Das [68]investigated the effect of EDM process parameters such as voltage (V), current (I), pulse-on time (Ton), and pulse-off time (Toff) on the performance characteristics of Aluminium Metal Matrix Composites (AMMCs) manufactured using the Stir Casting method, such as Electrod Wear Rate (EWR), Surface Roughness (SR), and Material Removal Rate (MRR). The combination of Al7075, Boron Carbide (3%), and Zirconium dioxide (15%) is used to analyze the EDM process. Experimentation demonstrates that the current is the most influential parameter on the MRR, EWR, and SR, and confirmed the ideal values of the input parameters.

Studies Related to Mechanical Properties of Aluminum Matrix Composites.				
Authors	**Materials**	**W%**	**properties studied**	**Results**
Senthilvelan et al. [47]	Al/B_4C Al/SiC Al/Al2O3	10 wt% of B4C, SiC, and Al2O3	tensile strength elongation Vickers hardness	Al/B_4C exhibited the highest improvment in mechanical properties while Al/SiC the lowest .
Baradeswaran and Elaya Perumal [48]	Al 7075 /Al_2O_3 Gr	5 % wt Gr, 2, 4, 6 and 8 wt.% of Al_2O_3	Hardness, tensile, compression, and flexural strength	The presence of graphite reduces mechanical characteristics, which was countered by the addition of Al_2O_3 particles in hybrid composites
Krishna and Xavior[49]	Al6061-SiC and Al6061-SiC/Graphite	5, 10, and 15%	tensile strength	The mechanical characteristics of SiC/Gr reinforced hybrid composites outperformed those of single reinforcement
Pugalethi et al., [50]	Al 7075 , Al_2O_3, and SiC	3,5,7,9 wt. % of Al_2O_3 and 2 wt. % of SiC	Strength ,hardness ductility	the addition of SiC and Al2O3 increases tensile strength and hardness while decreasing ductility
Fadhil [53]	Al, B4C, Mg	2wt%Mg with (0,2,4, and 6wt%) of B4C	tensile strength, modulus of elasticity	Particles of B4C improve the mechanical properties of Al-matrix yield stress, tensile strength, and the modulus of elasticity were increased by 11%, 51%, and

				51% respectively.
Raju and Principal [54]	Al,Fly ash	15%, 20%, and 25%. Of Fly ash	tensile strength, hardness, and impact strength	sample 20% fly ash exhibits good mechanical properties
Subramaniam et al. [55]	Aluminium 7075, (B4C) and coconut shell fly ash	(0, 3, 6, 9, and 12wt. percent) B4C and 3wt. percent CSFA	hardness and tensile strength	mechanical properties improve with increased reinforcement but ductility decreases.
Suresh et al. [56]	Al-7075 nano-Al_2O_3	(1, 2,3, and 4) w%Al_2O_3	tensile strength, hardness, and toughness	When the wt% is increased the tensile strength, hardness, and toughness steadily improve.
Studies related to machining properties of Aluminum matrix composites				
Authors	**Materials**	**Process parameters**	**properties studied**	**Results**
Habib[13]	Al/SiC composite (5, 10, 20, and 25)%	current, voltage, pulse on time, and weight percent SiC	MRR, EWR, Ra, and gap size	Process parameters have a significant impact on theMRR, EWR, Ra, and gap siz
S. Gopalakannan et al. [58]	Aluminium 7075	EDM process parameters; (V) ,(I), (Ton), and (Toff)	(MRR), (EWR) and (SR).	(MRR), (EWR) and (SR). significantly affected by current process parameters
Kumar et al. [59]	(Al 6351) matrix reinforced with 5% (SiC) and 10% (B4C)	Pulse current (I), (Ton), Pulse duty factor (τ), (V)	(EWR), surface roughness (Ra), and energy consumption	(EDM) input parameters have a significant impact on the output parameters,
Vinoth	Al–MMC	current, pulse	EWR, Ra	I, (Ton),, and

Kumar, et al. [60]	with 10% SiCp reinforcing	on time, and gap voltage		(V)have the most significant effect on EWR while (Ton) with I, had the most significant effect on Ra.
P. Kumar and R. Parkash [61]	5% (wt) B4C particles in Al 6061 metal matrix	current, (Ton), (Toff) and electrode material	(MRR), (EWR), (Ra)	The I is the most important factor for MRR and Ra, whereas tool material is the most critical component for EWR
V.K. Jain [62]	aluminum matrix reinforced with SiC particles	Ip, spark gap and electrode type (varying size and geometry).	MRR, EWR, Ra	the presence of SiC particles affects EDM efficacy owing to their tendency to not melt currentwas impact on MRR, EWR
K. Ponappa et al.,[64]	Al 7075-TiC-B4C2.5, 5, and 7.5 %	pulse current and pulse duration	EWR, MRR, and Ra	the Ip was the most influential in impacting MRR, EWR, and SR. The other variables have little influence on the response variable.
Mahanta et al. [65]	Al 7075)-enhanced with (B4C) (1.5 wt%) and fly ash	voltage, current, pulse-on time, and pulse-off time	MRR, PC, and Ra	the current (I) and pulse-on time (Ton) are important factors for performance measurements
Malhotra et al. [66]	Al7075, 10% SiC, and Magnesium nanoparticles	EDM process parameters	EWR and MRR	Rotary EDM has a greater MRR and a lower EWR than traditional EDM

Palanisamy et al. [67]	LM6-Alumina	(I, Toff, and Ton)	MRR, EWR, and SR	Ip is the most significant parameter influencing MRR and Ra
Vijaya Prakash and V. Chittarangan Das [68]	Al7075, Boron Carbide (3%), and Zirconium dioxide (15%)	(V), (I), (Ton), (Toff)	MRR (EWR), (SR),	Ip is the most influential parameter on the MRR, EWR, and Ra,
Present study	Al7075, (3%,6%, 9%) SiC (3%,6%, 9%) B4C (3%,6%, 9%) SiC+ B4C	Reinforcement material Reinforcement Percentage (V), (I), (Ton), (Toff)	VHN, YS UTS, UCS, FS, and e% MRR, EWR, and Ra	The type and content of reinforcement particles have a significant effect on the mechanical properties of the composites **Except** for Toff, all input variables in the EDM process are direct proportion to outputs

2.14.3 Summary of Previous Studies

Summary of Studies Related to Mechanical Properties of Aluminum matrix Composites.

- The mechanical properties of hybrid composites are better than single composites and base alloy
- The AL 7075 based composite has superior properties as compared to some other aluminum alloys,
- Stir casting process is considered as best fabrication process for Al 7075 matrix composite.
- The addition of SiC and B4C reinforced particles in aluminum-based composite increases the tensile strength, hardness, yield strength, compressive strength, and flexural strength, whereas ductility is decreased.
- Reinforced with SiC/B_4C are better than those of Al MMCs reinforced with B_4C or SiC.
- The Al/B_4C composite exhibited a strong interfacial bonding.

The Summary of Studies Related to Machining Properties of Aluminum Matrix Composites

- Among the process variables studied, the pulse current was determined to be the most influential in impacting MRR, EWR, and SR, and the Ton comes after current. The other variables have little influence on performance measures.
- Increasing discharge current resulting in a higher material removal rate together with a higher tool wear rate.
- Reinforcing particles percentage has a significant impact on the metal removal rate, electrode wear rate, gap size, and surface roughness.
- Most of EDM process parameters have a significant impact on the metal removal rate, electrode wear rate, and surface roughness.

Chapter Three

Experimental Work

3.1 Introduction

This chapter describes the experimental setup, techniques and equipment, and physical, mechanical, and machining tests used in this study. Mechanical and characterization tests include hardness test, tensil test, compression test, bending test, chemical composition analysis, optical microscope analysis, scanning electron microscope SEM, and XRD. The machining tests include MRR, EWR, and Ra of the machined surface in the EDM process.

3.2 Materials Used

Master alloy:Among all series of aluminum alloys, alloy 7075-T6 was chosen for its superior properties, good strength and formability can be considered the most important, which allow it to be widely used in various engineering fields, especially in the automotive and aerospace industries. Table (3.1) show the results of Al7075-T6 Chemical Composition test.

Table (3.1): Aluminum 7075–T6 Chemical Composition,

Material	Si	Fe	Cu	Mn	Mg	Cr	Ni	Zn	Ti	P	Pb	Al
%weight	0.107	0.288	1.85	0.0296	2.25	0.212	0.0154	5.78	0.0369	0.0063	0.0887	89.2

Among the commonly used ceramic reinforcements, boron carbide (B_4C) and Silicon Carbide were selected as reinforcement particles due to their good mechanical, physical, and thermal properties. The specifications,purity and origins of powders used in this work are shown in Table (3.2).

Table (3.2): Specifications of Materials Used in this work. Figure (3.1)

Materials	Specifications	Purity	Origin
Boron carbide	19.28 μm	99.8%	Changsha Santech Materials Co. Ltd
Silicon carbide	11.6 μm	99.0	

3.3 Outlines of Present Study

The Program of Present Study Shown in. Figure (3.2)

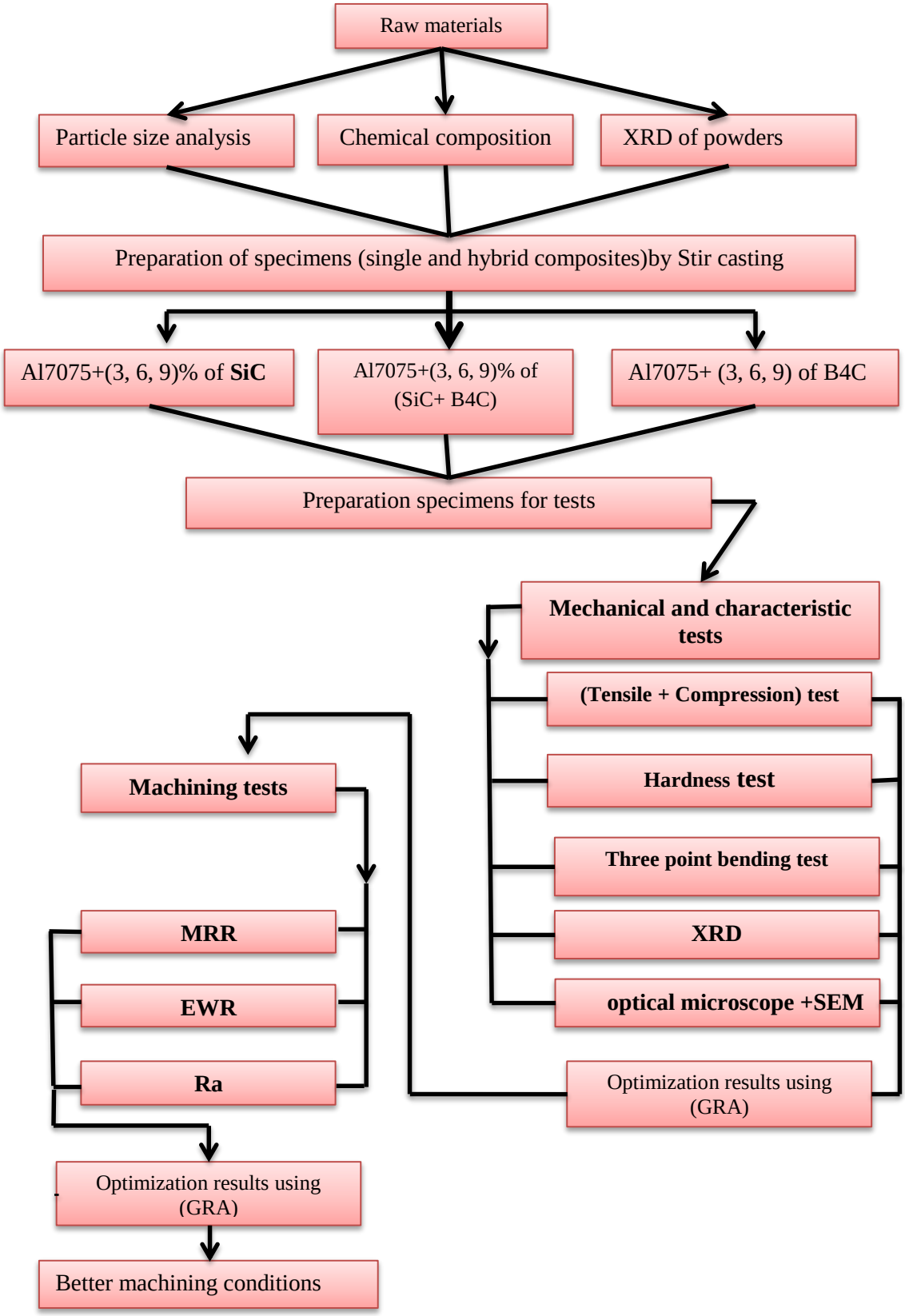

Figure (3.2): Outlines of the Present Work.

3.4 Tests of Materials before Preparation of specimen:

3.4.1 Chemical Composition

Chemical composition analysis for base alloy (Al 7075–T6) used in this work. Metal analysis using the SPECTRO model (SPECTROMAXx) shown in figure (3.3) was performed at the General Engineering Inspection and Qualification Company-Baghdad.

Figure (3.3): SPECTRO Analyzer

Table (3.2): Aluminum 7075–T6 Chemical Composition,

Material	Si	Fe	Cu	Mn	Mg	Cr	Ni	Zn	Ti	P	Pb	Al
%weight	0.107	0.288	1.85	0.0296	2.25	0.212	0.0154	5.78	0.0369	0.0063	0.0887	89.2

3.4.2 Particle Size Measurement (Analysis)

The analysis of particle size was performed for boron carbide and silicon carbide. The test was achieved by laser particle size shown in Figure (3.4) In the laboratories of ceramics and building materials at the University of Babylon/ College of Materials Engineering Figures (3.5) and (3.6) show the particle size analysis reports. The average particle size of B4C powder was 19.28 μm and of SiC was 11.6 μm.

Figure (3.4): Laser Particle Size Analyzer.

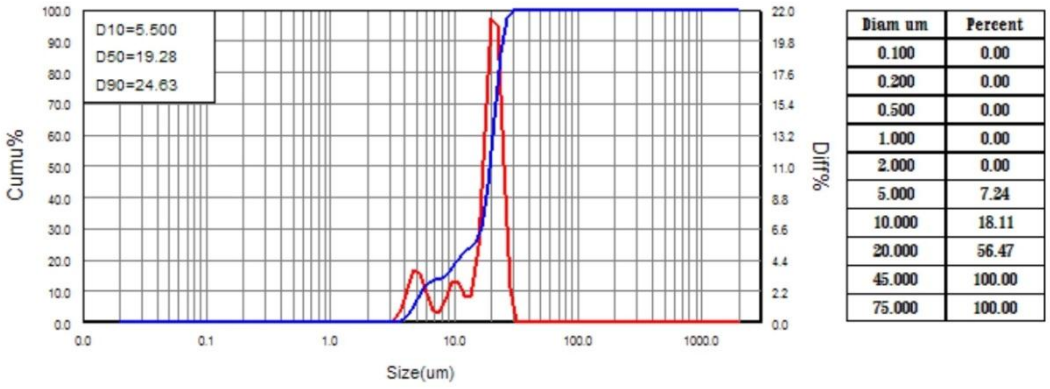

Diam um	Percent
0.100	0.00
0.200	0.00
0.500	0.00
1.000	0.00
2.000	0.00
5.000	7.24
10.000	18.11
20.000	56.47
45.000	100.00
75.000	100.00

Figure (3.5): analysis of particle size for boron carbide.

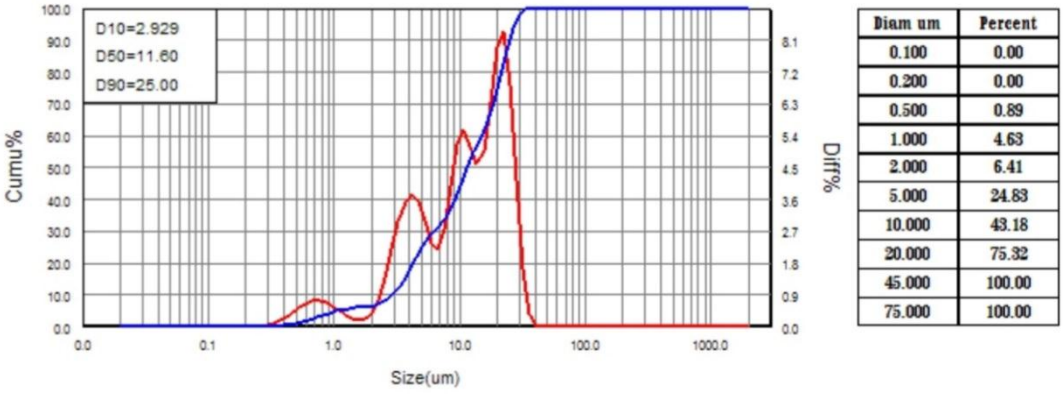

Diam um	Percent
0.100	0.00
0.200	0.00
0.500	0.89
1.000	4.63
2.000	6.41
5.000	24.83
10.000	43.18
20.000	75.32
45.000	100.00
75.000	100.00

Figure(3.6): analysis of particle size for silicon carbide.

3.4.3 X-Ray Diffraction (XRD)

The powders of SiC and B4C tested by XRD to ascertain the phases of the particles and whether they contain impurities. The analysis had been done at Ceramic Engineering Department / College of Materials Engineering - University of Babylon). Figure (3.7) shows XRD device.

Figure (3.7): X-Ray Machine used

3.5 Preparation of Composite Specimens by Stir Casting

All of the composite specimen were prepared using an aluminum 7075 T6 bar. The aluminum bar was melted in a ceramic crucible after cutting into small pieces to assist in melting and kept at 750°C in the furnace. Each piece of aluminum alloy, magnesium, (boron and/or silicon carbide) was weighted to the necessary amount (weight percentage wt), Mg reduced the aluminum melt's surface tension while as well increasing the wettability between the aluminum and reinforcing particles in the molten state. The weighted particles were preheated at (300ºC) for two hours (this agreed with [53]), to eliminate the content of moisture and increase wettability between Al7075 matrix and particles. A small pieces of Al7075 were loaded into a SiC crucible, then the furnace temperature was elevated to a liquid temperature (750)ºC, and slags were removed from the melt. To achieve the semi-solid condition, the temperature of melt after that was reduced to slightly below the liquid temperature (630ºC) to improve the wettability and Mixability of reinforcing particles in molten which is done in the presence of (1 percent wt) of magnesium ribbons, this agreed with [69]. The preheated boron carbide and/or silicon carbide particles, were gradually added to

the base alloy's molten, mechanical mild steel stirrer with a four-blade was used to stir the molten alloy slurry at a constant speed of 670rpm, this agreed with [70] [21]. To prevent gases from accessing the molten metal, the operation was carried out under an argon gas shield. Using a thermocouple, the temperature was measured to be (620-630)^{o} C while stirring. The temperature was then raised above the liquid's temperature once more, the molten was stirring continuously at the same speed and for a total time of 10 minutes, this agreed with[70]. Then , the molten was poured into steel molds that had been preheated at (300^{o}C). It is subsequently homogenized at 450°C for 8 hours. Figure 3.8 show stir casting process.

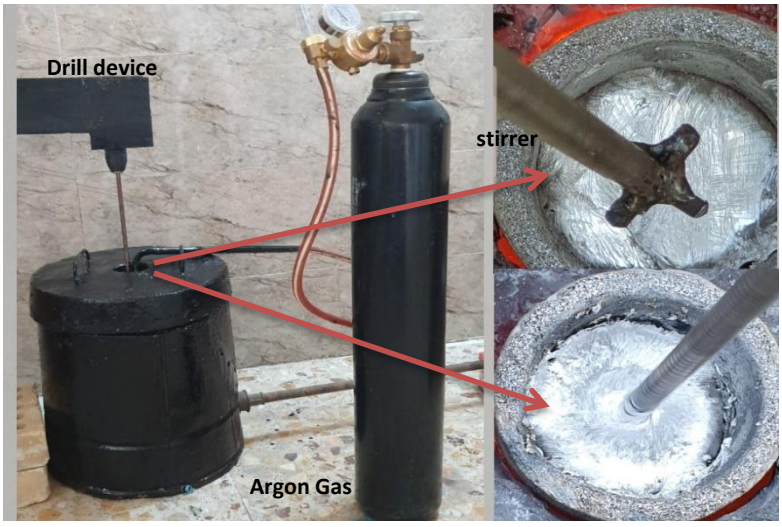

Figure (3.8) stir casting setup.

3.6 Tests after Preparation of specimens:

3.6.1 Vickers Hardness Test

The test was carried out according to ASTM E92-82 [21]. Each specimen was properly grinded and polished. The test was performed using a Vickers hardness testing machine with a load of (100 Kg) for (10 seconds). Five hardness values were measured for each specimen and their average was taken.

3.6.2 Tensile Test

The specimens with the dimensions presented in Figure (3.9) were manufactured following ASTM E08-8. This test was done through a universal testing machine that is controlled by a computer type (WDW). The tensile speed rate was (0.5)mm/min . The figure (3.10) shows the specimens before and after testing.

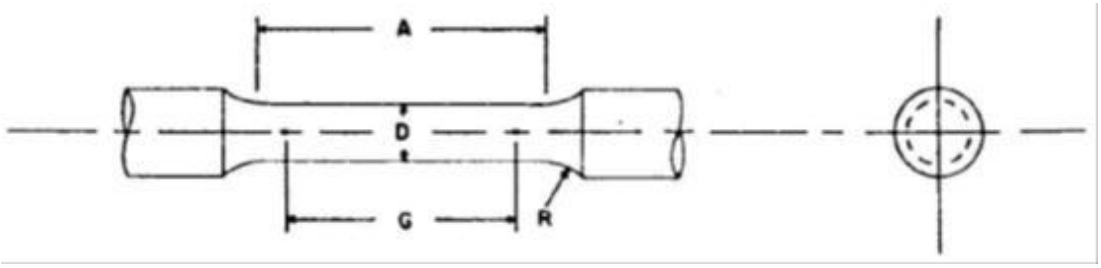

Figure (3.9): Standard Tensile Test Specimen. Gage length (G): (25.0 + 0.10) mm; the diameter (D): (6.25 + 0.12) mm; Radius of fillet (R) : 5mm; reduced section Length (A):32 mm

Figure (3.10): specimen before and after testing.

3.6.3 Compression Test

The compression test was carried out using dimensions according to ASTM (E9-09) at room temperature. The test was done via a computer control electronic testing machine (WDW). The dimensions of the specimens are (10mm in diameter and15 mm in height). Universal testing equipment was used with compression speed rate (0.1) mm/min. Figure (3.11) shows the specimen before

and after the testing.

Figure (3.11): specimen before and after testing

3.6.4 The Bending Test

The bending test was investigated for Al 7075 matrix composites using the three-point method. This flexural test was carried out using the universal testing equipment, to determine the flexural strength of the composites and base alloy according to ASTM A: 370[71]**,** this test was carried out to determine the flexural strength of the Al 7075 composite reinforced with 3, 6 and 9 wt. % of B4C and/or SiC, maximum bending load was evaluated. By using equations (3.1) to (3.5) the value flexural strength (MPa) will be obtained from the value of the load above as below:

$$\sigma = \frac{\boldsymbol{M} \times \boldsymbol{y}}{\boldsymbol{I}} \qquad \ldots\ldots\ldots\ldots\ldots\ldots\ldots\ldots (3.1)$$

Where σ is the stress of the flexural; M is the moment of bending; I is the moment of inertia, while y is the distance from the natural axis. The maximum flexural stress of the surface happens in the specimen's midpoint [48]. As shown in Figure(3.12).

$$M = \frac{P \times L}{4} \dots\dots\dots\dots\dots\dots\dots\dots\dots\dots\dots\dots\dots\dots (3.2)$$

$$y = \frac{t}{2} \dots\dots\dots\dots\dots\dots\dots\dots\dots\dots\dots\dots\dots\dots (3.3)$$

$$I = \frac{b \times t^3}{12} \dots\dots\dots\dots\dots\dots\dots\dots\dots\dots\dots\dots\dots\dots (3.4)$$

$$\sigma_{max.} = \frac{(3 \times P \times L)}{(2 \times b \times t^2)} \dots\dots\dots\dots\dots\dots\dots\dots\dots\dots (3.5)$$

Where P is the applied force by the test machine, b is the specimen breath, t is the specimen thickness, and L is the span length [48].

Figure (3.12): The testing specimen.

3.6.5 Scanning Electron Microscope (SEM) Analysis

The images of SEM were made of optimally prepared specimens in order to clearly and precisely examine the microstructure. The specimens were ground and polished using a suitable grinding sheet. This test was carried out at the High-Resolution Scanning Electron Microscope Laboratory Laboratory/ Baghdad, using Field Emission Scanning Electron Microscope(FE-SEM) device model (INSPECT F50) shown in Figure (3.13).

Figure. (3.13) FE-SEM device.

3.6.6 Optical Microscope

In order to effectively study the microstructure, optical microscope images were obtained for optimally prepared specimen. The specimen were ground using the proper grinding sheets, polished, and etched. with Keller's solution. This test was carried out at the Laboratory of Metallurgical Engineering Department / College of Materials Engineering - University of Babylon

3.7 Machining Tests

Electro-discharge machining was used in this work. The test was conducted to study the effect of machining variables on the required output of the machining operation for specimens of hybrid Al7075% (4.5% B_4C+4.5% SiC). Optimum machining conditions will be determined. The machining tests were focused to measure the output parameters: (MRR), (EWR), and (Ra) of the machined specimens for a wide range of machining conditions. The variable parameters used in this work were: discharge current (I_p); Pulse duration (T_{on}), Pulse interval (T_{off}), and voltage (V).

3.7.1 Machining Device

In this study, all the machining experiments were done using electrical discharge machining, CNC sinking machine type (CHMER CH323C/50N) installed at the Workshop of Technology University - Baghdad. Figure(3.14).

Figure (3.14): EDM machine

3.7.2 Workpiece Material

The specimens that were prepared for machining test are 18 mm in diameter and 12 mm in height, which are set as negative polarity during the machining process. Figure 3.15 shows the used specimen.

Figure (3.15): Workpiece used in EDM

3.7.3 Tool Electrode

The machining operation was performed to make a blind hole in the workpiece's smooth surface. As an electrode tool, A rod with diameter of 10mm and a length of 30mm was chosen. The rod was manufactured of 99.9% pure copper and had a positive polarity, as shown in Figure (3.16).

Figure (3.16): Copper Electrode.

3.7.4 Measurement of (MRR) and (EWR)

After the end of the machining process, the workpiece was taken, dried, and cleaned of dirt, debris, and the remains of the dielectric fluid, to be weighed after that using a high-accuracy electronic balance (0.0001)g in the method of weight loss. Eighteen machining experiments were carried out by the EDM process with different parameters for each specimen made of al7075 (4.5% B4C and 4.5% SiC). For each experiment, the weight of the electrode and workpiece before and after experiments was measured in order to determine MRR and EWR. The machining time was 5 minutes for each experiment. The formula for MRR (g/min) and EWR (g/min) is stated according to Equations(3.6) and (3.7) [72]:

$$MRR(\ mm^3/min) = \frac{(w1 - W2)}{tm \times \rho 1} \qquad (3.6)$$

$$EWR(mm^3/min) = \frac{((wi - (Wf))}{tm \times \rho 2} \qquad (3.7)$$

Where (w1) **is** the workpiece Initial weight, (W2) is the workpiece Final weight, (wi) weight of electrode before machining, (Wf) weight of electrode after machining, ρ_1 is the density of specimens, ρ_2 is density of electrode, (t_m) is the time of machining. The density was calculated using the Archimedes principle in an experimental setting. The workpiece weighed was done in both air and water, and the values of density (ρ) were computed using the formula below. [73]:

$$\rho = \frac{weight\ in\ air}{weight\ in\ air - weight\ in\ water} \times \rho_{water} \qquad (2)$$

ρ_{water}= water density at room temperature.

ρ was 2.8007g/cm^3

3.7.5 Measurement of Surface Roughness

The surface roughness of freshly machined specimens was measured under various machining settings. The surface roughness tester type (TR210) was used for this test, as indicated in Figure (3.17). The probe scans the surface, comparing peaks and valleys to determine the (SR). After each test, the value of Ra in(µm) was recorded, and the specimen was shifted slightly so that the measurements are more representative of the specimen surface. An average of four measurements to each specimen were taken in this test. This test was carried out at the Laboratory of Metallurgical Engineering Department / College of Materials Engineering - University of Babylon

Figure (3.17): surface roughness tester.

Chapter Four

Results and Discussion

4.1 Introduction

In this chapter, all the results obtained from the mechanical, characterization, and machining tests that were conducted in this study are discussed. The results were discussed from different aspects, the effect of the type and percentage of the reinforcement particles on the mechanical properties, as well as the impact of the machining parameters on output machining parameters, to choose the chemical composition of the composite material with the better mechanical properties, and then choose the optimum machining conditions for this specimen. It was all done by applying a GRA uses two factors and three levels built on the Taguchi method

4.2 Results of Mechanical Properties

The mechanical tests were carried out for Al 7075reinforced by B4C and/ or SiC to find out the effect of the type and percentage of the reinforcement particles on the responses (VHN, YS, UTS, UCS, FS and elongation). Type of reinforcement materials, percentage of reinforcement materials and its levels are shown in Table (4.1).

Table (4.1): Significant variable and their levels.

Parameter	Designation	Unit	Coded/ Actual levels		
			1	2	3
Reinforcement material	RM	---	SiC	B_4C	SiC + B_4C
Reinforcement Percentage	RP	%	3	6	9

Taguchi orthogonal array L9 was selected to design the experiments under two variables and three levels as shown in Table (4.2).

Table 4.2: Matrix and assessed mechanical properties.

Exp. No.	RM	RP	VHN	YS MPa	UTS MPa	UCS MPa	FS MPa	e %
0	Base alloy	0%	115.00	182.96	233.51	248.51	290.42	3.34
1	SiC	3%	136.98	195.894	276.5	298.62	330	2.2448
2	SiC	6%	157.098	205.45	284.075	306.7875	362.56	1.5738
3	SiC	9%	152.49	212.18	287.875	310.905	368.72	1.2505
4	B4C	3%	150.861	202.162	285.35	308.1825	345.84	2.0008
5	B4C	6%	167.226	210.928	291.65	314.9775	380.16	1.4335
6	B4C	9%	160.509	219.624	297.975	321.8175	386.32	1.098
7	SiC+ B4C	3%	165.9	216.57	290.4	313.6275	362.56	2.0923
8	SiC+ B4C	6%	169.2	227.626	299	322.92	398.64	1.4762
9	SiC+ B4C	9%	178.2	239.99	309.325	334.0575	404.8	1.1407

4.2.1 Identifying the Influence Factors

Based on the following hypothesis in the terminology of statistical modeling that the effect of factors on output is based on 95 % confidence interval or 5 % significance level having almost P-values less or equal to 0.05 affecting the all responses (VHN, YS, UTS, UCS, FS and elongation) [74] The insignificant factors were removed from the models' structures using the backward elimination method[75]and the ANOVA was conducted for each reduced quadratic model generated including just these significant factors that contributed to model building as significant terms. as illustrated in Table 4.3. From the ANOVA, it can be conclude that all the input parameters either significant when ($0 < p\text{-value} < 0.05$) or it is more significant when ($p\text{-value} = 0$) surely, all these were done after removing the non- significant factors.

Table 4.3: ANOVA Table for the Trimmed (VHN, YS, UTS, UCS, FS and e %).

Source	DF	Adj SS	Adj MS	F-Value	P-Value
VHN					
Regression	4	1179.77	294.942	845.01	0.000
RM	1	254.37	254.374	728.78	0.000
RP	1	353.44	353.442	1012.61	0.000
RP*RP	1	265.33	265.329	760.16	0.000
RM*RP	1	37.27	37.271	106.78	0.000
Error	4	1.40	0.349		
Total	8	1181.17			
YS					
Regression	2	1376.88	688.44	55.71	0.000
RM	1	832.19	832.19	67.35	0.000
RP	1	544.70	544.70	44.08	0.001
Error	6	74.14	12.36		
Total	8	1451.03			
UTS					
Regression	2	728.36	364.178	111.06	0.000
RM	1	421.26	421.263	128.47	0.000
RP	1	307.09	307.093	93.65	0.000
Error	6	19.67	3.279		
Total	8	748.03			
UCS					
Regression	2	849.33	424.667	111.41	0.000
RM	1	491.28	491.279	128.89	0.000
RP	1	358.05	358.054	93.94	0.000
Error	6	22.87	3.812		
Total	8	872.20			
FS					
Regression	3	4682.15	1560.72	1727.48	0.000
RM	1	1827.71	1827.71	2023.00	0.000
RP	1	717.73	717.73	794.41	0.000
RP*RP	1	396.49	396.49	438.86	0.000
Error	5	4.52	0.90		
Total	8	4686.67			
e %					
Regression	4	1.44350	0.360875	447.62	0.000
RM	1	0.03515	0.035151	43.60	0.003
RP	1	0.13453	0.134533	166.87	0.000
RM*RM	1	0.02830	0.028298	35.10	0.004
RP*RP	1	0.04110	0.041098	50.98	0.002
Error	4	0.00322	0.000806		
Total	8	1.44672			

4.2.2 Vickers Hardness Number

The Vickers's hardness of the matrix alloy and Al7075 (SiC and/or B_4C) composites given in Figure. (4.1). It is clear from this figure that the hardness value improve with increase reinforcement particles content reaches maximum value at 6 wt. % reinforcement then decreases with increasing the addition percentage of the reinforcement, this could be caused by the agglomeration of the reinforcement particles after this percentage, this leads to a decrease in hardness. The Vicker's hardness of the composites has increased due to very hard reinforcement particles, acceptable uniform reinforcements distribution in the matrix, and increased density of dislocations due to hardness of $B_4C$and SiC particles itself which acting as barriers to dislocations motion, this agreed with [76]. Brittle ceramic particles embedded in a soft and ductile aluminium matrix can also effectively enhance hardness values owing to a mismatch in the coefficients of thermal expansion of the ceramic reinforcing particles and the matrix, this agreed with [77].

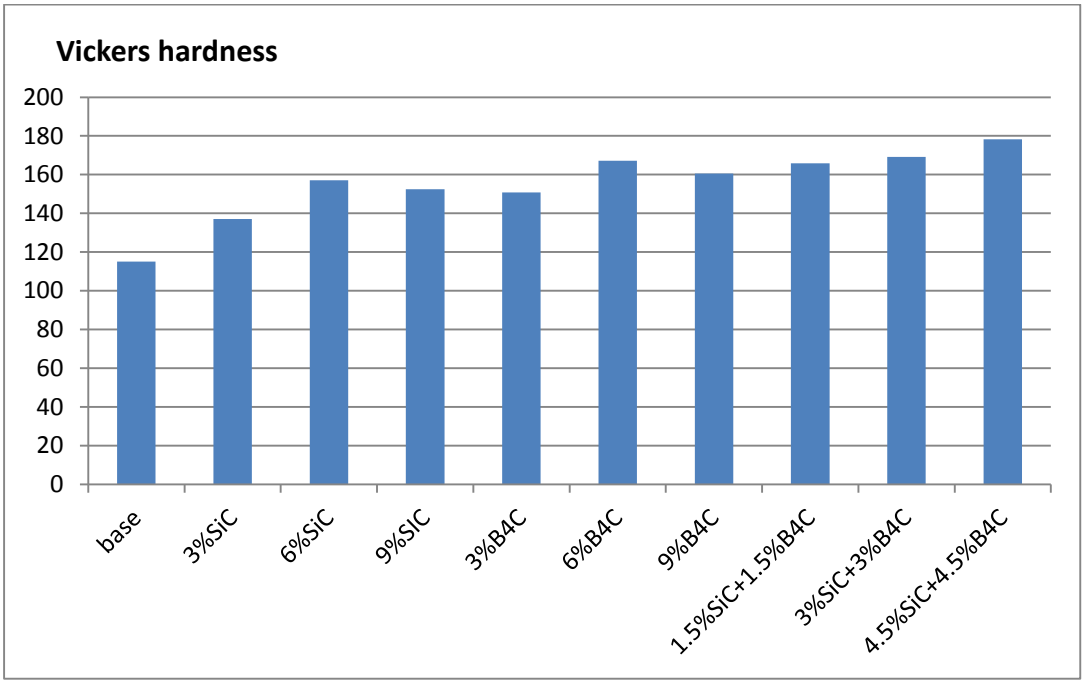

Figure(4.1) Variation of vickers hardness of al7075 composites with varying content of SiC and B_4C.

Because of the hardness of B4C is higher than of SiC, the Vickers hardness improves with the addition type of reinforcing materials when compared to unreinforced Al7075. Therefore, according to the figure(4.2) and based on what was mentioned above it can be concluded that all type and contents of reinforcements are very impacting parameters it might be due to a mismatch in the coefficient of thermal expansion (CTE) between the base alloy and the reinforcement, as well as between boron carbide and silicon carbide.

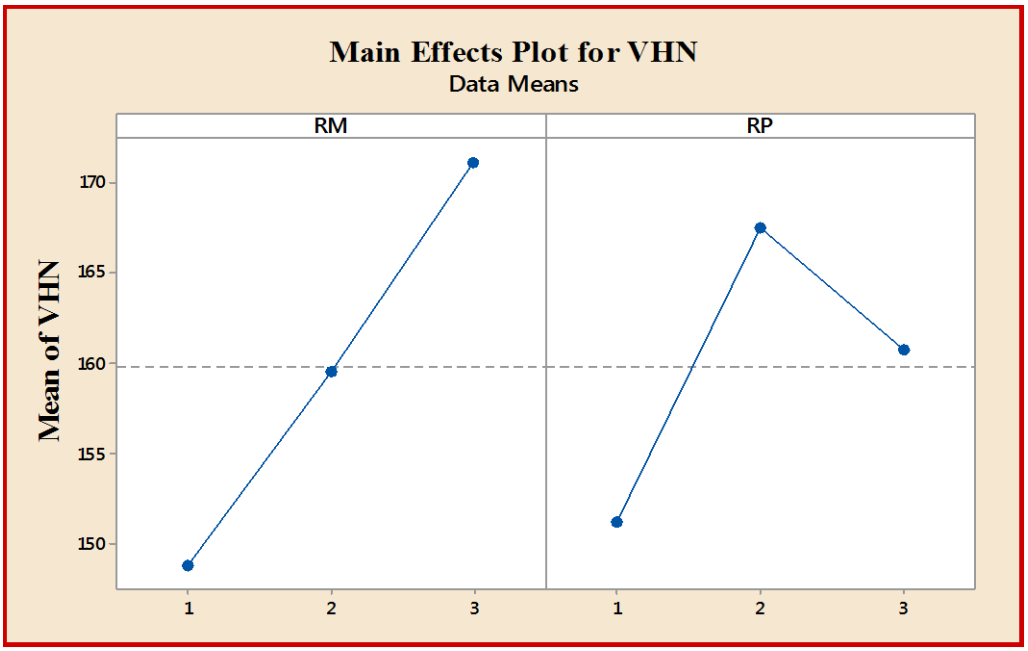

Figure 4.2: Effect of factors on VHN.

4.2.3 Yield Strength

The yield strength values are shown in Figure (4.3), which indicates the improvement in yield strength as the weight fraction of SiC and/or B4C particles increases. Based on experimental data the yield strength of Al7075 matrix alloy improves from 182.96 MPa to 239.99 MPa when reinforced with (4.5 % SiC+4.5 % B4C) as shown in figure (4.3). The composite's maximum tensile strength was improved by 31.1 percent when compared to baes alloy. In addition to the reasons that will be discussed, this increase in yield strength is because of the presence of reinforcing particles in aluminum7075 matrix, which increases resistance to crack

initiation, resulting in increased tensile strength.

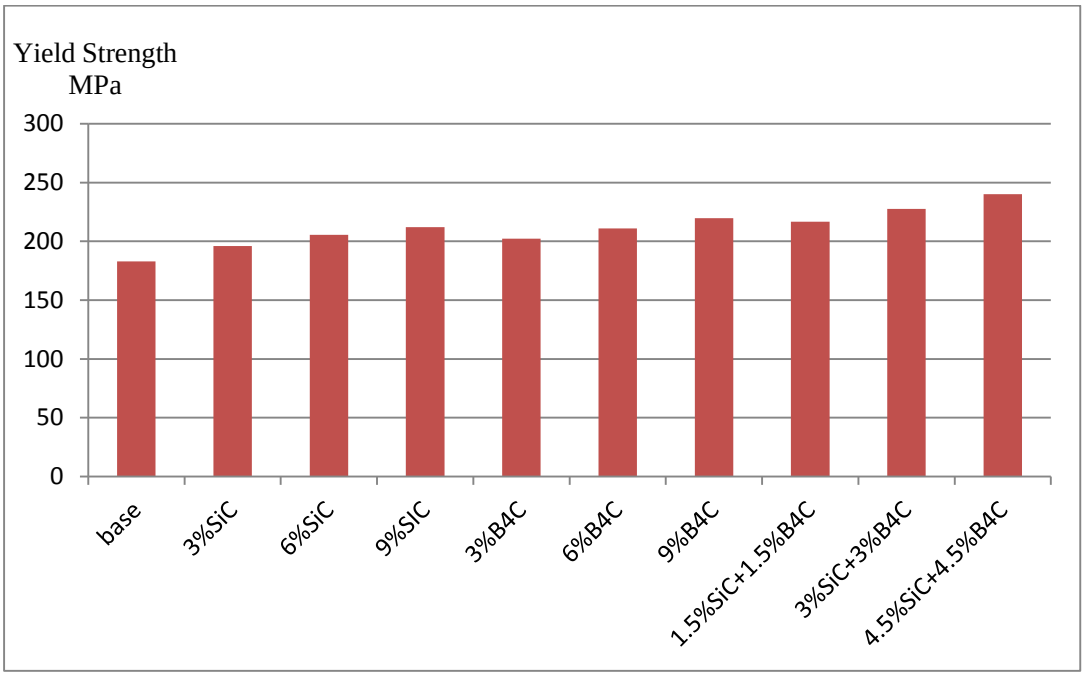

Figure (4.3) Variation of yield strength of al7075 composites with varying content of SiC and B_4C.

As shown in Figure (4.4), the yield strength of composites improves as the particle type varies and amount of reinforcing material increases. The tensile strength of these composites is enhanced by the addition of Boron carbide and/or Silicon carbide particles. The presence of reinforcing particles in the Al7075 composite, which act as a barrier to dislocation motion, results in a yield strength increase. Furthermore, the addition of magnesium in the aluminum matrix improved the interfacial bonding between the matrix and the reinforcement, allowing the load to be transferred more effectively from the matrix alloy to the reinforcement content. As a result of the strong bonding, the yield strength has improved, this agreed with [78].

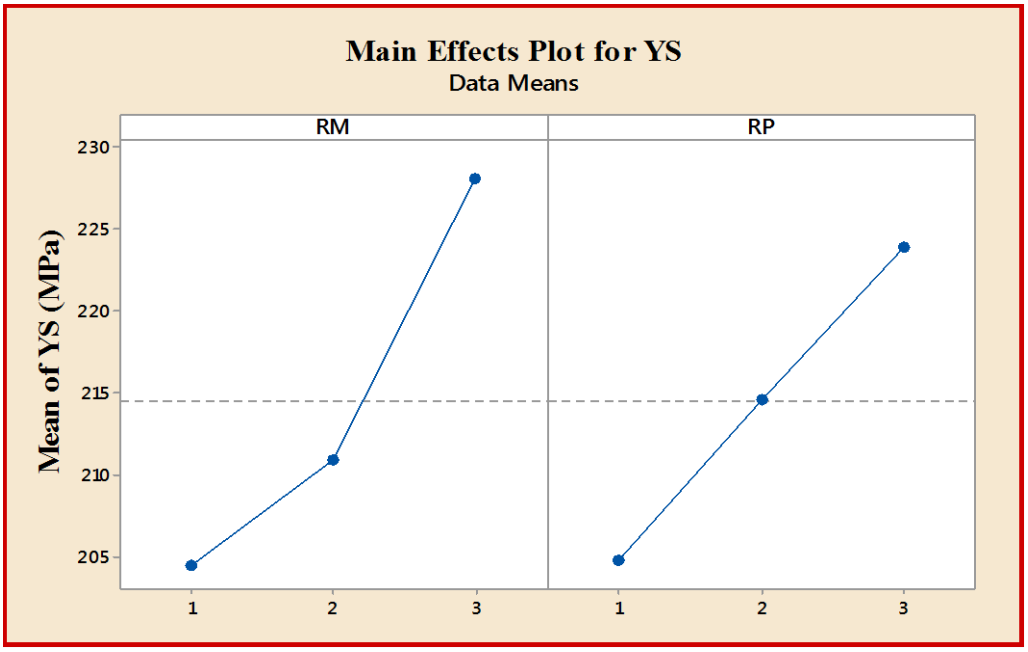

Figure 4.4: Effect of factors on YS.

4.2.4 Ultimate Tensile Strength

The ultimate tensile strength of the composite specimens and of the base alloy are shown in Figure (4.5). The UTS is usually determined by performing a tensile test and analyzing the stress versus strain curve.

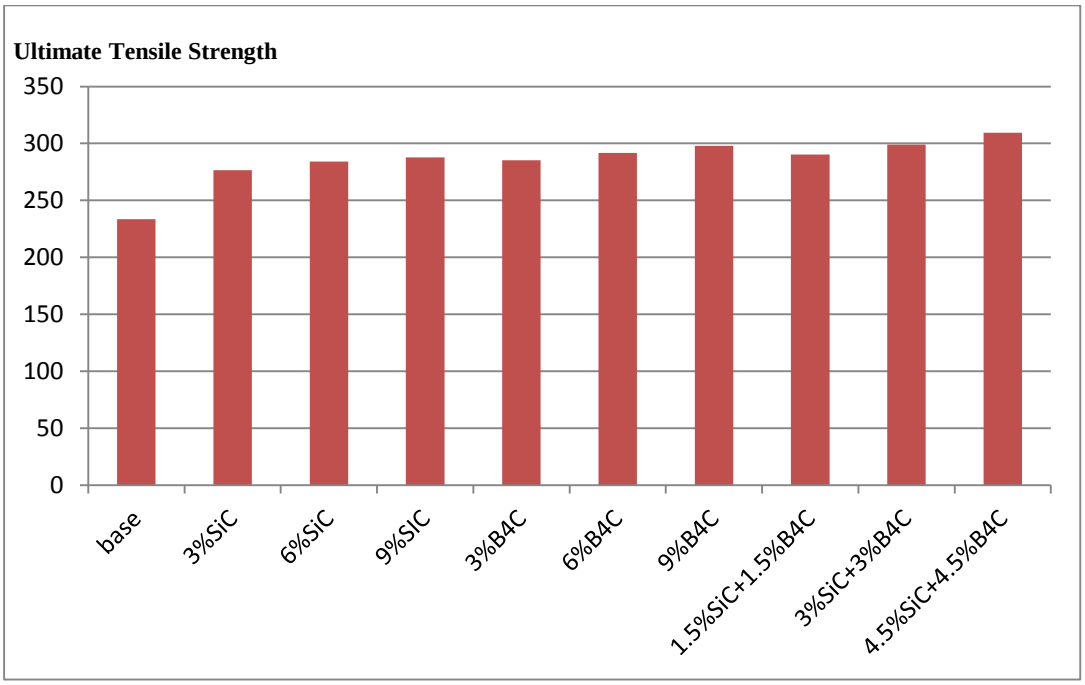

Figure (4.5)Variation of Ultimate Tensile Strength with varying content of SiC and B_4C.

In terms of reinforcement materials type and its percentage, the UTS behavior of composites is close to the yield strength for the same reason as shown in Figure (4.6). The ultimate tensile strength has been shown to improve as the SiC and/or B4C particle volume fraction increases and is much more than the strength of the parent alloy, (from 233.51 Mpa for base alloy to 309.325Mpa for (4.5%SiC+4.5% B4C composite) with improvement of 32.4%. The increased strength seen with the presence of the (B4C+ SiC) particles might be attributed to the creation of greater strength in matrix, allowing it to resist tensile stresses effectively. This is due to the fact that increase load transfer from matrix to reinforcement increases composite tensile strength, this agreed with [76]

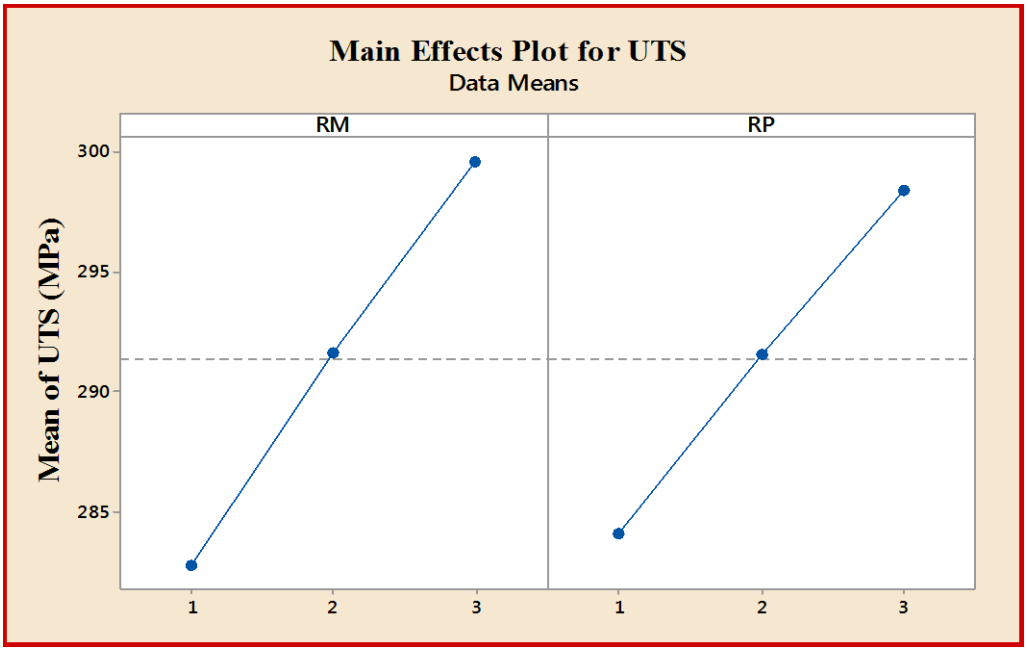

Figure (4.6): Effect of factors on UTS.

The increase in ultimate tensile strength is mostly due to (B4C+ SiC) particles working as a dislocation barrier, similar to what was discussed before in yield strength. The matrix strengthening is responsible for the increased strength. The mismatch in thermal expansion between the three components of composite (B4C, SiC and matrix) causes significant dislocation density to form in the Al 7075 matrix that leads to more increasing in (UTS).

4.2.5 Ultimate Compressive Strength

The ultimate compressive strength (UCS) of the composite specimens and of the base alloy are shown in Figure (4.7). The ultimate compressive strength have been observed to increase with increasing the content of SiC and/or B_4C, reaches a maximum value of (334.05) MPa at (4.5%SiC+4.5% B_4C) and are considerably higher than (UCS) of matrix alloy (248.51) MPa with an improvement of 34.42% compared to the matrix alloy.

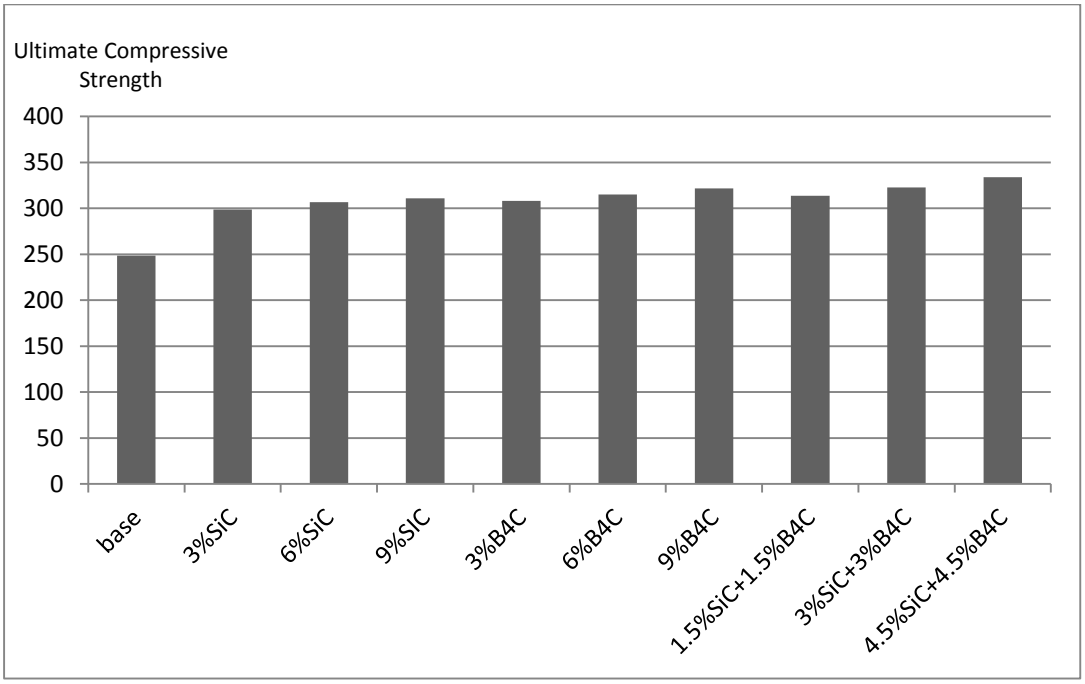

Figure (4.7): Variation of Ultimate Compressive Strength with varying content of SiC and B_4C

Figure (4.8) shows the behavior of the composites' (UCS) in term of type and content of reinforcements. Because of the high compressive strength of hard B4C particles (more than silicon carbide) present in the matrix, the (UCS) of composite improves with the addition of type of reinforcing materials. Furthermore, (UCS) increases when the weight % of reinforcing particles in the Al7075 composite increases, as reinforcement particles work as a barrier to dislocation motion, resulting in an additional increase in (UCS). Moreover, the

presence of magnesium improves the interface, allowing for more effective load transfer from the base phase to the reinforcement, which raises the (UCS).

Also The compression strength of hybrid composites has been seen to improve as the amount of dual particles (hybrid) increases, and it is much greater than the basic alloy compressive strength. It might be due to a mismatch in the thermal coefficient of expansion (CTE) between the three components of composite (B4C, SiC and matrix), this agreed with [79].

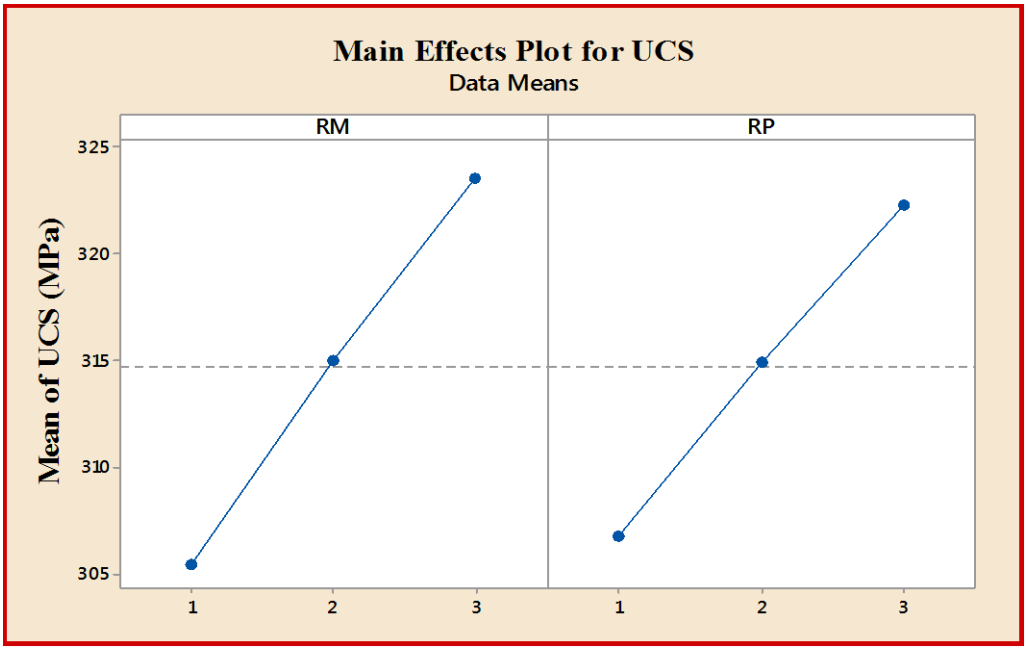

Figure 4.8: Effect of factors on UCS.

4.2.6 Flexural Strength

Flexural strength is the 3-point bending method to study the behavior and ability of the material under bending load. The load was gradually applied from the top roller Until failure. From the figure (4.9) which is show Flexural strength changes as the content of SiC and B4C increases. It was observed that the addition of B4C and/or SiC particles to the matrix enhanced flexural strength reaches a maximum value of (404.8)MPa at (4.5%SiC+4.5% B_4C) which is higher than flexural strength of base alloy (290.42) MPa with an improvement of 39.4% as compared to the base matrix alloy.

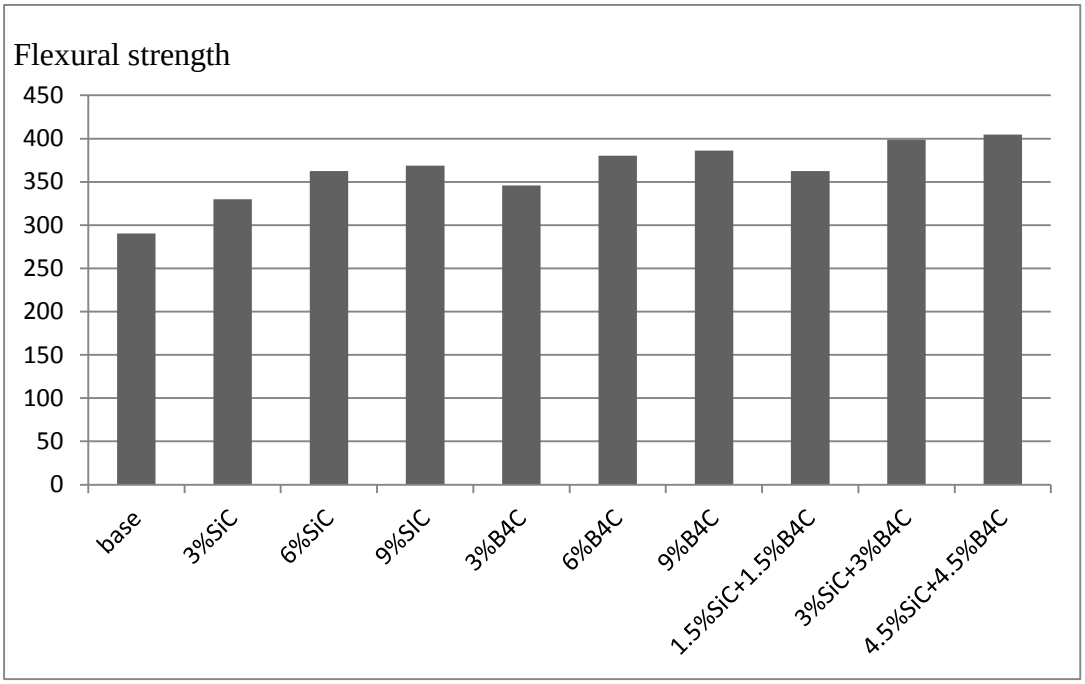

Figure (4.9): Variation of Flexural strength with varying content of SiC and B4C

As mentioned earlier in the discussion of UTS and YS, UCS, good bonding between the reinforcement particles and the matrix alloy increases the flexural strength of the composites, which is greater than that of the base alloy. Flexural strength increases as the percentage of reinforcing particles increases. This indicates that the composites have enough ductility to attain greater strength at (4.5 % SiC+4.5 % B4C), resulting in an increase in flexural strength to (404.8) MPa. The reinforcing particles prevent cracks from quickly expanding through the composite and restrict deformation, which enhances the flexural strength of the composites this agreed with [76]. From figure (4.10) In terms of reinforcing material type and reinforcing percentage, the flexural strength behaviour of MMCs is close to that of UTS and yield strength. for that reasons which mentioned in these Paragraphs.

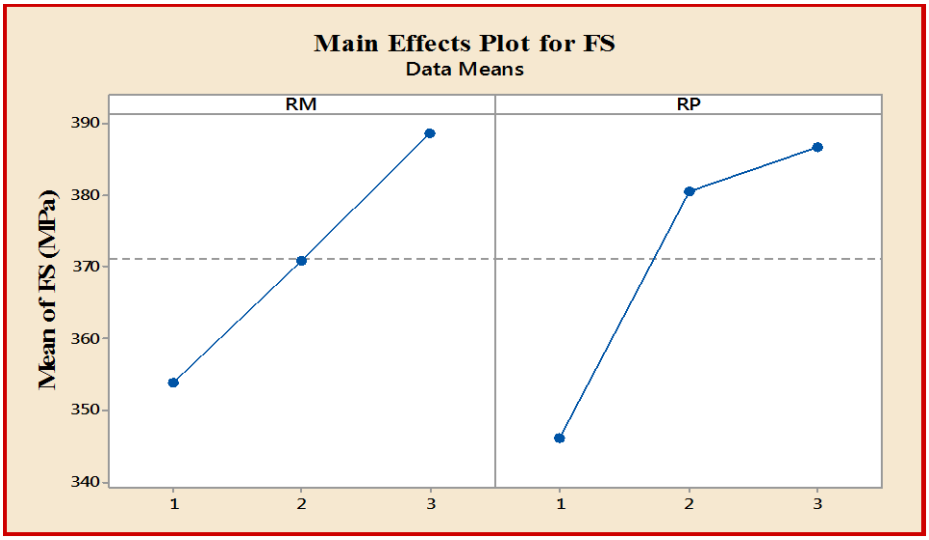

Figure 4.10: Effect of factors on FS.

4.2.7 Elongation

The elongation was determined from tensile test. From figure (4.11) It is apparent that as the percentage of reinforcement materials incorporated in the matrix alloy increased, the elongation percentage reduced. This is due to an increase in brittleness as the percent of reinforcing materials increased, improved hardness as reinforcing materials are added, as previously indicated, by impeding the movement of the dislocations, which leads to reduces the elongation.

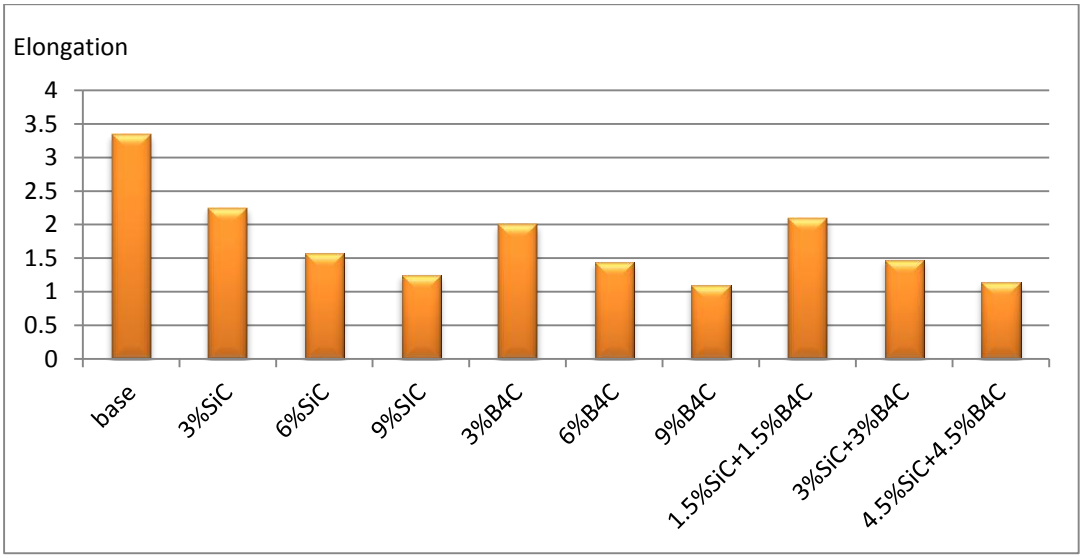

Figure (4.11): Variation of with elongation with varying content of SiC and B_4C

Regarding the percentage of reinforcement. The elongation of the MMC behaves in a completely opposite manner to the yield strength and UTS, in terms of the

content of reinforcing materials, as well as in terms of the type of reinforcement materials but at (4.5% SiC + 4.5% B4C) it improves slightly as shown in Figure (4.12).

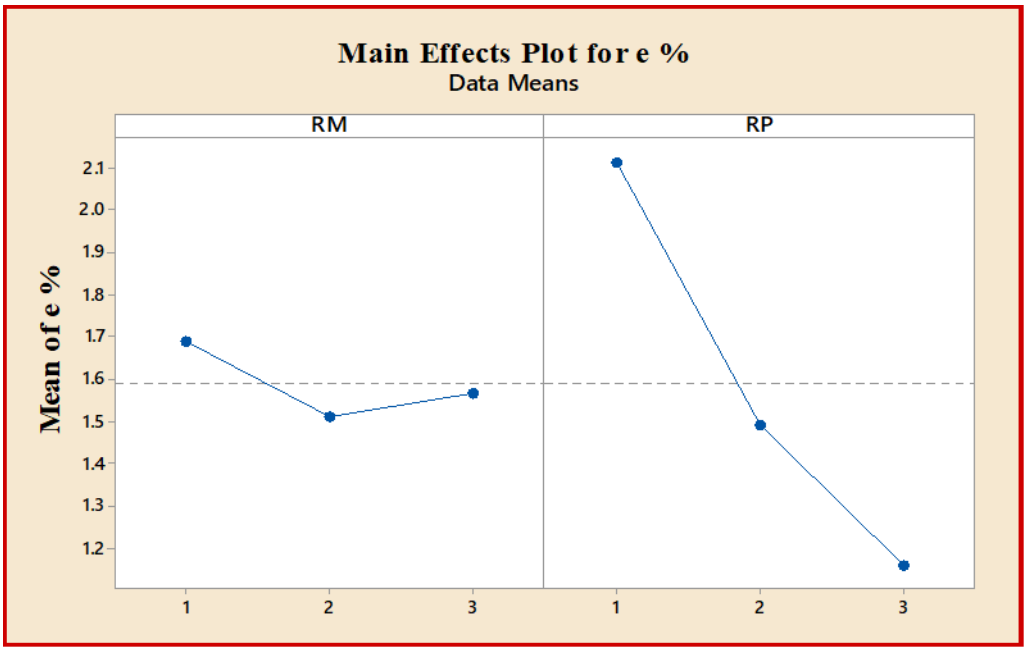

Figure 4.12: Effect of factors on elongation.

4.2.8 Improving of Model Fitting Capabilities of Mechanical Properties

The insignificant coefficients of some terms of the quadratic equation (4.1 to 4.6) have been omitted.

$$FS = 4.4 + 17.453\ RM + 132.88\ RP - 14.080\ RP \times RP \quad (4.1)$$

$$UCS = 247.56 + 9.049\ RM + 7.725\ RP \quad (4.2)$$

$$UTS = 229.22 + 8.379\ RM + 7.154\ RP \quad (4.3)$$

$$YS = 129.27 + 11.78\ RM + 9.53\ RP \quad (4.4)$$

$$VHN = -129.08 + 23.33\ RM + 109.10\ RP - 11.518\ RP^2 - 3.053\ RM \times RP \quad (4.5)$$

$$e\ \% = 7.751 - 1.012\ RM - 1.622\ RP + 0.1189\ RM^2 + 0.1433\ RP \times RP \quad (4.6)$$

4.2.9 Checking the adequacy of Mechanical Properties's Model

Another criteria for determining the model's sufficiency is the coefficient of determination (R^2). For VHN, YS, UTS, UCS, FS, and e percent, the measured R^2 values are above 99.88, percent 94.89, 97.37, 97.38, 99.90, and 99.78 percent, respectively. These numbers show that the regression models are adequate. Drawing scatter plots is used to assess the validity of the regression models that have been built. Figure(4.13) shows typical scatter plots for all of the models. The predicted and experimental response values suggest a near-perfect fitting of the empirical models developed.

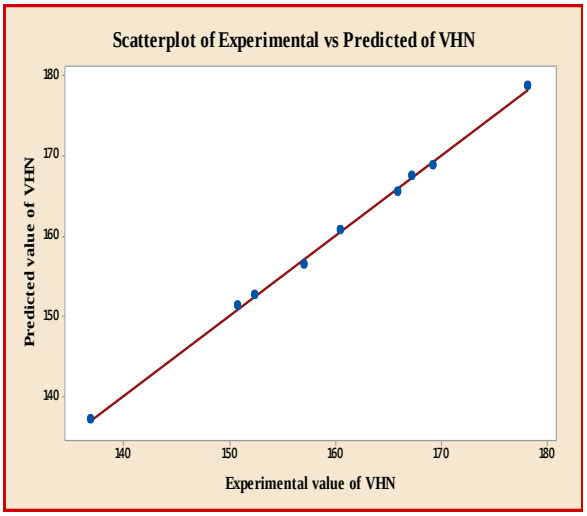

A

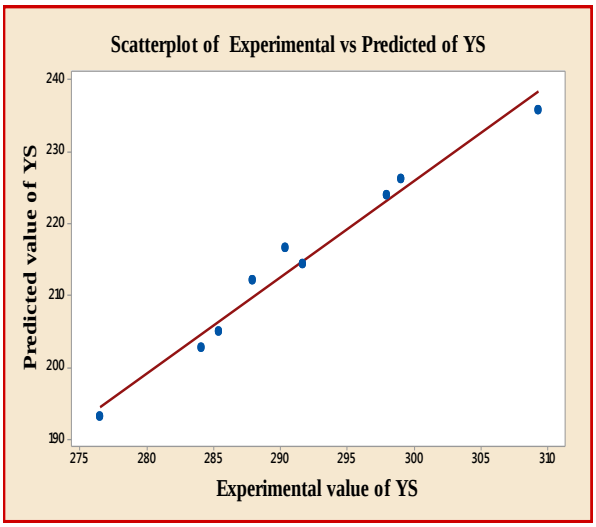

B

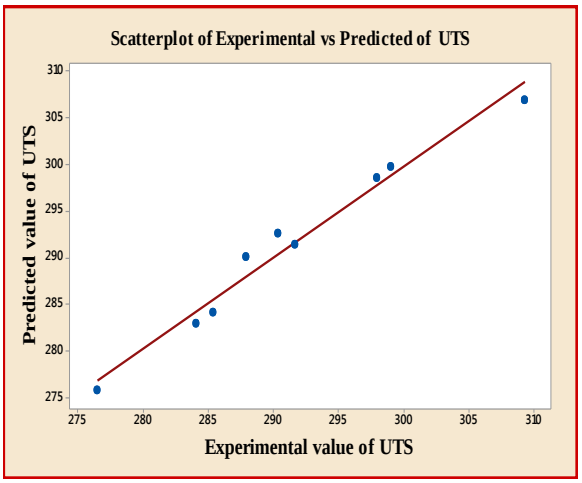

C

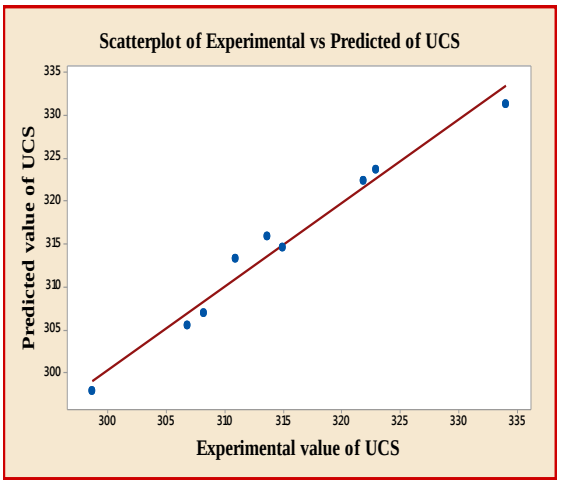

D

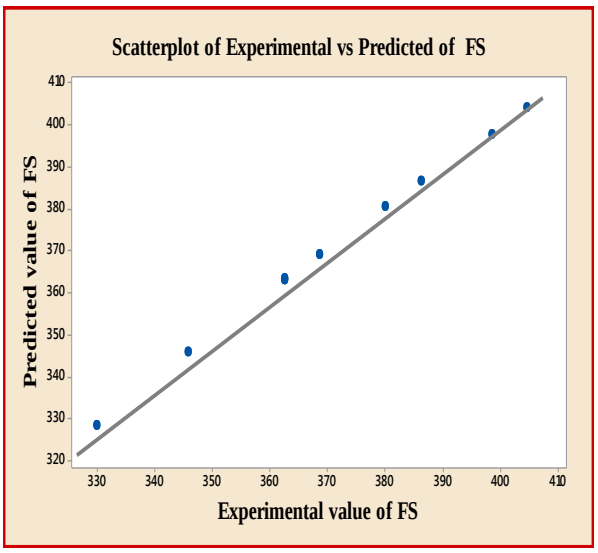

E

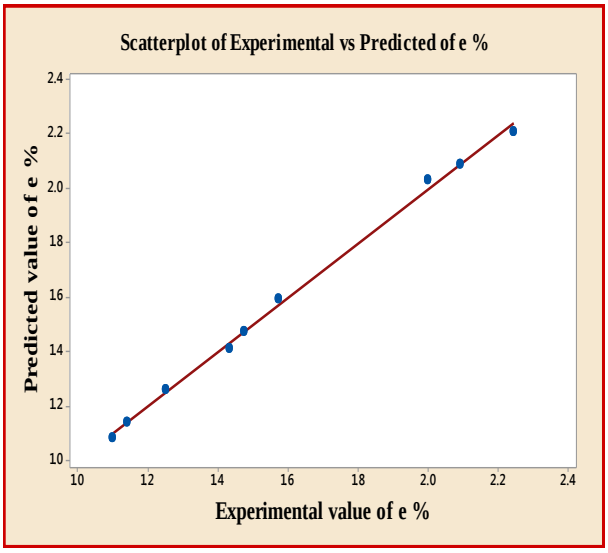

F

Figure 4.13: Scatter plot for: A(VHN), B(YS), C(UTS), D(UCS), E(FS) and F (e %).

4.2.10 Optimization by Grey Relational Analysis Method of Mechanical Properties

Table 4.2 indicates the experimental layout, it provides a total 9 experimental runs. From the results of these three replications, the mean values of VHN, YS, UTS, UCS, FS, and e percent are listed in column 4, 5, 6, 7, 8 and 9 of Table 4.2, respectively. Since it is difficult to identify the optimum process parameters for achieving larger VHN, YS, UTS, UCS, FS, and e percent, thus, the next step is by normalizing the experimental results using GRA. As the VHN, YS, UTS, UCS, FS, and e percent respectively, have been characterized as larger-is-better to improve the quality of the mechanical properties, equation (2.1) was used to normalize the experimental data produced.

The column two, three, four, five, six and seven of Table (4.4) lists the processed experimental data after grey relational generation (i.e. normalization).

The normalised values vary from one to zero, as can be seen. Following normalising, all sequences are labelled $X_0^*(k)$ to the reference sequence and $X_j^*(k)$ for comparability sequence.

The better normalizd result must be equal to one and greater normalizd results mean to better behavior. Next, the absolute value of deviation sequence of Δ_i (k) is governed using equation (2.4). In this work, the VHN, YS, UTS, UCS, FS, and e percent, are influence equally by all the process parameters. To calculate the GRC as given in column eight, nine, ten, eleven, twelve and thirteen of Table (4.4), the distinguishing coefficient ξ= 0.5 was replaced in equation (2.3) by considering all process parameters have equal weightage.

Then, equation (2.5) was used to determine the GRG. The experiments order according to GRG values are listed in column fourteen of Table (4.4). The higher GRG value, 0.793524, shows that the experimental results is getting closer to e ideally normalized experimental results. It's worth mentioning that experiment 9 has the greatest GRG and hence may be considered the best multi-performance mechanical properties experimental sequence. In addition, Figure 4.14 displays GRG from Table 4.2 for all nine experiments conducted using the L9 orthogonal array. Figure (4.16) shows the variations in a response as factors progress from one level to the next, and it is apparent that experiment 9 has the greatest GRG value. As a result, it's clear that each of the nine runs has the optimum combination of process parameter settings for the best multi-performance features.

Table (4.4): The sequences of each performance characteristic after data processing.

Exp. No.	Normalized						GRC						GRG	Rank
	VHN	YS	UTS	UCS	FS	e %	VHN	YS	UTS	UCS	FS	e %		
1	0.201098	0.372158	0.383875	0	0.360406	0.97561	0.384941	0.443325	0.447978	0.333333	0.57241	0.953489	0.522579	6
2	0.375631	0.587916	0.564486	0.610311	0.491117	0.731707	0.444694	0.548195	0.534466	0.561994	0.62722	0.650793	0.561227	5
3	1	0.807113	0.729528	0.776167	0.57868	0.089431	1	0.721618	0.648953	0.690767	0.670209	0.354467	0.681002	3
4	0	0	0	0.891634	0	0.642276	0.333333	0.333333	0.333333	0.821874	0.46127	0.582938	0.477680	8
5	0.085337	0.243522	0.47842	0.350584	0.379442	0.235772	0.353441	0.397938	0.489438	0.435004	0.579789	0.395498	0.441851	9
6	0.133868	0.441962	0.553727	0.692218	0.408756	0.219512	0.365997	0.472573	0.528389	0.618979	0.591531	0.390476	0.494658	7
7	0.239537	0.725806	0.669409	0.728113	0.463198	1	0.39668	0.645833	0.601981	0.647763	0.614649	1	0.651151	4
8	0.289552	0.830645	0.853816	0.886187	0.643782	0.902439	0.41307	0.746988	0.773773	0.81458	0.706196	0.836735	0.715224	2
9	0.331256	1	1	1	1	0	0.42781	1	1	1	1	0.333333	0.793524	1

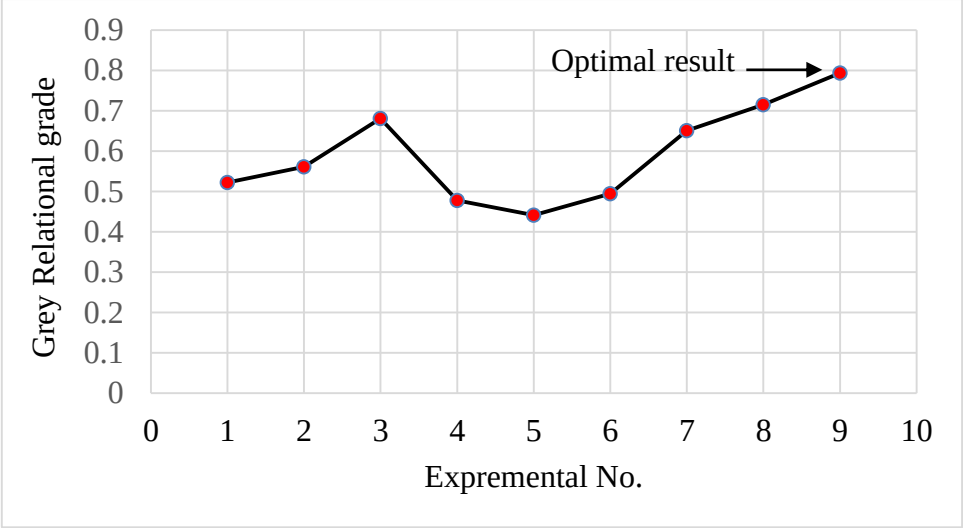

Figure 4.14. Grey relational grade for multi-response.

The multiple responses of performance characteristics of mechanical properties can be evaluated using a response table using GRG as shown in Table (4.5). Because the orthogonal experiments design, as seen in the same table,the influence of each the GRG input parameter can be separated at various levels. It confirms that the RM is more influence compared to RP parameter on the mechanical properties as illustrated in the first rank (Table 4.5) from this table and Figure 4.15, it is also confirmed that the RM (SiC + B_4C) and RP (9 %) characterize the highest value of GRG. Hence, the combination of level 3 of RM and level 3 of RP is the optimal combination of process parameter in mechanical properties to obtain largest VHN, YS, UTS, UCS, FS and e %.

Table 4.5: Response table for the GRG.

Parameters	GRG			Main effect (max-min)	Rank
	Level 1	Level 2	Level 3		
RM	0.58826933	0.47139633	0.719966*	0.248570	1
RP	0.55047	0.57276733	0.656395*	0.105925	2
Total mean value of GRG γ_m= 0.59321067 GRG optimum * Levels					

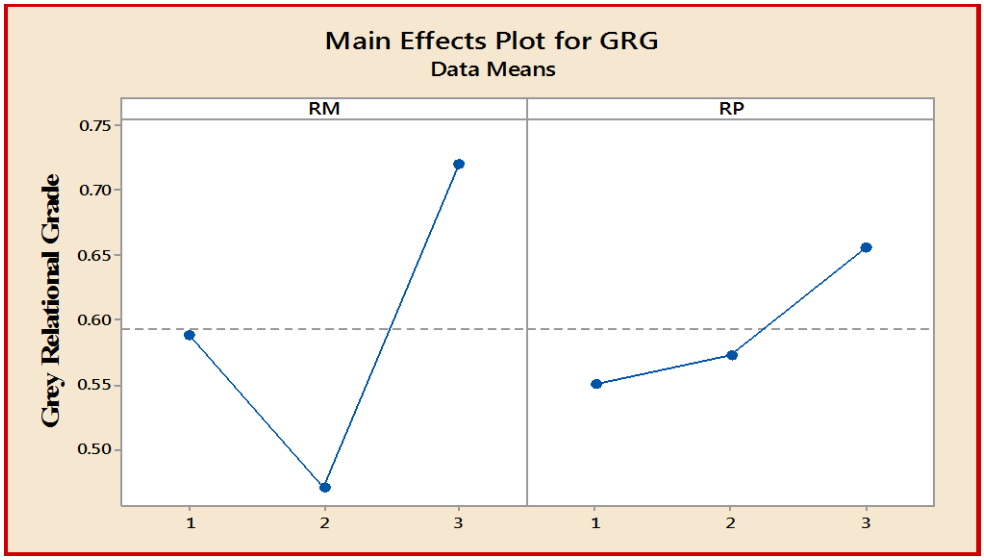

Figure 4.15: Main Effect of factors on GRG.

After the optimum parameters is attained, the optimal combination of process Parameters must be predicted, and a confirmation test must be performed to ensure that quality characteristics have improved. Equation(4.7) can be used to compute the estimation or prediction GRG $(\widehat{\gamma})$ at the optimal level of a process parameter[80].

$$\hat{\gamma} = \gamma_m + \sum_{i=1}^{q} (\gamma_i - \gamma_m) \dots\dots\dots\dots\dots\dots\dots\dots\dots\dots\dots\dots\dots\dots (4.7)$$

Where γ_m is the total mean of GRG, γ_i is the mean of the GRG at the optimum level and q is the number of the process parameter that the performance characteristics.

The results of confirmation test are shown in Table (4.6) and it can be verified that the value of value of mechanial properties have have been improved as fowlloing; VHN 161.91 to 178.2, UTS from 296.312 MPa to 309.325 MPa, UCS from 315.78 MPa to 334.0575 MPa, YS from 224.26 MPa to 239.99 MPa, FS increased from 390.11 MPa to 404.8 MPa, and e %1.032 to 1.1407 %.

Furthermore, it also shows that the optimization method enhanced the GRG value in the confirmation experiment from 0.733024 to 0.78315033 when compared to the predicted value. The outputs of the confirmation test indicate that the results of optimising the process parameters of mechanical properties utilizing GRA for multi-performance characteristics are acceptable.

Table 4.6: Improvements in grey relational grade with optimized parameters.

Condition description	Optimum mechanical properties	
	Predicted experiment	Confirmation experiment
VHN	161.91	178.2
YS (MPa)	224.26	239.99
UTS (MPa)	296.312	309.325
UCS (MPa)	315.78	334.0575
FS (MPa)	390.11	404.8
e %	1.032	1.1407
GRG	0.793524	0.8436503
Improvement in GRG = 0.0501263 %		

4.2.11 Microstructure Analysis

Figures (4.16) shows the microstructures of Al7075 (4.5%B4C+4.5%SiC) composites. The microstructures reveal an uniform distribution of dual particles and good bonding between reinforcement particles and matrix (no gap between matrix and reinforcing partical). This explains why the mechanical properties have improved significantly. It should increase the composites' load-bearing capability. The presence of dual particle content in the Al matrix alloy can significantly change the microstructure and mechanical properties of the AMC.

It has been evidenced that using stir casting to prepare these composites resulted in an acceptable distribution of the reinforcing (B4C+SiC) particles in the matrix with minimal segregation. The proper selection of each stir casting parameter,

such as stirring speed, stirring time, stirrer blade design, stirring in two phases at different temperatures, and the use of argon gas, was essential in improving the distribution of reinforcing particles in the base alloy. Regular casting defects like porosity and contraction were minimally present in the microstructure.

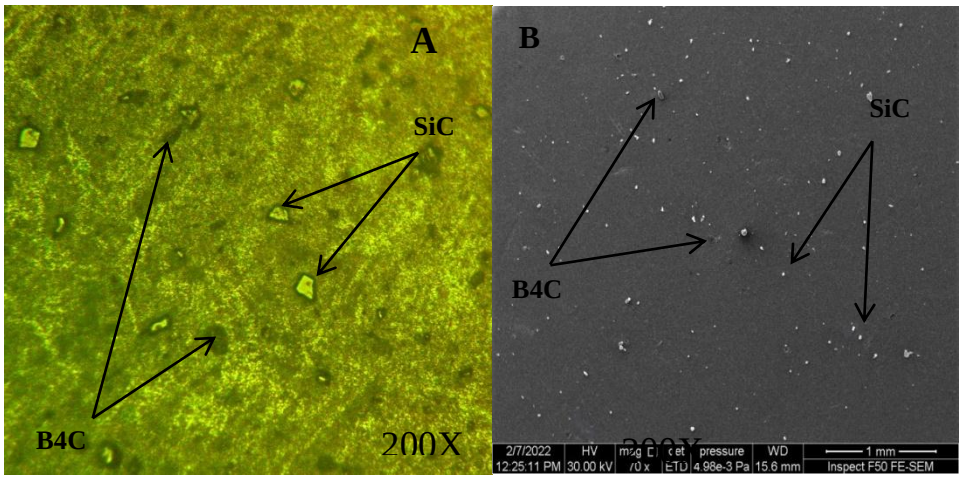

Figure(4.16): Al(4.5%B4C+4%SiC) microwstructure (A) optical microwscope image (B) SEM image for

4.2.12 XRD Analysis

X-ray diffraction patterns of SiC and B4C powders and Al7075 composite reinforced with (4.5%B4C+4.5%SiC) are shown in Figure (4.17A,B,C). The peak in figure (4.17A) at 26.68º, 34º, 35.6º, 38.3º, and 43.2º correspond to the presence of SiC and the peak in figure (4.17B) at 19.7º, 22º, 23.5º, 34.9º, and 37.8º correspond to the presence of B4C**.** From figure (4.17C)The XRD results reveal that the main elements present in the hiybrd composites was Al (solid solution). The presence of components like SiC and B4C particles were not clearly detected by XRD due to their low concentration, the intensities peaks increase with increasing wt .% of components, this agreed with [81]. Furthermore, XRD pattern did not reveal any presence of secondary phases.

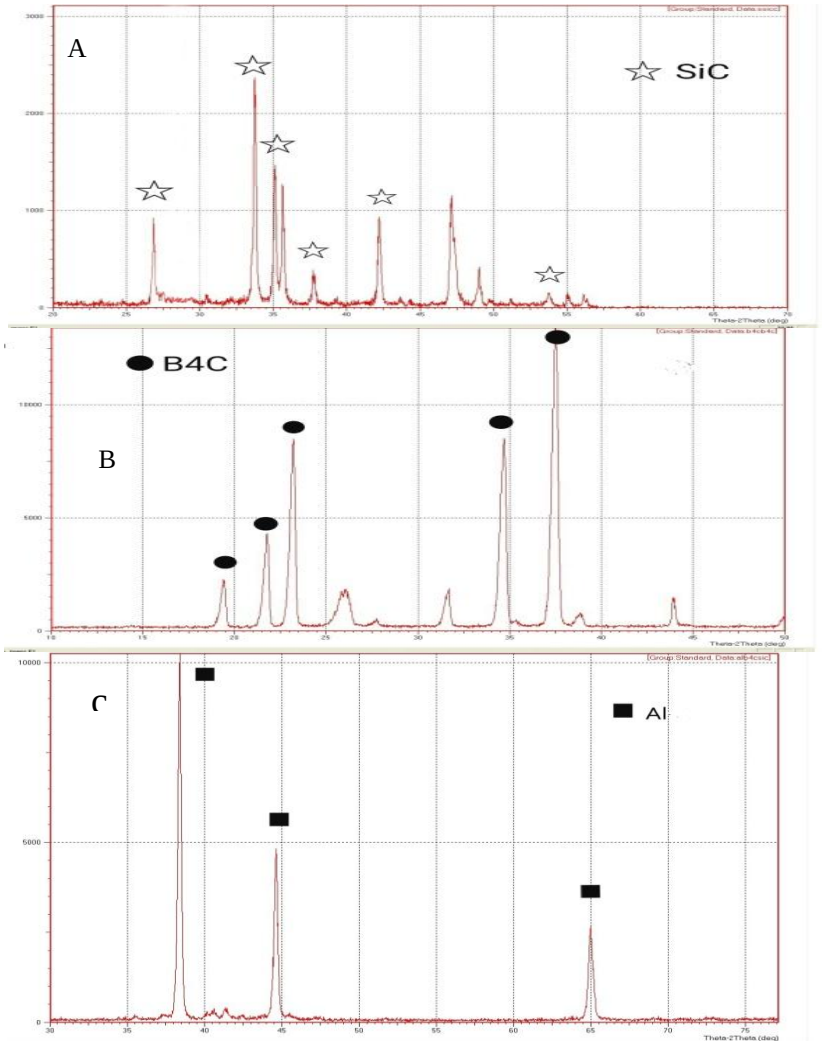

Figure (4.17): XRD Patterns: (A)for SiC powder, (B) for B4Cpowder, and(C) for Al7075 (4.5%B4C+4.5%SiC) composite.

4.3 Results of Machining Tests

Machining test carried out on the optimum specimen of the mechanical properties test (Al7075 reinforced with 4.5% SiC and 4.5% B_4C) specimen under various conditions of controlled factors (Ip, V, Toff and Ton), while the EWR, MRR and Ra was recognized as a performance measure. The designations, and levels of controlled factors are shown in Table 4.7.

Table 4.7: Machining Parameters and Levels.

Parameters	Designation	Units	Levels		
Voltage of discharge	V	volt	140	240	---
Pulse current	Ip	Amp.	10	16	22
Pulse duration	Ton	µsec	50	100	150
Pulse interval	Toff	µsec	25	50	75

The machined specimens using a programme created using the Taguchi Method. orthogonal array (OA) as shown in Table (4.8) L18 to achieve the best machining conditions. For predicting response variables, a regression model is developed. In this investigation, Minitab (Version 2017) software was employed.

Table 4.8: Design of Experiments L_{18} ($2^1 3^3$) array and output.

S. No.	V volt	Ip Amp.	Ton µs	Toff µs	MRR mm^3/min.	EWR mm^3/min.	Ra (µm)
1	140	10	50	25	38.954	0.913	2.451
2	140	10	100	50	37.282	0.938	2.558
3	140	10	150	75	32.649	0.924	2.487
4	140	16	50	25	63.917	0.954	3.268
5	140	16	100	50	56.715	0.938	3.215
6	140	16	150	75	46.786	0.917	3.268
7	140	22	50	50	63.500	0.880	4.317
8	140	22	100	75	51.287	0.861	4.512
9	140	22	150	25	75.315	1.247	5.116
10	240	10	50	75	29.796	0.927	2.682
11	240	10	100	25	44.731	0.927	3.322
12	240	10	150	50	42.877	1.261	3.499
13	240	16	50	50	57.538	1.065	3.872
14	240	16	100	75	47.473	1.028	3.890
15	240	16	150	25	75.075	1.499	4.725
16	240	22	50	75	54.123	0.932	3.695
17	240	22	100	25	79.880	1.404	6.235
18	240	22	150	50	69.040	1.343	6.224

4.3.1 Identifying the Influence Factors

As we mentioned earlier in paragraph 4.2.1 to determine the influencing factors and depending on the hypothesis in the terminology of statistical modeling that the effect of factors on output is based on 95 % confidence interval or 5 % significance level having almost P-values less or equal to 0.05 affecting the all responses (MRR, EWR and Ra) [74]. The insignificant factors were removed from the models' structures using the backward elimination method[75]and the ANOVA was conducted for each reduced quadratic model generated including just these significant factors that contributed to model building as significant terms. as illustrated in Table 4.9. From the ANOVA, it can be conclude that all the input parameters either significant when ($0 < \text{p-value} < 0.05$) or it is more significant when (p-value = 0) surely, all these were done after removing the non- significant factors.

Table 4.9: ANOVA Table for the Trimmed EWR, MRR, and Ra.

Source	DF	Seq SS	Adj SS	Adj MS	F	P
MRR						
Regression	11	3853.96	3853.96	350.36	309.56	0.000
V	1	64.71	16.25	16.25	14.36	0.009
Ip	1	2320.08	1757.11	1757.11	1552.50	0.000
Ton	1	95.85	15.43	15.43	13.63	0.010
Toff	1	1116.66	629.77	629.77	556.43	0.000
Ip^2	1	158.65	173.15	173.15	152.99	0.000
V × Ip	1	1.63	7.78	7.78	6.87	0.040
V × Ton	1	0.06	11.41	11.41	10.08	0.019
V × Toff	1	1.67	7.11	7.11	6.28	0.046
Ip × Ton	1	10.17	10.17	10.17	8.99	0.024
Ip × Toff	1	69.84	69.84	69.84	61.71	0.000
Ton × Toff	1	14.65	14.65	14.65	12.94	0.011
Residual Error	6	6.79	6.79	1.13		
The Total	17	3860.75				
EWR						
Regression	4	0.578657	0.578657	0.144664	16.58	0.000
V	1	0.182811	0.182811	0.182811	20.96	0.001
Ip	1	0.050311	0.050311	0.050311	5.77	0.032
Ton	1	0.192533	0.192533	0.192533	22.07	0.000

Toff	1	0.153002	0.153002	0.153002	17.54	0.001
Residual Error	13	0.113402	0.113402	0.008723		
The Total	17	0.692059				
Ra						
Regression	7	21.4522	21.4522	3.0646	24.44	0.000
V	1	2.6850	2.6850	2.6850	21.42	0.001
Ip	1	14.3008	14.3008	14.3008	114.06	0.000
Ton	1	2.1118	1.5749	1.5749	12.56	0.005
Toff	1	1.7503	1.2653	1.2653	10.09	0.010
Ip^2	1	0.1910	0.1910	0.1910	1.52	0.245
Ip × Ton	1	0.2437	0.1868	0.1868	1.49	0.250
Ip × Toff	1	0.1696	0.1696	0.1696	1.35	0.272
Residual Error	10	1.2538	1.2538	0.1254		
The Total	17	22.7060				

4.3.2 The Effect of Process Parameters on MRR

Figure 4.18 displays the main effect plot of each variable (V, Ip, Ton, and Toff) on MRR at a 95% confidence interval or 5% significant level. As can be seen, the MRR increases steadily as the voltage increases. Increasing V raises the discharge power in sparks area and, as a result, increasing the MRR on the surface. The MRR tends to rise as Ip increases. The product of pulse energy and frequency is thought to be proportionate to MRR. Increasing the Ip at a constant frequency raises the pulse energy, which is agrees with the reference. [82].

T_{on} little effect on MRR when Ton grows from 50 µs to 150 µs, as seen in Figure (4.18). The shorter the Ton, the less vaporization occurs, and longe pulse length, mean plasma channel expands more and more. The extension of plasma channel results in a lower energy intensity on workpiece, that is not enough to melt and/or evaporate the material of the workpiece [83] Thus, throughout the range of investigation, MRR was highest at Ton approximately 150 s.

Finally, when Toff increases, the MRR decreases. This is because a rise in Toff causes heat to be dissipated, resulting in a reduced MRR[84].

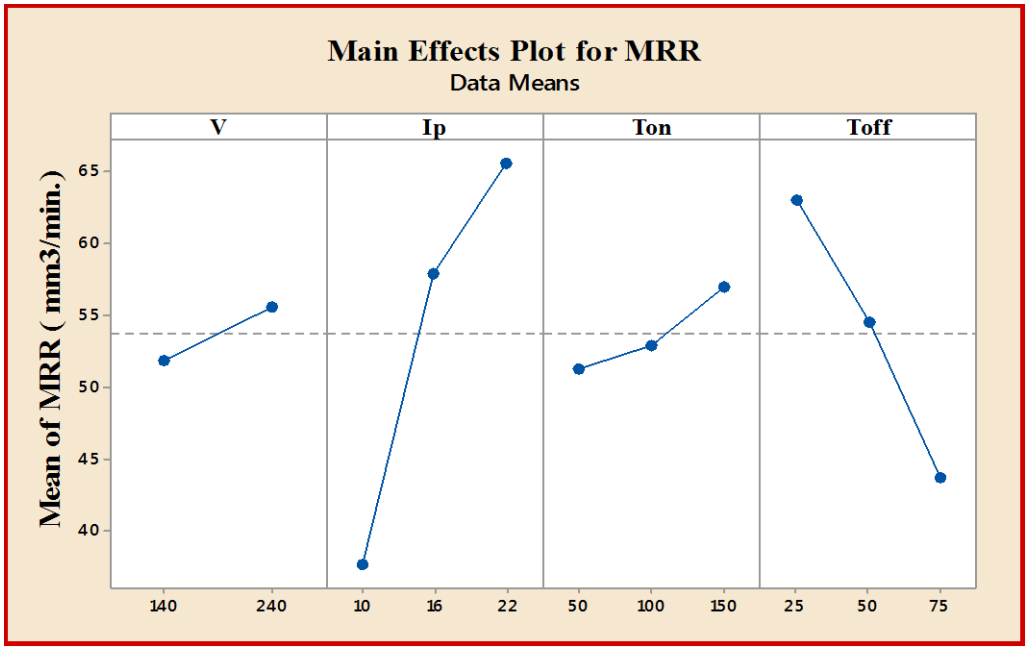

Figure 4.18: process parameters Effect on MRR.

Figures 4.19 - 4.24 display the estimated outputs of MRR in relation to the control parameters of V, Ip, Ton and Toff. As can be seen from the Fig. 4.19 the MRR increases considerably with increase in V and Ip, similarly for V and Ton, Ip and Ton as well shown in Figures 4.20 and 4.22 respectively. However, for every amount of pulse duration, the MRR increases with respect to voltage and pulse current. This is because they have a control on the incoming energy [85]. As a result, the greatest levels of V, Ip, and Ton for MRR are significant parameters. Furthermore, Figure 4.21 depicts the influence of V and Toff on MRR. It is observed that the MRR values are higher when V is higher with lower Toff, Likewise for Ip and Toff, Ton and Toff as well shown in Figures 4.16 and 4.17 respectively. The explanation is the same, as stated earlier, however, the increase in Ip, Ton generates a strong spark as well as the temperatures of the workpiece does not drop remarkably before the next spark starts when there is decrease in Toff and therefore MRR increases.

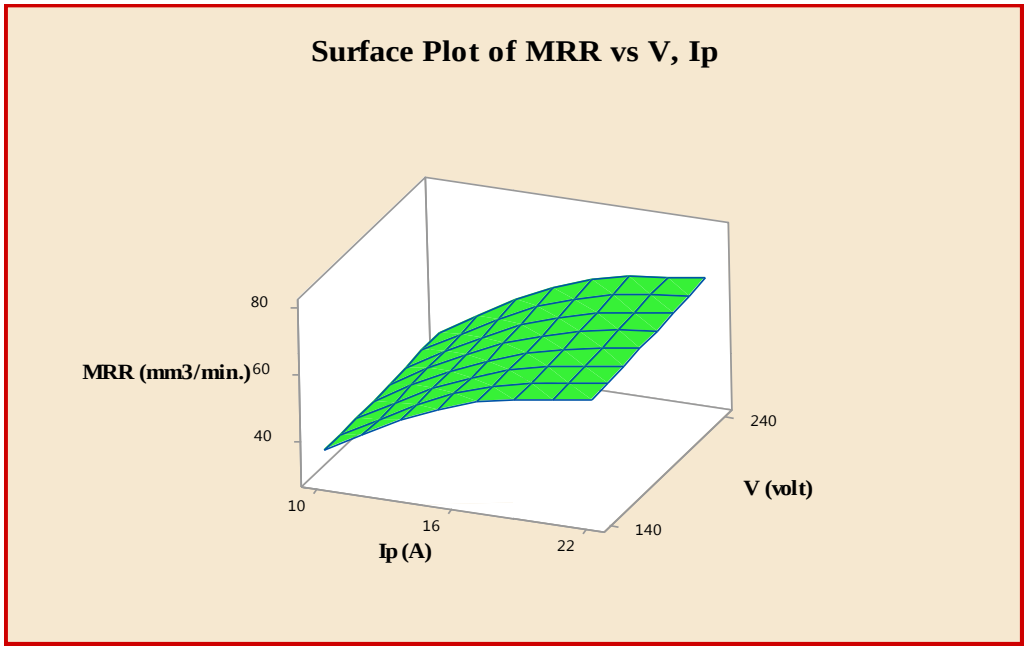

Fig. 4.19: Response Surface Plot of MRR × V and Ip.

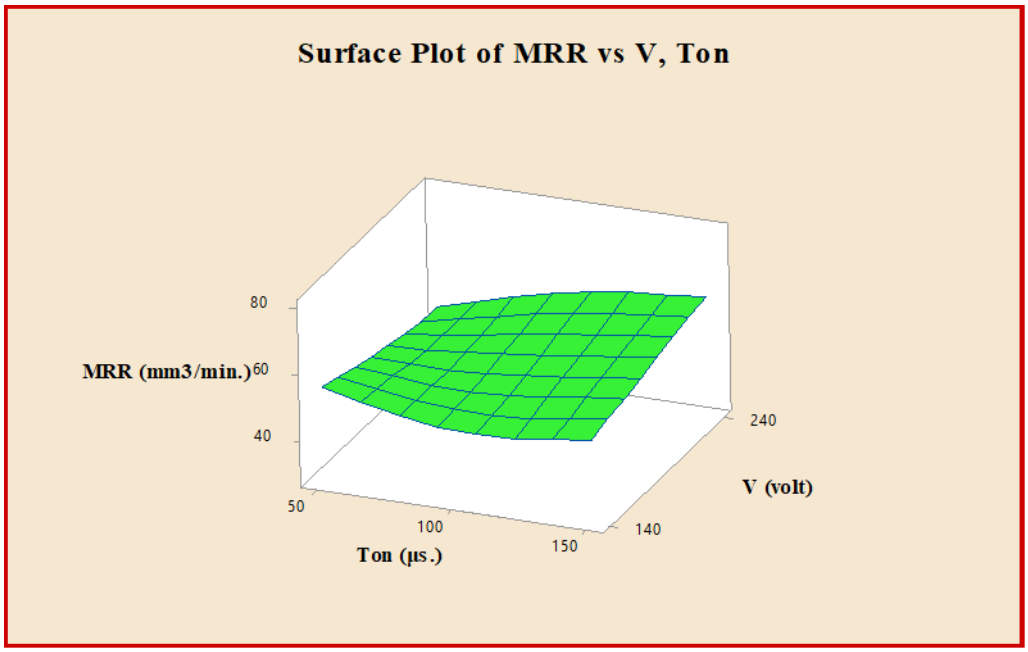

Fig. 4.20: Surface Plot of Response for MRR × V and Ton.

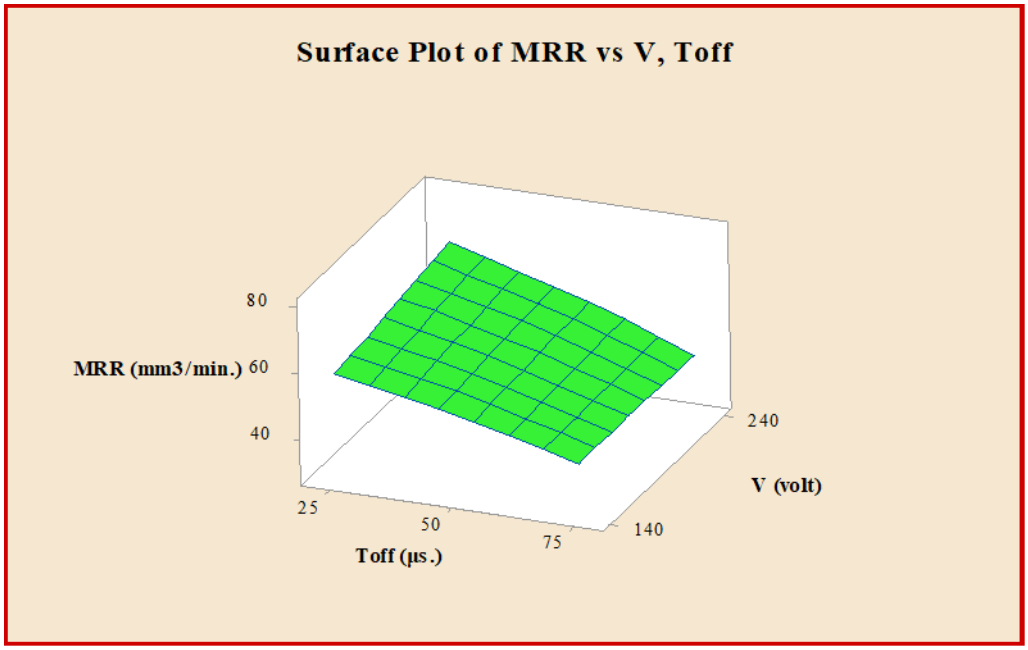

Fig. 4.21: Surface Plot of Response for MRR × V and Toff.

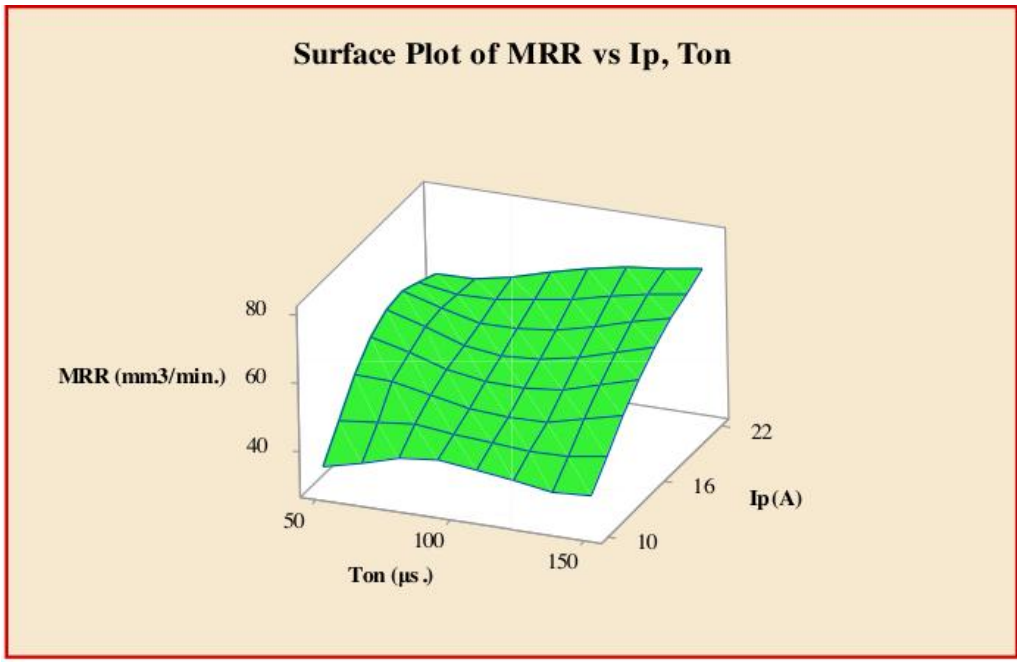

Fig. 4.22: Response Surface Plot of MRR × Ip and Ton.

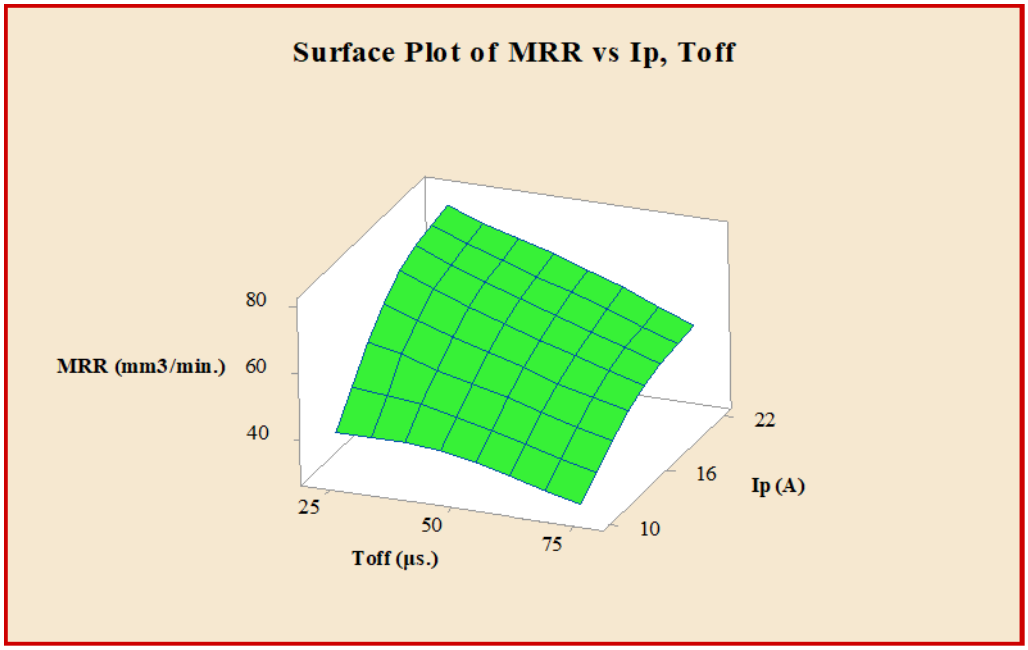

Fig. 4.23: Response Surface Plot of MRR × Ip and Toff.

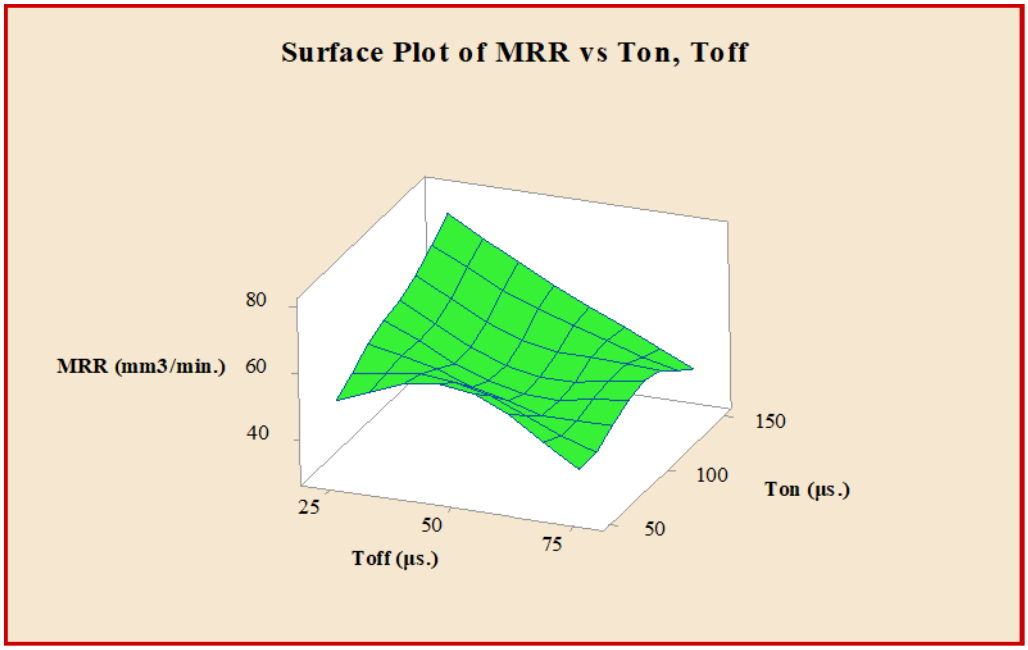

Fig. 4.24: Response Surface Plot of MRR versus Ton and Toff.

4.3.3 The Effect of Process Parameters on EWR

Figure 4.25 shows the four main effect plots of EWR. A similar trend is observed compared to the MRR effect plots. With voltage, discharge current and pulse duration directly proportional with the electrode wear rate (EWR) for the same reason for the MRR. From the effect plot of pulse off-time (Toff), it is clear that setting longer pulse off-times can favour it as shorter pulse durations will deteriorate tool wear. This is the same explanation for the MRR, which can certainly be used here.

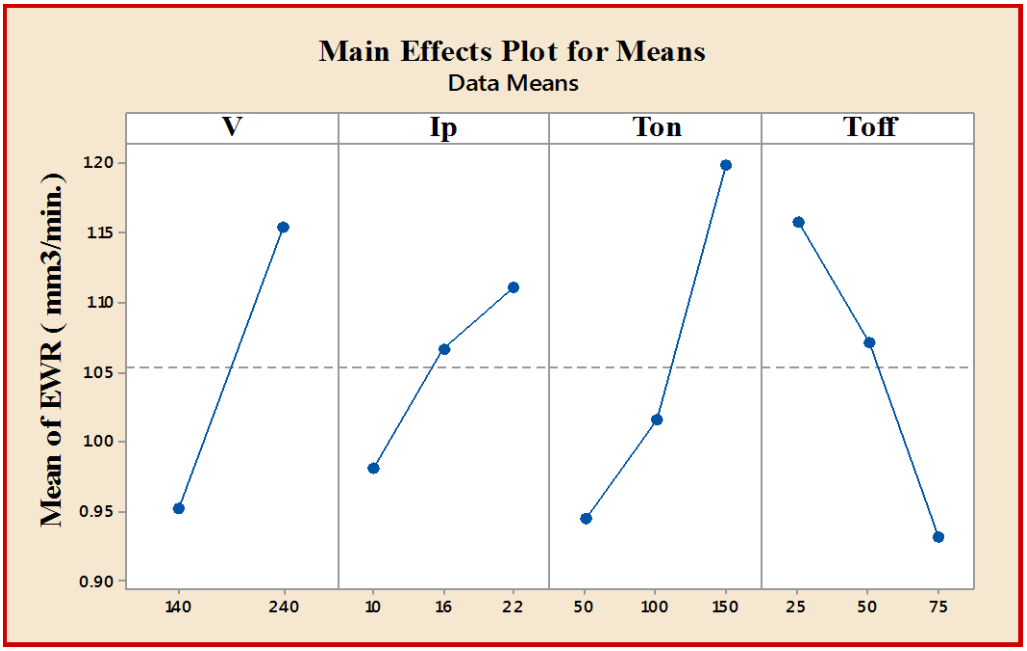

Figure 4.25: Effect of process parameters on EWR.

4.3.4 Influence of Process Parameters on (Ra)

The primary effect charts for the four controllable factors on Ra are shown in Figure 4.26. It is obvious that all factors have a greater influence on Ra.

Furthermore, when Ip increases, so does Ra. In other words, when Ip increase, discharge impacts the specimen's surface more intensely, exerting a force of impact on the liquid in the crater, as a result, additional liquid metal is forced away from the crater, increasing the surface roughness. of the machined surface, this is agreed with Ref. [86].

Likewise, Ra raised when Ton went from low to high levels, while the other parameters stayed constant at the mid values. The long Ton creates more heat transmission to the machine area because the flushing pressure is constant, and the dielectric fluid cannot expel the molten metals.

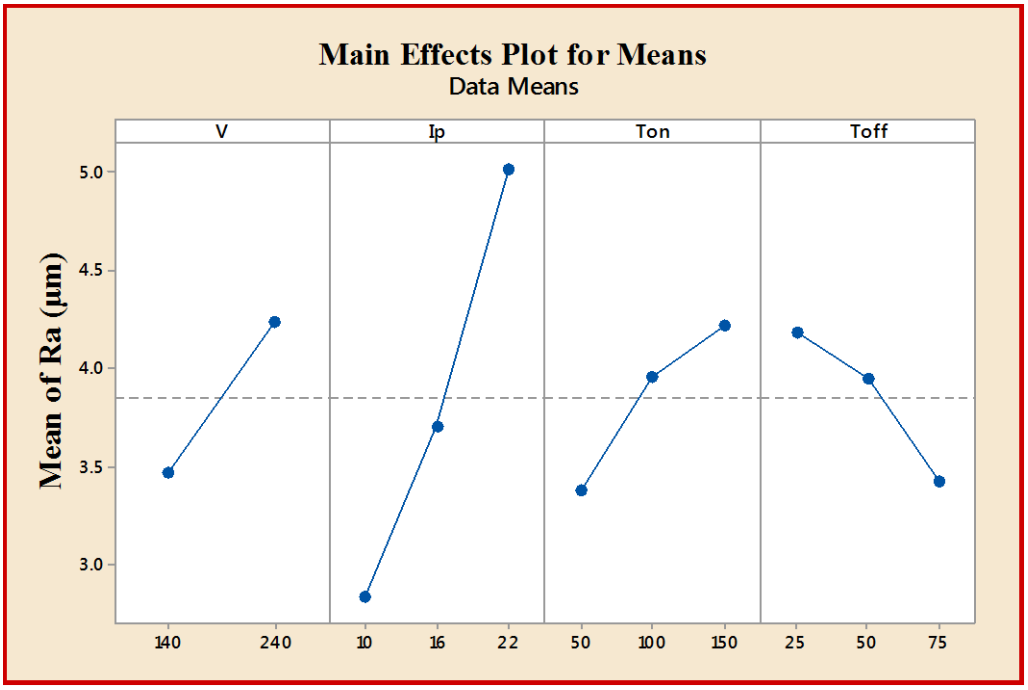

Figure 4.26. Effect of process parameters on Ra.

In other words, as the ton increases, the molten isothermal penetrates more deeply into the core of the material, allowing the molten to spread deeper into the material, which leads to the production of a thicker white layer. Accordingly, the higher the Ton, the greater the Ra, this is agreed with the reference [87]. The most influential factors for surface roughness are Ip and Ton. When either of these parameters is increased, the surface roughness value increases. The high energy pulse creates a crater on the machined surface, resulting in a poor surface finish quality.

Figure 4.28: Surface Plot response of Ra vs Ip and Toff. Figure 4.27 depicts the estimated output for Ra in relation to the control parameters Ip and Ton. This is because they have a control on the input energy. The combined effects of Ip and Toff on the Ra are seen in Figure 4.28. It is obvious that smooth surfaces may be created when high Toff and low Ip

values are achieved. This is due to the discharge striking the specimen's surface less intensively with a low current and a cooling effect on the tool and workpiece, a longer Toff reduces the Ra.

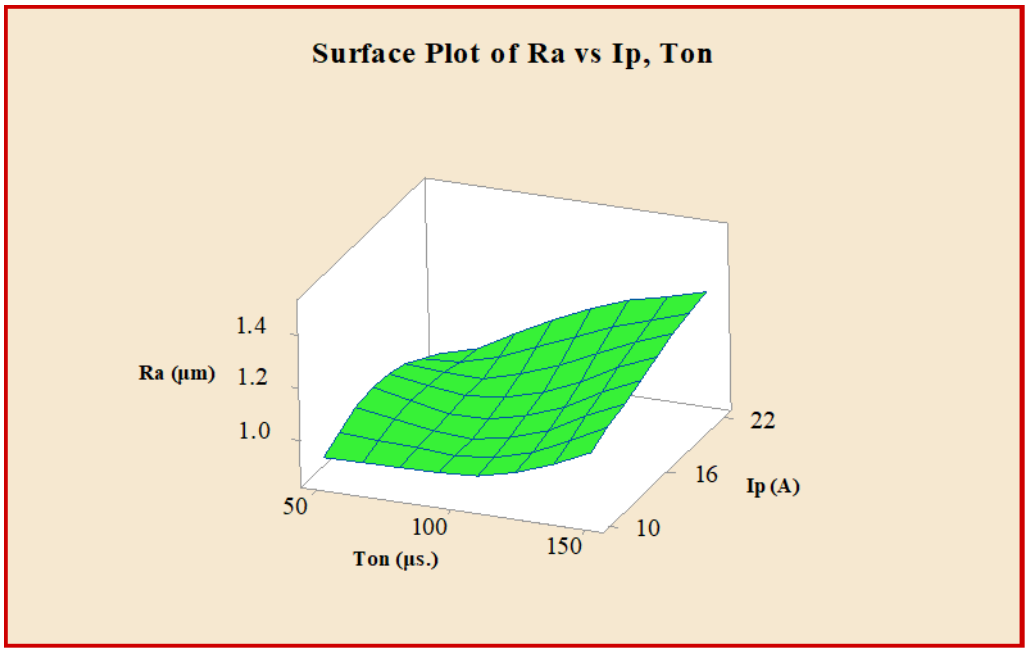

Figure 4.27: Surface Plot Response of Ra vs Ton and Ip.

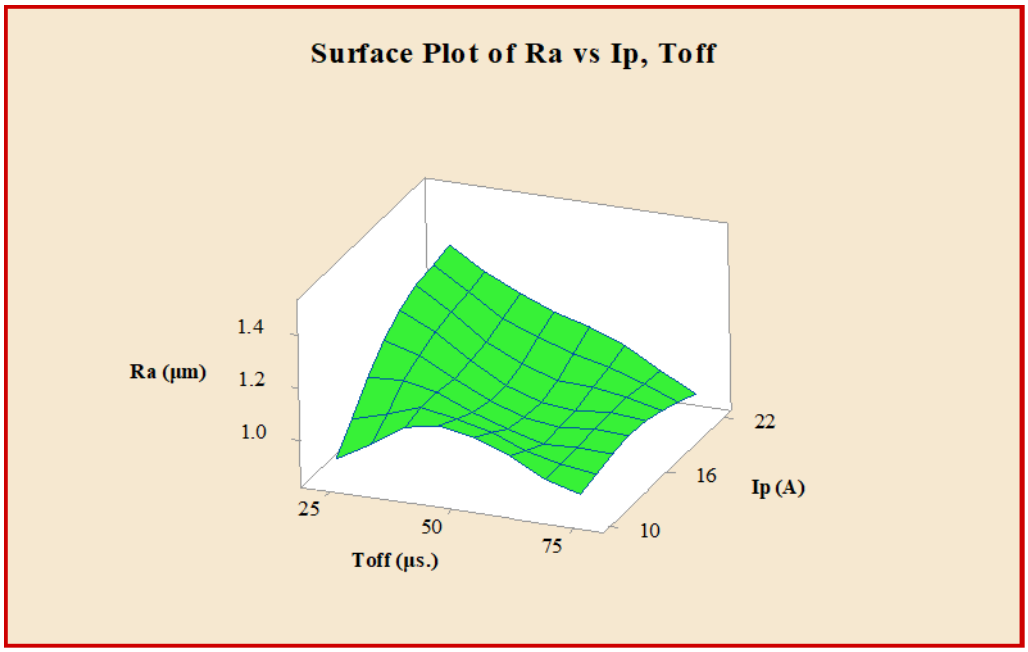

Figure 4.28: Surface Plot Response of Ra vs Toff and Ip.

4.3.5 Improving of Model Fitting Capabilities of Machining

Equations 4.8 – 4.10 shown below are the predicted regression models for calculating output (MRR, EWR and Ra). Equations of output are developed with 95% confidence levels.

$$MRR = -37.13 - 0.0345\ V + 9.300\ Ip + 0.0830\ Ton + 0.315\ Toff - 0.1894\ Ip^2 + 0.00297\ V \times Ip + 0.000522\ V \times Ton - 0.000823\ V \times Toff - 0.00434\ Ip \times Ton - 0.02275\ Ip \times Toff - 0.001670\ Ton \times Toff \quad (4.8)$$

$$EWR = 0.470 + 0.002016\ V + 0.01079\ Ip + 0.002533\ Ton - 0.00452\ Toff \quad (4.9)$$

$$Ra = 0.84 + 0.00772\ V - 0.015\ Ip - 0.00102\ Ton + 0.0028\ Toff + 0.00607\ Ip \times Ip + 0.000540\ Ip \times Ton - 0.001029\ Ip \times Toff \quad (4.10)$$

4.3.6 Verifying the model's sufficiency of Machining

Another criteria for determining the model's adequacy is the coefficient of determination (R^2). For MRR, EWR, and Ra, the measured R^2 values are more than 99.82 percent, 83.61 percent, and 94.48 percent, respectively. These results reveal that the models of regression are adequate. The developed regression models' validity is further examined by producing scatter plot diagrams. Figure 4.29 displays typical scatter plot diagrams for all models. The actual and predicted values of the responses show that the developed empirical models fit very well.

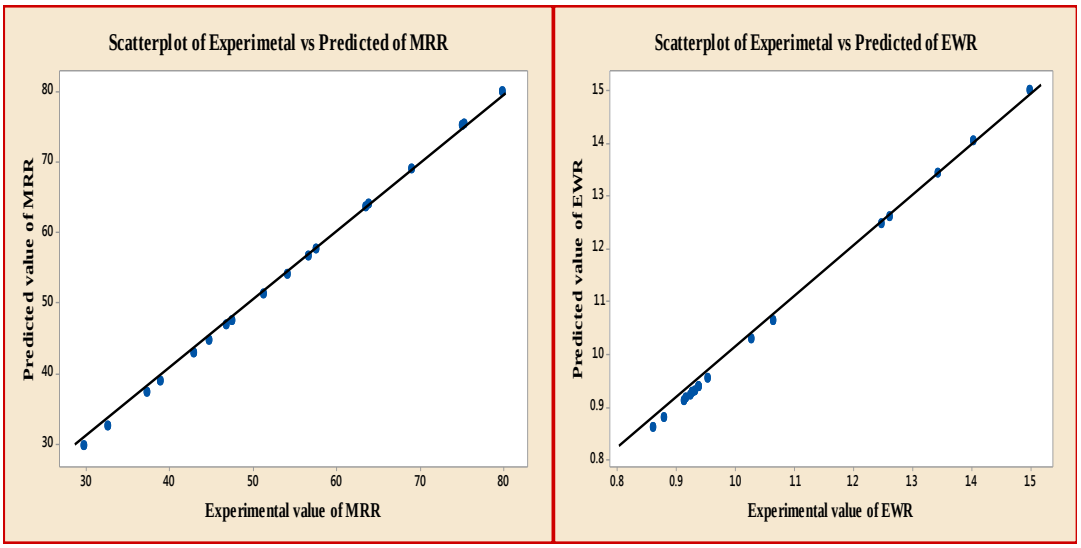

A B

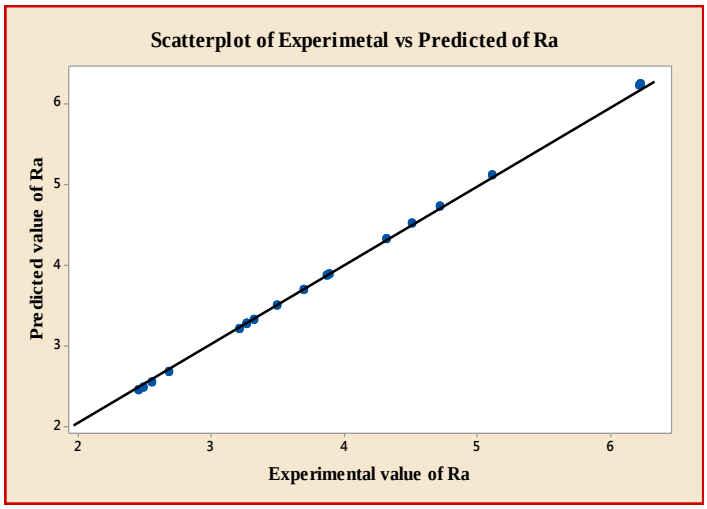

C

Figure 4.29: Scatter plot diagram of the A (MRR), B (EWR) and C (Ra).

4.3.7 Optimization by GRA Method for Machining

The column two, three and four of Table 4.10 lists the processed experimental data after grey relational generation (i.e. normalization). As can be seen, the normalized values vary from one to zero. After normalizing, all sequences are designate as $X_0^*(k)$for reference sequence and $X_j^*(k)$for comparability sequence.

Best normalized value should be one. and larger normalized results mean to better performance. Next, the absolute value of deviation sequence of

Δ_i (k) is governed using equation (2.4).In this swork, the MRR, EWR and Ra are influence equally by all the process parameters. To compute the GRC stated in column five, six and seven of Table 4.10, the distinguishing coefficient ξ= 0.5 was replaced in equation (2.3) by considering all process parameters have equal weightage.

Table 4.10: The sequences of each performance characteristic after data processing.

Exp. No.	Normalized			GRC			GRG	Rank
	MRR	EWR	Ra	MRR	EWR	Ra		
1	0.182853	0.918495	1	0.379608	0.859838	1	0.746482	1
2	0.149469	0.87931	0.971723	0.370225	0.805555	0.946473	0.707418	3
3	0.056964	0.901254	0.990486	0.346492	0.835079	0.981327	0.720966	2
4	0.681275	0.854232	0.784091	0.610706	0.774272	0.698413	0.694463	4
5	0.537477	0.87931	0.798097	0.519468	0.805555	0.712349	0.679124	7
6	0.33923	0.912226	0.784091	0.430749	0.850667	0.698413	0.659943	8
7	0.672949	0.970219	0.506871	0.604558	0.943786	0.503459	0.683934	6
8	0.429099	1	0.455338	0.466897	1	0.478624	0.648507	9
9	0.908853	0.394984	0.295719	0.845813	0.452482	0.415185	0.571160	12
10	0	0.896552	0.938953	0.333333	0.828572	0.891191	0.684365	5
11	0.298199	0.896552	0.769820	0.416042	0.828572	0.684763	0.643126	10
12	0.261181	0.373041	0.723044	0.40361	0.443672	0.643537	0.49694	17
13	0.553909	0.680251	0.624471	0.52849	0.609943	0.571083	0.569839	13
14	0.352947	0.738245	0.619715	0.4359	0.656379	0.567998	0.553426	15
15	0.904061	0	0.399049	0.839012	0.333333	0.454153	0.542166	16
16	0.485724	0.888715	0.671247	0.492962	0.817949	0.603316	0.638076	11
17	1	0.148903	0	1	0.37007	0.333333	0.567801	14
18	0.783564	0.244514	0.002907	0.697899	0.398252	0.333981	0.476711	18

Then, equation (2.5) was used to determine the GRG. The experiments order according to GRG values are listed in column eight of Table 4.10. The greater GRG value, 0.746482, means that the associated experimental datarss are close to the optimally normalised experimental data. The experiment number one has the greatest GRG and hence may be considered the finest experimental sequence of the EDM's multi-performance properties. Furthermore, Figure 4.30 displays the GRG from Table 4.10 for all eighteen trials carried out using the L18 orthogonal array. Figure 4.30 shows the variations in response when factors are changed from one level to another, and it is obvious that experiment number 1 has the greatest GRG value. As a result, all

eighteen runs have an optimum combination of process parameters set for the best multi-performance qualities.

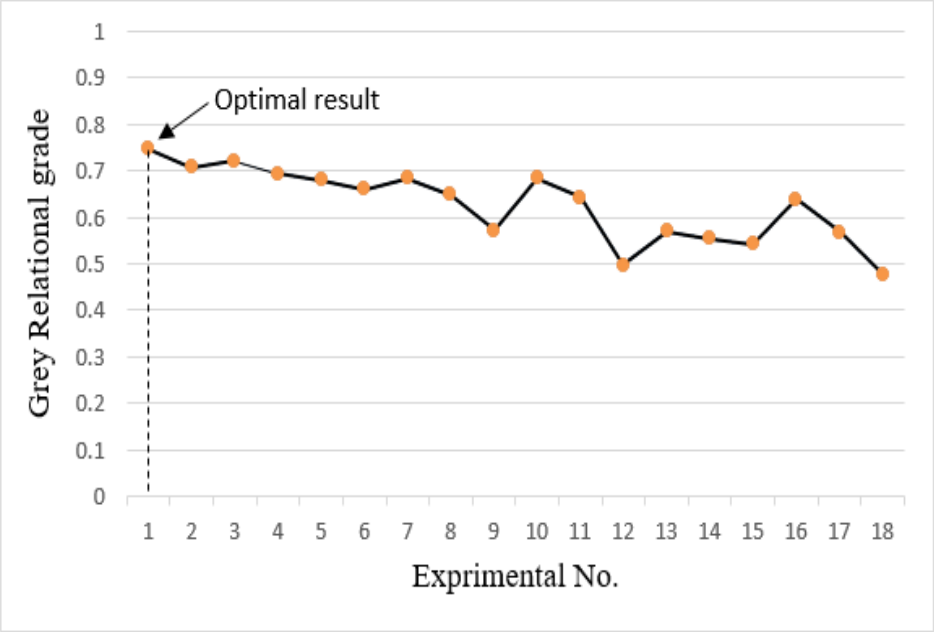

Figure 4.30: Grey relational grade for multi-response

The multiple responses of performance characteristics of EDM can be evaluated using a response table using GRG as shown in Table 4.10. Because the experimental design was orthogonal, it was easy to separate the influence of each input parameter at various levels on GRG easily, as shown in the same table.

It confirms that the voltage is more influence compared to rest parameters on the MRR, EWR and Ra as illustrated in the first rank (Table 4.11) from this table and Figure 4.31, it is also confirmed that the V (140 volt), Ip (10 A), Ton (50 µs) and Toff (75 µs) characterize the highest value of GRG. Hence, the combination of level 1 of V, Ip, Ton and level 3 of Toff is the optimal combination of process parameter in EDM to obtain largest MRR with lowest EWR and Ra.

Table 4.11: GRG response table.

Parameters	GRG			Main effect (max-min)	Rank
	Level 1	Level 2	Level 3		
V	0.67911078*	0.57471700	---	0.104394	1
Ip	0.66654950*	0.61649350	0.59769800	0.068851	2
Ton	0.66697000*	0.63323367	0.57798100	0.033736	3
Toff	0.6275330	0.60232767	0.65088100*	0.023350	4
The mean of GRG total value γ_m= 0.6269137 * Levels for optimal GRG					

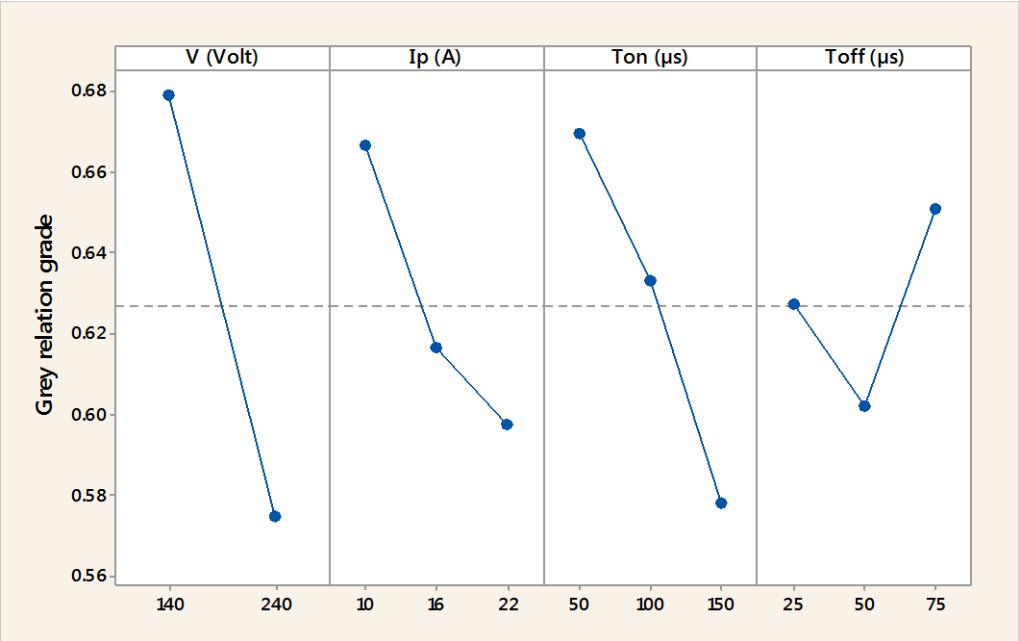

Fig. 4.31: Main Effect of factors on GRG.

After the optimum parameter is attained, the optimal combination of process parameter needs to be predicted and a confirmation test should be carried out to Confirm the enhancement of quality characteristics. Equation (4.7) can be used to determine the estimation or prediction GRG at the optimal level of process parameter [18]. The results of confirmation test are shown in Table 4.12 and it can be verified that the value of (MRR) increased from 38.954 mm^3/min. to 41.577 mm^3/min, value of electrode wear rate and surface roughness have been improved from 0.913 mm^3/min to 0.862 mm^3/min and 2.451 to 2.220 µm respectively. Furthermore, it also indicates that the optimization method

increased the GRG value in the confirmation experiment from 0.746482 to 0.78277 when comparing to the predicted value. The result of confirmation tests verify that the results in optimising the process parameters of EDM process using GRA for multi performance characteristics are acceptable.

Table 4.12: Improvements in GRG with optimized output.

Condition description	Optimal machining properties	
	Predicted experiment	Confirmation experiment
MRR (mm^3/min)	38.954	41.577
EWR (mm^3/min)	0.913	0.862
Ra (μm)	2.451	2.220
GRG	0.746482	0.78277
Improvement in GRG = 0.036288 %		

Chapter Five

Conclusion and Suggestion

5.1 Conclusion:

1. The stir casting methods is successfully used to produce single or hybrid aluminum composites with 3, 6 and 9 percentage reinforcement particles.
2. In term of type of reinforcement materials the mechanical properties of (Al 7075-SiC+ B_4C) composites are better than the rest of the composites, and the Al 7075-B4C composites are better than the Al 7075-SiC composites, at the same weight percentages
3. The content of reinforcement particles have a significant effect on the mechanical properties of the composites.
4. By adding reinforcing particles, the mechanical properties of all composites are effectively improved, except for the hardness of single composite, it reaches a maximum value at 6% of the reinforcement particles and then decreases, while the elongation decreases with increasing the amount of reinforcement particles
5. The improvements in VHN, YS, UTS, UCS, and FS were 54.95 %, 31.1 %, 32.46, 34.42, and 39.4 respectively
6. The Better mechanical properties (VHN, YS, UTS, UCS, and FS) were obtained at reinforcement percentage of (4.5%B4C+SiC4.5%
7. The experiment showed the optimal factor combination, and predicted values were more similar to observed values.
8. The specimens at (4.5%B4C+SiC4.5%)has been successfully machined by EDM.
9. Except for Toff, all input variables in the EDM process are direct proportion to outputs.

10. The best combination of EDM process parameters were V 140 volts, Ip 10 A, Ton 50 µs, and Toff 25 µs where greater MRR, lower EWR, and lower Ra are attained.

5.2 Suggestion:

1. Studying the effect of type and content of reinforcement for aluminum matrix on some other properties like wear, corrosion resistance.
2. Investigate the effect of some other reinforcement materials such as TiC, BN and Graphene for HMMCs to obtain better mechanical properties.
3. Studying the preparation of MMCs by powder metallurgy under different parameters
4. Machining of HAMMCs through wire-EDM, powder mixed EDM, and the effect of geometric tolerances
5. Studying the effect other machining parameters for HMMCs like pressure of flushing, material of tool and dielectric fluid, polarity, and content and type of some reinforcement materials on machining outputs.

References

[1] M. O. Bodunrin, K. K. Alaneme, and L. H. Chown, “Aluminium matrix hybrid composites: A review of reinforcement philosophies; Mechanical, corrosion and tribological characteristics,” *J. Mater. Res. Technol.*, vol. 4, no. 4, pp. 434–445, 2015, doi: 10.1016/j.jmrt.2015.05.003.

[2] M. C. Fadhil and B. S. Ravikiran, “Characterization of Aluminium Alloy / SiC Metal Matrix Composites,” *Int. J. Eng. Res. Adv. Technol.*, vol. 2, no. 09, pp. 1–5, 2016, [Online]. Available: http://www.ijerat.com/uploads/2/3213_pdf.pdf.

[3] K. K. . M. and A. C. Ravindra Mamgain, Alakesh Manna, “Effect of volume fraction (Al2O3) on tensile strength of Aluminium 6061 by varying stir casting furnace parameters: A Review,” *Int. J. Sci. Eng. Res.*, vol. 6, no. 5, pp. 189–198, 2015.

[4] S. S. Irhayyim, H. S. Hammood, and A. D. Mahdi, “Mechanical and wear properties of hybrid aluminum matrix composite reinforced with graphite and nano MgO particles prepared by powder metallurgy technique,” *AIMS Mater. Sci.*, vol. 7, no. 1, pp. 103–115, 2020, doi: 10.3934/MATERSCI.2020.1.103.

[5] T. Panneerselvam, T. K. Kandavel, K. S. Arun, and V. Dineshkumar, “Tribological study on hybrid reinforced aluminium-based metal matrix composites,” *Int. J. Surf. Sci. Eng.*, vol. 12, no. 5–6, pp. 449–466, 2018, doi: 10.1504/IJSURFSE.2018.096763.

[6] “Investigations of mechanical, microstructural and tribological properties of Al2024 nanocomposite reinforced by TiO2 nanoparticles,” 2018.

[7] T. Division, “EDM machinability and parametric optimisation of 2014Al / Al 2 O 3 composite by RSM Akhil Khajuria * and Raman Bedi Balbir Singh Modassir Akhtar,” vol. 20, no. 6, pp. 536–555, 2018.

[8] A. Sharma and P. M. Mishra, “Effects of various reinforcements on mechanical behavior of AA7075 hybrid composites,” *Mater. Today Proc.*, vol. 18, pp. 5258–5263, 2019, doi: 10.1016/j.matpr.2019.07.526.

[9] R. R. Mishra, S. Sameer, S. Kumar, R. Muni, and P. Mishra, “FABRICATION & TESTING OF ALUMINIUM METAL MATRIX COMPOSITES,” no. 05, pp. 167–172, 2020.

[10] H. Kala, K. K. S. Mer, and S. Kumar, “A Review on Mechanical and Tribological Behaviors of Stir Cast Aluminum Matrix

Composites.," *Procedia Mater. Sci.*, vol. 6, no. Icmpc, pp. 1951–1960, 2014, doi: 10.1016/j.mspro.2014.07.229.

[11] P. S. Bains, S. S. Sidhu, and H. S. Payal, "Fabrication and Machining of Metal Matrix Composites : A Review," *LMMP*, vol. 31, no. 5, pp. 553–573, 2016, doi: 10.1080/10426914.2015.1025976.

[12] H. Bisaria and P. Shandilya, "Machining of Metal Matrix Composites by EDM and its Variants: A Review," pp. 267–282, 2015, doi: 10.2507/daaam.scibook.2015.23.

[13] S. S. Habib, "Study of the parameters in electrical discharge machining through response surface methodology approach," *Appl. Math. Model.*, vol. 33, no. 12, pp. 4397–4407, 2009, doi: 10.1016/j.apm.2009.03.021.

[14] K. H. Ho and S. T. Newman, "State of the art electrical discharge machining (EDM)," *Int. J. Mach. Tools Manuf.*, vol. 43, no. 13, pp. 1287–1300, 2003, doi: 10.1016/S0890-6955(03)00162-7.

[15] B. C. Kandpal, J. Kumar, and H. Singh, "Electrical Discharge Machining Characteristics of Aluminium Metal Matrix Composites - A Review," *Mater. Today Proc.*, vol. 2, no. 4–5, pp. 1665–1671, 2015, doi: 10.1016/j.matpr.2015.07.094.

[16] Rajan Verma, Saurabh Sharma, and Dinesh Kumar, "Analysis of Mechanical Properties of Aluminium based Metal Matrix Composites Reinforced with Alumina and Sic," *Int. J. Eng. Res.*, vol. V6, no. 03, pp. 454–459, 2017, doi: 10.17577/ijertv6is030506.

[17] K. Nagahara, "Ceramic and metal matrix composites: route and properties," *Otolaryngol. - Head Neck Surg.*, vol. 71, no. 9, pp. 633–638, 1999.

[18] S. C. Tjong, *Processing and Deformation Characteristics of Metals Reinforced with Ceramic Nanoparticles*, Second Edi. Elsevier Ltd, 2014.

[19] 2016 Bharath et al., "Experimental Investigations on Mechanical and Wear Behavior of Hybrid Aluminium Alloy," *Int. J. Res. Eng. Technol.*, vol. 05, no. 25, pp. 128–131, 2016, doi: 10.15623/ijret.2016.0525024.

[20] R. Narayanan, C. Saravanan, V. Krishnan, and K. Subramanian, "Effect of Particulate Reinforced Aluminium Metal Matrix Composite – A Review," *Mech. Mech. Eng.*, vol. 19, no. 1, pp. 23–30, 2015.

[21] M. Imran and A. R. A. Khan, "Characterization of Al-7075 metal matrix composites: A review," *J. Mater. Res. Technol.*, vol. 8, no. 3, pp. 3347–3356, 2019, doi: 10.1016/j.jmrt.2017.10.012.

[22] W. Jiang, Z. Jiang, G. Li, Y. Wu, and Z. Fan, "Microstructure of Al / Al bimetallic composites by lost foam casting with Zn interlayer Microstructure of Al / Al bimetallic composites by lost foam casting with Zn interlayer," no. November, 2017, doi: 10.1080/02670836.2017.1407559.

[23] W. D. Callister, "Materials science and engineering: An introduction (2nd edition)," *Mater. Des.*, vol. 12, no. 1, p. 59, 1991, doi: 10.1016/0261-3069(91)90101-9.

[24] H. H. Hlail, "Multiple Optimization of Mechanical and Machining Properties of Hybrid MMCs," *Thesis, MSC Babyon Univ.*, 2020.

[25] M. . Rajesh, A. M., & Kaleemulla, "Experimental investigations on mechanical behavior of aluminium metal matrix composites," *Mater. Sci. Eng.*, vol. 149, No. 1.

[26] K. K. C. Marc Andr´e Meyers, *Mechanical Behavior of Materials*. 2006.

[27] D. K. Sharma, M. Sharma, and G. Upadhyay, "Boron carbide (B4C) reinforced aluminum matrix composites (AMCs)," *Int. J. Innov. Technol. Explor. Eng.*, vol. 9, no. 1, pp. 2194–2203, 2019, doi: 10.35940/ijitee.A4766.119119.

[28] D. Patidar and R. S. Rana, "Effect of B4C particle reinforcement on the various properties of aluminium matrix composites: A survey paper," *Mater. Today Proc.*, vol. 4, no. 2, pp. 2981–2988, 2017, doi: 10.1016/j.matpr.2017.02.180.

[29] M. K. Sahu and R. K. Sahu, "Aluminum Based Hybrid Metal Matrix Composites : A Review of Selection Philosophy and Mechanical Properties for Advanced Aluminum Based Hybrid Metal Matrix Composites : A Review of Selection Philosophy and Mechanical Properties for Advanced Applications," *Int. J. Mech. Prod. Eng. Res. Dev.*, vol. 10, no. October, pp. 8–28, 2020, [Online]. Available: http://www.tjprc.org/conference-archives.php?page=117.

[30] A. Kumar and R. N. Rai, "Fabrication, Microstructure and Mechanical Properties of Boron Carbide (B4Cp) Reinforced Aluminum Metal Matrix Composite - A Review," *IOP Conf. Ser. Mater. Sci. Eng.*, vol. 377, no. 1, 2018, doi: 10.1088/1757-899X/377/1/012092.

[31] K. J. Joshua, S. J. Vijay, and D. P. Selvaraj, "Effect of nano TiO2 particles on microhardness and microstructural behavior of AA7068 metal matrix composites," *Ceram. Int.*, vol. 44, no. 17, pp. 20774–20781, 2018, doi: 10.1016/j.ceramint.2018.08.077.

[32] M. T. Sijo and K. R. Jayadevan, "Analysis of Stir Cast Aluminium Silicon Carbide Metal Matrix Composite: A Comprehensive Review," *Procedia Technol.*, vol. 24, pp. 379–385, 2016, doi: 10.1016/j.protcy.2016.05.052.

[33] S. Gopalakannan and T. Senthilvelan, "Effect of Electrode Materials on Electric Discharge Machining of 316 L and 17 - 4 PH Stainless Steels," *J. Miner. Mater. Charact. Eng.*, vol. 11, no. 07, pp. 685–690, 2012, doi: 10.4236/jmmce.2012.117053.

[34] K. P. Rajurkar and J. Narasimhan, "A REPORT ON TECHNOLOGY ASSESSMENT OF ELECTRICAL DISCHARGE AND ELECTRO-CHEMICAL MACHINE TOOLS," no. July, pp. 1–105, 2003.

[35] K. W. LaBarge, "Electrical discharge machining.," *J. Dent. Technol.*, vol. 14, no. 9, pp. 19–22, 1997, doi: 10.1016/0141-6359(84)90045-x.

[36] B. C. Kandpal, J. kumar, and H. Singh, "Machining of Aluminium Metal Matrix Composites with Electrical Discharge Machining - A Review," *Mater. Today Proc.*, vol. 2, no. 4–5, pp. 1665–1671, 2015, doi: 10.1016/j.matpr.2015.07.094.

[37] S. Singh, "Optimization of machining characteristics in electric discharge machining of 6061Al/Al2O3p/20P composites by grey relational analysis," *Int. J. Adv. Manuf. Technol.*, vol. 63, no. 9–12, pp. 1191–1202, 2012, doi: 10.1007/s00170-012-3984-8.

[38] R. K. Garg, K. K. Singh, A. Sachdeva, V. S. Sharma, K. Ojha, and S. Singh, "Review of research work in sinking EDM and WEDM on metal matrix composite materials," *Int. J. Adv. Manuf. Technol.*, vol. 50, no. 5–8, pp. 611–624, 2010, doi: 10.1007/s00170-010-2534-5.

[39] N. Mohd Abbas, D. G. Solomon, and M. Fuad Bahari, "Current research trends in variants of Electrical Discharge Machining: A review," *Int. J. Mach. Tools Manuf.*, vol. 47, no. 7–8, pp. 1214–1228, 2007, doi: 10.1016/j.ijmachtools.2006.08.026.

[40] M. Rizwee, S. S. Minz, M. Orooj, M. Z. Hassnain, and M. J. Khan, "Electric discharge machining method for various metal matrix composite materials," *Int. J. Innov. Technol. Explor. Eng.*, vol. 8, no. 9, pp. 1796–1807, 2019, doi: 10.35940/ijitee.i8112.078919.

[41] B. C. Kandpal, J. Kumar, and H. Singh, "Optimization and characterization of EDM of AA 6061/10%Al2O3 AMMC using Taguchi's approach and utility concept," *Prod. Manuf. Res.*, vol. 5, no. 1, pp. 351–370, 2017, doi: 10.1080/21693277.2017.1389315.

[42] H. El-Hofy, *advanced machining processes non-traditional and hybrid machining processes*. .

[43] H. H. Hlail and S. H. Al-Shafaie, "Multi-Response Optimization of Mechanical Properties of Al reinforced by Al2O3 and/or SiC using Grey Relational Analysis," *IOP Conf. Ser. Mater. Sci. Eng.*, vol. 671, no. 1, 2020, doi: 10.1088/1757-899X/671/1/012012.

[44]] S. H. Al-Shafaie, "Multi-Objective Optimization to Improve Surface Integrity in WEDM of Al/ WCp Metal Matrix Composites Using Grey Relational Analysis," *Int. J. Mech. Eng. Technol.*, vol. 10, no. 1, pp. 10173–10181, 2018.

[45] K. D. S. Kachhap, A. Singh, "A Study of Material Removal during Electrical-Discharge Drilling of Hybrid Metal Matrix Composites," *J. Sci. Ind. Res.*, vol. 78, pp. 364–367, 2018.

[46] A. O. Al-Roubaiy, S. H. Al-Shafaie, and M. Wurood Asaad, "Modeling and optimization of brazing for AA 6061/ AISI 304lusing grey relational analysis," *Int. J. Mech. Eng. Technol.*, vol. 10, no. 1, pp. 107–118, 2019.

[47] T. Senthilvelan, S. Gopalakannan, S. Vishnuvarthan, and K. Keerthivaran, "Fabrication and characterization of SiC, Al2O3 and B4C reinforced Al-Zn-Mg-Cu alloy (AA 7075) metal matrix composites: A study," *Adv. Mater. Res.*, vol. 622, pp. 1295–1299, 2013, doi: 10.4028/www.scientific.net/AMR.622-623.1295.

[48] A. Baradeswaran and A. Elaya Perumal, "Study on mechanical and wear properties of Al 7075/Al2O 3/graphite hybrid composites," *Compos. Part B Eng.*, vol. 56, pp. 464–471, 2014, doi: 10.1016/j.compositesb.2013.08.013.

[49] M. V. Krishna and A. M. Xavior, "An investigation on the mechanical properties of hybrid metal matrix composites," *Procedia Eng.*, vol. 97, pp. 918–924, 2014, doi: 10.1016/j.proeng.2014.12.367.

[50] P. Pugalethi, M. Jayaraman, and A. Natarajan, "Evaluation of Mechanical Properties of Aluminium Alloy 7075 Reinforced with SiC and Al_2O_3 Hybrid Metal Matrix Composites," *Appl. Mech. Mater.*, vol. 766–767, pp. 246–251, 2015, doi: 10.4028/www.scientific.net/amm.766-767.246.

[51] P. Kittali, J. Satheesh, G. A. Kumar, and T. Madhusudhan, "A Review on Effects of Reinforcements on Mechanical and Tribological behavior of Aluminum based Metal matrix composites," pp. 2412–2416, 2016.

[52] N. Verma, "Review on Effect of Various Types of Reinforcement Particles on Mechanical Behavior of 6061 and 7075 Aluminium Alloy Matrix .... Review on Effect of Various Types of Reinforcement Particles on Mechanical Behavior of 6061 and 7075 Aluminium Alloy Matrix Co," *Int. J. Emerg. Technol. Eng. Res.*, vol. 5, no. October, pp. 4–9, 2017.

[53] Z. Fadhil, "Influence of Boron Carbide Reinforcement on Mechanical Properties of Aluminum Base Composite Prepared by Stir and Squeeze Casting," no. 5, pp. 1645–1651, 2017.

[54] F. A. Raju and V. Principal, "Micro Structure and Mechanical Behavior of AL-7075-T6 and Fly Ash Metal Matrix Composite Produced by Stir Casting Process," vol. 12, no. 2, pp. 365–374, 2017.

[55] B. Subramaniam, B. Natarajan, B. Kaliyaperumal, and S. J. S. Chelladurai, "Investigation on mechanical properties of aluminium 7075 - boron carbide - coconut shell fly ash reinforced hybrid metal matrix composites," *China Foundry*, vol. 15, no. 6, pp. 449–456, 2018, doi: 10.1007/s41230-018-8105-3.

[56] S. Suresh, G. H. Gowd, and M. L. S. Deva Kumar, "Experimental investigation on mechanical properties of Al 7075/Al 2 O 3 /Mg NMMC's by stir casting method," *Sadhana - Acad. Proc. Eng. Sci.*, vol. 44, no. 2, pp. 1–10, 2019, doi: 10.1007/s12046-018-1021-9.

[57] K. Kumar, B. M. Dabade, and L. N. Wankhade, "Influence of B4C and SiC particles on aluminium metal matrix composites: A brief overview," *Mater. Today Proc.*, vol. 44, pp. 2726–2734, 2021, doi: 10.1016/j.matpr.2020.12.697.

[58] S. Gopalakannan, T. Senthilvelan, and S. Ranganathan, "Modeling and optimization of EDM process parameters on machining of Al7075-B4C MMC using RSM," *Procedia Eng.*, vol. 38, pp. 685–690, 2012, doi: 10.1016/j.proeng.2012.06.086.

[59] S. Suresh Kumar, M. Uthayakumar, S. Thirumalai Kumaran, P. Parameswaran, and E. Mohandas, "Electrical discharge machining of Al (6351)-5% SiC-10% B4C hybrid composite: A grey relational approach," *Model. Simul. Eng.*, vol. 2014, 2014, doi: 10.1155/2014/426718.

[60] S. Vinoth Kumar and M. Pradeep Kumar, "Machining process

parameter and surface integrity in conventional EDM and cryogenic EDM of Al-SiCp MMC," *J. Manuf. Process.*, vol. 20, pp. 70–78, 2015, doi: 10.1016/j.jmapro.2015.07.007.

[61] P. Kumar and R. Parkash, "Experimental investigation and optimization of EDM process parameters for machining of aluminum boron carbide (Al–B4C) composite," *Mach. Sci. Technol.*, vol. 20, no. 2, pp. 330–348, 2016, doi: 10.1080/10910344.2016.1168931.

[62] I. Shyha and M. Rudd, "Electro-discharge machining of metal matrix composite materials," *Adv. Mater. Process. Technol.*, vol. 2, no. 2, pp. 235–244, 2016, doi: 10.1080/2374068X.2016.1164525.

[63] S. K. Lalmuan, S. Das, M. Chandrasekaran, and S. K. Tamang, "Machining Investigation on Hybrid Metal Matrix Composites- A Review," *Mater. Today Proc.*, vol. 4, no. 8, pp. 8167–8175, 2017, doi: 10.1016/j.matpr.2017.07.158.

[64] K. Ponappa, K. S. K. Sasikumar, M. Sambathkumar, and M. Udhayakumar, "Multi-objective optimization of edm process parameters for machining of hybrid aluminum metal matrix composites (Al7075/TiC/B4C) using genetic algorithm," *Surf. Rev. Lett.*, vol. 26, no. 10, 2019, doi: 10.1142/S0218625X19500719.

[65] S. Mahanta, M. Chandrasekaran, S. Samanta, and R. M. Arunachalam, "EDM investigation of Al 7075 alloy reinforced with B4C and fly ash nanoparticles and parametric optimization for sustainable production," *J. Brazilian Soc. Mech. Sci. Eng.*, vol. 40, no. 5, 2018, doi: 10.1007/s40430-018-1191-8.

[66] P. Malhotra, R. K. Tyagi, N. K. Singh, and B. Singh, "Experimental investigation and effects of process parameters on EDM of Al7075 / SiC composite reinforced with magnesium particles," *Mater. Today Proc.*, no. xxxx, 2019, doi: 10.1016/j.matpr.2019.11.069.

[67] D. Palanisamy, A. Devaraju, N. Manikandan, K. Balasubramanian, and D. Arulkirubakaran, "Experimental investigation and optimization of process parameters in EDM of aluminium metal matrix composites," *Mater. Today Proc.*, no. xxxx, 2019, doi: 10.1016/j.matpr.2019.08.145.

[68] E. D. M. Investigation and O. F. Al, "EDM INVESTIGATION OF AL 7075 /B4C/ZRO2 HYBRID METAL MATRIX COMPOSITE BY APPLYING RESPONSE SURFACE METHODE," vol. 12, no. 3, pp. 152–164, 2021.

[69] S. Sunil Kumar Reddy, C. Sreedhar, and S. Suresh, "Investigations

on Al 7075 /nano-SiC/ B4C hybrid reinforcements using liquid casting method," *Mater. Today Proc.*, vol. 46, no. xxxx, pp. 8540–8547, 2021, doi: 10.1016/j.matpr.2021.03.536.

[70] P. Chellapandi, S. K. A, and A. V. S, "Experimental investigations on aluminum based metal matrix composites with B4C, SiC and Mg," vol. 1, pp. 59–68, 2015.

[71] M. Satheesh and M. Pugazhvadivu, "Flexural Strength Behavior of Al 6061matrix Reinforced with SiC and Coconut shell ash," *SSRG Int. J. Mech. Eng. (SSRG-IJME)-Special Issue*, pp. 12–15, 2018, [Online]. Available: http://www.internationaljournalssrg.org.

[72] V. Senthilkumar and B. U. Omprakash, "Effect of Titanium Carbide particle addition in the aluminium composite on EDM process parameters," *J. Manuf. Process.*, vol. 13, no. 1, pp. 60–66, 2011, doi: 10.1016/j.jmapro.2010.10.005.

[73] R. A. Abdulwahid, H. Al-Ethari, and S. H. Al-Shaafaie, "Influence of mechanical mold vibration on EDM parameters of aluminum-alumina composite," *Int. Conf. Adv. Sustain. Eng. Appl. ICASEA 2018 - Proc.*, pp. 221–226, 2018, doi: 10.1109/ICASEA.2018.8370985.

[74] F. Gillani *et al.*, "Parametric Optimization for Quality of Electric Discharge Machined Profile by Using Multi-Shape Electrode," 2022.

[75] A. H. Taieb and S. Msahli, "Optimization of the Knitted Fabric Quality by using Multicriteria Phenomenon tools," *Int. J. Fiber Text. Res.*, vol. 3, no. 4, pp. 66–77, 2013.

[76] A. Baradeswaran and A. Elaya Perumal, "Influence of B4C on the tribological and mechanical properties of Al 7075-B4C composites," *Compos. Part B Eng.*, vol. 54, no. 1, pp. 146–152, 2013, doi: 10.1016/j.compositesb.2013.05.012.

[77] K. Sekar and D. V. Ananda Rao, "Investigation of Hybrid Composite A7075/SiC/B4C by Stir and Squeeze Casting method," *Mater. Today Proc.*, vol. 22, pp. 1398–1408, 2019, doi: 10.1016/j.matpr.2020.01.483.

[78] H. A. Al-salihi, A. Akram, and H. J. Alalkawi, "Mechanical and wear behavior of AA7075 aluminum matrix composites reinforced by Al 2 O 3 nanoparticles," *Nanocomposites*, vol. 5, no. 3, pp. 67–73, 2019, doi: 10.1080/20550324.2019.1637576.

[79] M. Venkateswarlu, "Synthesis and Mechanical Characterization of duel particle reinforced hybrid composites," vol. 13, no. 2, pp. 178–

182, 2018.

[80] F. Puh, Z. Jurkovic, M. Perinic, M. Brezocnik, and S. Buljan, "Optimizacija parametara obrade tokarenja s više kriterija kvalitete uporabom Grey relacijske analize," *Teh. Vjesn.*, vol. 23, no. 2, pp. 377–382, 2016, doi: 10.17559/TV-20150526131717.

[81] W. Melik, Z. Boumerzoug, and F. Delaunois, "Effect of SiC Amount on the Properties of Al6061 Matrix Produced by Powder Metallurgy," 2020.

[82] S. Gopalakannan and T. Senthilvelan, "Optimization of machining parameters for EDM operations based on central composite design and desirability approach," *J. Mech. Sci. Technol.*, vol. 28, no. 3, pp. 1045–1053, 2014, doi: 10.1007/s12206-013-1180-x.

[83] A. Singh, P. Kumar, and I. Singh, "Process optimization for electro-discharge drilling of metal matrix composites," *Procedia Eng.*, vol. 64, pp. 1157–1165, 2013, doi: 10.1016/j.proeng.2013.09.194.

[84] H. Yan, B. Djo Kabongo, H. Zhou, C. Wu, and Z. Chen, "Analysis and optimization of the machining characteristics of high-volume content sicp/al composite in wire electrical discharge machining," *Crystals*, vol. 11, no. 11, 2021, doi: 10.3390/cryst11111342.

[85] S. Gopalakannan, T. Senthilvelan, and S. Ranganathan, "Modeling and optimization of EDM process parameters on machining of Al7075-B4C MMC using RSM," *Procedia Eng.*, vol. 38, no. January, pp. 685–690, 2012, doi: 10.1016/j.proeng.2012.06.086.

[86] F. Gillani, T. Zahid, S. Bibi, R. S. U. Khan, M. R. Bhutta, and U. Ghafoor, "Parametric Optimization for Quality of Electric Discharge Machined Profile by Using Multi-Shape Electrode," *Materials (Basel).*, vol. 15, no. 6, p. 2205, 2022, doi: 10.3390/ma15062205.

[87] M. T. Mohammed, "Investigate WEDM Process Parameters on Wire Wear Ratio, Material Removal Rate and Surface Roughness of Steel 1012 AISI," *Eng. Technol. J.*, vol. 36, no. 3, 2018, doi: 10.30684/etj.36.3a.3.

الخلاصة

تستخدم المواد المتراكبة ذات الاساس المعدنيMMCs على نطاق واسع في تطبيقات صناعية وهندسية مختلفة بسبب خصائصها الفائقة، مثل المقاومة النوعية العالية ، ومقاومة الصدمة العالية ، ومتانة الكسر العالية عند مقارنتها بالمواد التقليدية. تستخدم سبيكة Al 7075t6 على نطاق واسع في تطبيقات النقل ، وخاصة الفضاء والطيران والاستخدام البحري والسيارات بسبب النسبة العالية للمقاومة الى الوزن . على الرغم من أن سبائك سلسلة Al 7075-t6 تتمتع بخصائص ميكانيكية وحرارية أفضل بالإضافة إلى مقاومة عالية للتآكل ، إلا أنها لا تزال بحاجة إلى التحسين لاستخدامها في التطبيقات الهندسية.

في هذا البحث تم دراسة الخصائص الميكانيكية والتشغيلية لمادة متراكبة ذات اساس من Al-7075 (AMMCs) المعزز بـ (3و6 و 9)% من B_4C و / أو SiC المصنع بطريقة السباكة بالتحريك. الخصائص الميكانيكية لـ AMMCs ، وهي صلادة فيكرز ، ومقاومة الشد ، ومقاومة الانضغاط ، ومقاومة الانحناء ، والاستطالة ؛ تم مراجعة بعض الدراسات السابقة حول السلوك الميكانيكي وسلوك التشغيل لـ .AMMCs .تم دراسة و توصيف المواد باستخدام XRD ، وجهاز قياس الحجم الحبيبي ، و SEM ، والمجهر الضوئي. تبين نتائج الخواص الميكانيكية أن جميع مواد التقوية لها تأثير كبير على هذه الخواص. تميزت المادة المتراكبة المحضرة بنسبة ($SiC4.5\%+B_4C4.5\%$) بخواص ميكانيكية أفضل. تحسنت الخواص الميكانيكية كالاتي:الصلادة بنسبة 54.95% و مقاومة الشد القصوى بنسبة 32.46% ، اجهاد الخضوع بنسبة 31.1%، ومقاومة الانحناء بنسبة 39.48% في ، ومقاومة الانضغاط القصوى 34.42%بالمقارنة مع السبيكة الأساسية. ساعدت طريقة الامثلية المستخدمة على تحسين خواص AMMCالهجينة. تم إخضاع أفضل عينة من حيث الخواص الميكانيكية ($4.5\%B_4C+4.5\%$ SiC) لإجراء تشغيل بالتفريغ الكهربائي (EDM) لتحديد الظروف المثلى للتشغيل وتم استخدام طريقة تحليل العلاقة الرمادية .(GRA) عند مستوى ثقة95% ، تم تحليل النتائج التي تم جمعها من العمليات التجريبية في الاختبارات الميكانيكية والتشغيل باستخدام برنامج .Minitab17.

تم اختيار الاستجابة الرئيسية لتقييم تأثير عوامل عملية EDM مثل الجهد (V) والتيار (I)ومدة النبض (Ton) وفاصل النبض (Toff) على خصائص الأداء مثل معدل إزالة المعدن (MRR) ومعدل بلى العدة ((EWR) وخشونة الأسطح .(Ra) , بعض عوامل عملية EDM لها تأثير كبير على مخرجات التشغيل وفقًا للنتائج. تكشف نتائج GRA أن مجموعة معاملات العملية المثلى للتشغيل هي(الفولتية =140 فولت و التيار= 10 امبير و Ton=50 ميكروثانية و Toff= 25ميكروثانية

وزارة التعليم العالي والبحث العلمي
جـــامـــعـة بـــابـــل
كـــلـيـة هـنـدســة الـــمواد
قـــسـم هـــندسة الـمعـــادن

تأثير كاربيد السيليكون و البورون على الخواص الميكانيكية والتشغيلية لمادة مركبة ذات اساس AA7075-T6

رسالة
مقدمة الى قسم هندسة المعادن في كلية هندسة المواد/جامعة بابل وهي جزء من متطلبات نيل شهادة الماجستير في هندسة المواد/ هندسة المعادن

من قبل:
محـمد شاكـر نـاهي ساير

بإشراف:

أ. د .سعد حميد الشافعي
أ.م. سندس عباس جاسم

2022م 1443هـ